NTNU – Trondheim
Norwegian University of
Science and Technology

Effects of Ammonia and Organic Ligands to Cadmium (Cd) Toxicity on Marine Phytoplankton

Xixi Liu

Environmental Toxicology and Chemistry
Submission date: May 2012
Supervisor: Bjørn Munro Jenssen, IBI
Co-supervisor: Murat Van Ardelan, IKJ

Norwegian University of Science and Technology
Department of Biology

Acknowledgements

This thesis has been supported by WAFOW 3 that is a collaborative project between Norway and Chile on coastal ecosystem.

I would love to express my most sincere thanks to my scientific supervisor, Dr. Murat Van Ardelan (Department of Chemistry, NTNU), for his patient supervise, academic knowledge support and encouragement during my two years master study in NTNU.

I am appreciated my main supervisor, Prof Bjørn munro Jenssen (Department of Biology, NTNU) for his advice and master thesis support.

I also thank Prof. Øyvind Mikkelsen (Department of Chemistry, NTNU) for academic and technique support on anodic stripping voltammetry.

Besides, I am willing to thank Prof. Jose Luis Iriarte Machuca from Universidad Austral de Chile for statistical analysis, and thank Syverin Lierhagen (Department of Chemistry, NTNU) for HR-ICP-MS measurement.

Trondheim, May 2012,

Xixi LIU

Abstract

The effects of ammonia to Cd toxicity on marine phytoplankton have been studied. The phytoplankton biomass was significantly increased at higher ammonia flux after high Cd level exposure, which indicated high ammonia decreased Cd toxicity on phytoplankton. In addition, DGT labile Cd concentration was linear decreased with increasing ammonia flux in day 8, while DGT labile Cd concentration was increased at higher ammonia flux in day 12. Cd complexation capacity in seawater of Cd treatment was higher over 100 times than Cd complexation capacity in seawater of without Cd treatment. And high ammonia increased Cd complexation capacity in seawater after high Cd exposure in day 8, while Cd complexation capacity in seawater of Cd treatment was decreased due to high ammonia in day 12. Therefore, ammonia influences the amount of DOM released by phytoplankton and the Cd complexation with organic ligands, and finally leads to affect Cd bioavailability and toxicity on phytoplankton.

Abbreviation

ANOVA	Analysis of variation
ASV	Anodic Stripping Voltammetry
BLM	Biotic Ligand Model
CA	Carbonic Anhydrase
CASS-4	Nearshore Seawater Reference Material for Trace Metals
CC	Complexation Capacity
DGT	Diffusive Gradients in Thin-films
DOM	Dissolved Organic Matters
FIAM	Free Ion Activity Model
Ft	Instantaneous Chlorophyll Fluorescence
HR-ICP-MS	High Resolution Inductively Coupled Plasma Mass Spectrometry
K	Stability Constant
MQ	Milli-Q water
NASS-5	Seawater Reference Material for Trace Metals
NBS	National Bureau of Standards
RC	Reaction Centers
PS	Photosystem
SPM	Subcellular Partitioning Model
UP	Ultrapure
WAFOW	*Can Waste Emission from Fish Farms Change the Structure of Marine Food Webs? A comparative study of coastal ecosystems in Norway and Chile*

Contents

Figure list

Table list

1. Introduction

1.1 Aquaculture and eutrophication

The aquaculture has produced significant environmental influences and hence has been considered to control aquaculture developments (Porrello, et al., 2003, Gowen, 1994). Eutrophication is the typical impact of aquaculture due to nutrient discharges to the natural environment (Porrello, et al., 2003). Marine aquaculture systems release nutrients as dissolved inorganic nutrient through excretion from the fish (NH_4 and PO_4), particulate organic nutrients through defecation, and dissolved organic nutrients through re-suspension from the particulate fractions. The majority of the nitrogen (N) wastes are released to open waters (68% of total) in the form of NH_4 whereas the bulk of the phosphorus (P) is accumulated in sediments (63%). In addition, released ammonia due to aquaculture may have immediate toxic effect on biota besides its impact on primary production and changes in natural plankton community (Olsen, 2008). This altered nutrient ratio and increased releasing of nutrients affect the species composition of the phytoplankton (Olsen, 2008).

However, there is no scientific concept agreed upon for understanding how nutrient and organic wastes from aquaculture distribute and accumulate in ecosystem. And there is a rare understanding of how released nutrients and organic matter affect the structure and function of the ecosystem. Based on

these situations, WAFOW projects (*Can Waste Emission from Fish Farms Change the Structure of Marine Food Webs? A comparative study of coastal ecosystems in Norway and Chile*) start studying the effects of nutrient wastes released from aquaculture on marine microbial food webs both in Norway and Chile. Moreover, macronutrients released from aquaculture activities impact the distribution, transformation and transportation of trace metals in marine phytoplankton and zooplankton. Although the Cd toxicity on marine ecology has been studied, there are rare studies linking Cd toxicity and aquaculture activities. Therefore, this thesis, as a relevant studying of WAFOW project, was focusing on the Cd toxicity to phytoplankton affected by released and organic matters through aquaculture activities.

1.2 Biogeochemical cycles of trace metals

Marine plankton contribute over 50% carbon fixation via photosynthetic on the Earth (Morel and Price, 2003, Field, et al., 1998). In order to keep high primary production efficiency, plankton has to take up the essential micronutrients with trace concentrations (<0.1 μM), including carbon, nitrogen, phosphorus, and silicon. Besides, trace metals have vital roles for biochemical reactions for ocean organisms. The most important bioactive trace metals for marine organisms are iron (Fe), zinc (Zn), copper (Cu), manganese (Mn), cobalt (Co), nickel (Ni) and cadmium (Cd).

1.2.1 Trace metals in biogeochemical cycles

There are three important biogeochemical cycles in the marine environment: carbon cycle, nitrogen cycle and phosphate cycle (Morel and Price, 2003). Trace metals are essential for the growth of marine plankton, which also are involved in the biogeochemical cycles in seawater (Figure 1), and they have key roles in these cycles either directly or indirectly (Morel and Price, 2003). Organisms in seawater take up trace metals which are essential for their growth, and transform metals by complexation for biological use. Therefore, the trace metals play important roles in the microorganism growth and the biogeochemical cycles of C, N and P.

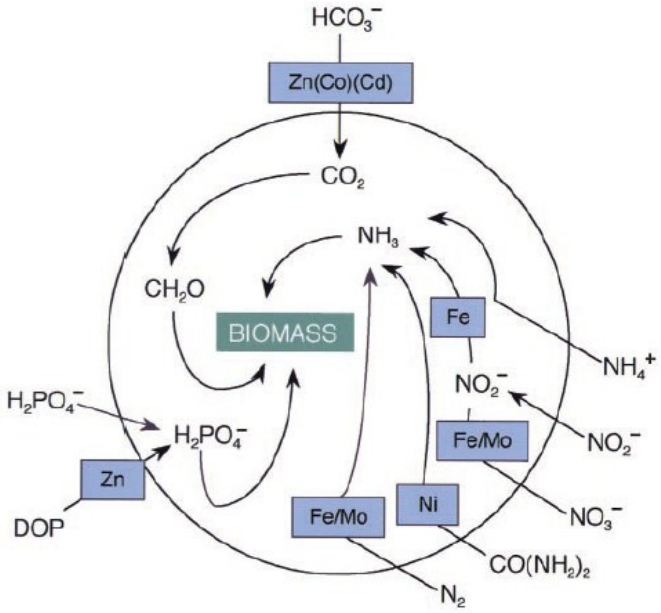

Figure 1 Trace metals requirements during biogeochemical process by marine phytoplankton, which involves carbon, nitrogen, and phosphorus acquisition and assimilation (Morel and Price, 2003).

There is a mutual interaction between trace metals and phytoplankton: essential and toxic metals somehow affect the growth of the microorganisms and their life cycle, phytoplankton in turn control the chemistry and biogeochemical cycling of trace metals.

1.2.2 Metal speciation

Metal speciation is essential for the chemical reactivity of trace metals in the aquatic environment, especially for bioavailability, toxicity, and the geochemical behavior of chemical species (Hirose, 2006). Metal speciation was defined in 'IUPAC Recommendations 2000' as the partitioning of total metal present in a particular system among all possible chemical forms through reactions with all available complexation sites (Templeton, 2000, Tessier, 1995, Hirose, 2006, Buffle, 1990). Chemical species classify as isotopic composition, electronic or oxidation state, and complex or molecular structure (Figure 2).

During the last four decades, the chemical speciation of trace metals in seawater has been studied (Hirose, 2006, Sillen, 1961, Stumm, 1975), which is important to clarify the chemical species of trace metals in seawater, and to understand their bioavailability and toxicity. Metal availability can be adjusted by biota in marine environment, such as bacterial, phytoplankton and zooplankton groups. The planktonic organisms excrete more DOM (Dissolved Organic Matters) to response the environmental condition changes, which

decrease the toxicity of metals due to metal-DOM complexation (Wen, et al., 2006). The characteristics of organic ligands produced by marine microorganisms include high-affinity, hydrophilic metal-specific, biologically more resistant hetero-polycondensates with amounts of binding sites, some of them are in colloids functions (Vasconcelos, 2002, Wells, 2002, Wen, et al., 2006).

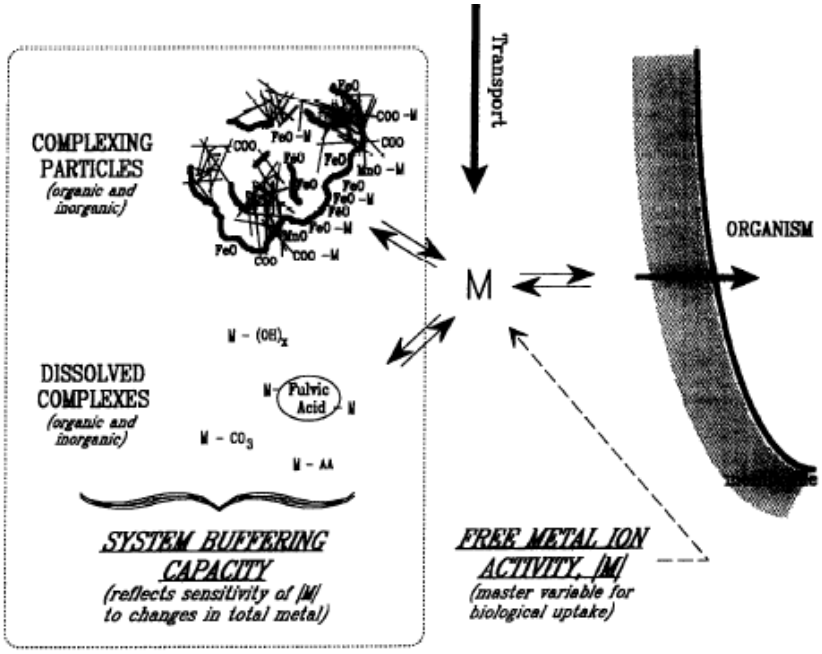

Figure 2 Metal complexation by dissolved and particulate complexants in natural waters (Buffle, 1990)

1.2.3 Metal chelation and complexation

The concentrations of trace metals are extraordinary low in seawater due to their less solubility and their effective removal from the water column. Such low concentration (nM and pM level) restrict the measuring technique and the sensitivity of detection instruments (Hirose, 2006). Moreover, seawater is so

chemically complicated system with many inorganic and organic chemical species dissolved in high saline water that the difficulty of measurement is also increased (Hirose, 2006). Regarding to planktonic uptake of most essential metals, trace metals are presented at extremely low concentration in surface. However, phytoplankton is still able to accumulate those essential trace metals at very low concentration.

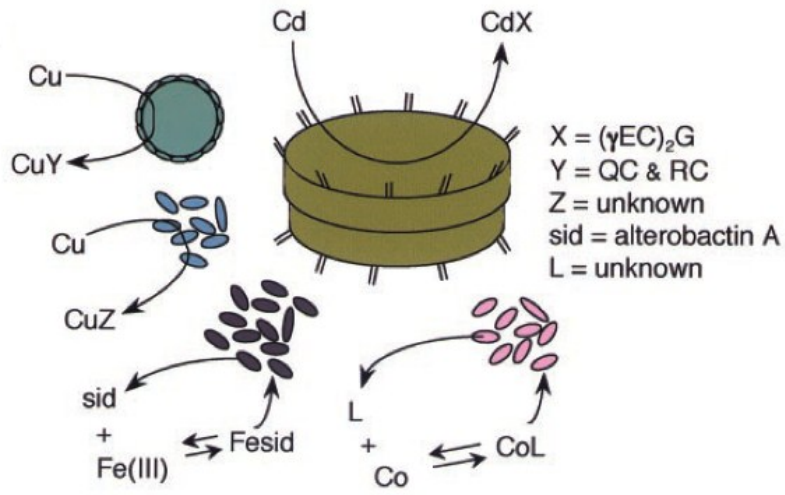

Figure 3 Examples of metal ligand complexes with complexing agents released from marine phytoplankton. CdX: phytochelatin-Cd complex released by diatoms; CuY: peptide complexes of Cu released by coccolithophorids; CuZ: unidentified Cu ligand complex released by synechococcus; Fesid: Fe-siderophore complex released by heterotrophic bacteria and cyanobacteria; CoL: Co complex with unidentified ligands released by prochlorococcus. (Morel and Price, 2003)

Some studies demonstrated that most the dissolved trace metals (Fe, Co, Cu, Zn, and Cd) are presented as nonreactive forms in surface seawater (Rue and Bruland, 1995, Morel and Price, 2003, Saito and Moffett, 2002). That is due to those metals are bound with some strong organic chelators released by marine microorganism in surface water. When phytoplankton is in high trace

metal concentration exposure, the main purpose of releasing complexing agents is to detoxify those metals (Figure 3). Although some of complexing agents have only been produced by plankton at relatively high metal concentrations exposure, the dissolved trace metals is dominated by organic complexes which may happened at either low or high molecular mass ligands (Morel and Price, 2003).

Small proportions of trace metals are existed as free hydrated cationic elements or complexes with inorganic ligands (Wen et al. 2006). The studies on the interactions between metal ions and inorganic ligands such as halogens and hydroxide, indicated insufficiency for understanding the ecological functions of trace metals in marine environment (Hirose, 2006). In addition, most amounts of trace metals are existed as complexation with organic ligands rather free elements or complexation with inorganic ligands (Wen, et al., 2006). For example, recent studies founds that more than 99 % of Cu species are presented as organic complexes in seawater (Hirose, 2006). Complexation between metals and organic ligands has been studies decades (Hirose, 2006, Morel and Price, 2003). Most bioactive trace metals in seawater form complexes with dissolved organic matters that are relevant to the growth of marine microorganisms, the bioavailability and toxicity of trace metals. The complexation capacity is the water capacity for complexing with metals ions and adjusting the dissolved metal concentration in water system (Zhang, 1990).

In addition, complexation capacity is important to determine the amount of the organic ligands in natural water, and it measures the metal-buffering capacity, and quantitatively assesses the fate of polluting metals in aquatic environment (Mantoura, 1981).

1.3 Cadmium

The vertical profiles of Cd concentration in oceans indicate that Cd is correlated with algal nutrient throughout the water column, especially with nitrate. The concentration of Cd is impoverished on the surface due to phytoplankton uptake, and reaches the maximum at depth corresponding to the chlorophyll *a* and nitrite maximum and re-mineralization of sinking organic ligands (Xu, et al., 2008, Wen, et al., 2006, Bruland, 1978). These evidences indicate the existence of interaction between Cd and nitrogen sources (nitrate, nitrite and ammonia). However, in some cases phosphate also affects Cd complexation process in marine system (Wen, et al., 2006, Xu, et al., 2008).

Cd is a toxic metal under high concentration, which has been proved in the history, such as itai-itai disease (Kasuya, 1992). However, the nutrient-like characteristic of Cd was recently discovered, when the concentration is low and low Zn content environment. One explanation is that Cd can replace Zn in carbonic anhydrase (CA) as a catalytic metal atom by diatoms (Lane, 2000, Morel, 1994, Xu, et al., 2008).

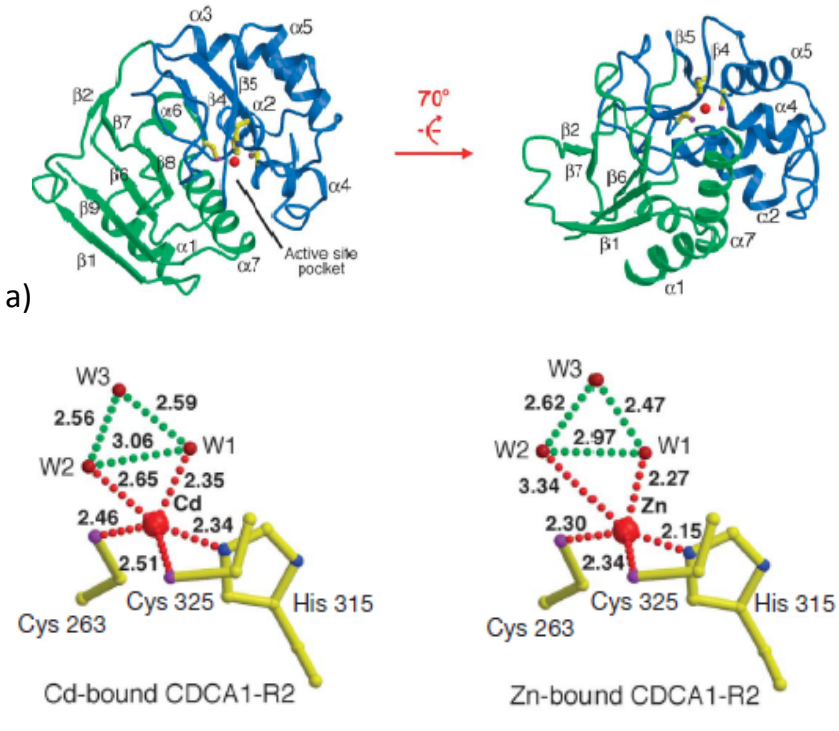

Figure 4 Structure of the second CA repeat of CDCA1 (CDCA1-R2). a) Overall structure of Cd-bound CDCA-R2. Two lobes of the structure are colored blue and green. The red point represents Cd, and Cd-coordinating residues are yellow. b) Comparison of Cd- and Zn- coordination in CDCA1-R2. Metals are colored as red point, coordination are marked by red dashed lines, and green is for hydrogen bonds (Xu, et al., 2008).

CA is one of the protein which catalyzes the reversible hydration of CO_2 (Xu, et al., 2008). Due to the physicochemical characteristic of CA, it is essential for acquisition of inorganic carbon for photosynthesis. In additional, CA contributes carbon uptake from atmosphere to ocean by phytoplankton which account for approximately 40 % of net marine primary production (Xu, et al., 2008, Falkowski, 2004, Badger, 2003). In total there are three categories of CA, α, β and γ, respectively. However they all only rely on Zn as catalytic metal atom. Two new types of CA have been discovered. One is δ-CA, represented

by TWCA1, which has the similar active sites as α-CA (Cox, 2000); another is ζ-CA, represented by CDCA1, which can utilize Cd directly (Lane, 2005). In fact, CDCA1 is a cambialistic enzyme, that is to say it can utilize and spontaneously exchange Zn and Cd as catalysis metal atom (Figure 4). Structural simulation could be an explanation for exchange Zn and Cd in active enzyme site. Cd can be biochemical catalyzed by CA in phytoplankton even in the low metal concentration condition, which could be one reason of atmospheric CO2 reduction following with diatoms radiation during the Cenozoic era (Xu, et al., 2008).

1.4 Phytoplankton

Phytoplankton (mainly Diatoms) account for nearly all primary production in the marine system (Sakshaug, 2005). The size of phytoplankton covers a wide range from 0.4 µm to 2 mm and photosynthesis is the main process to generate phytoplankton biomass in marine systems. For chlorophyll-containing species, photosynthesis is the typical process to produce carbohydrates and oxygen from carbon dioxide, water and light. The light (hv) is converted to heat and stored energy for organism growth. The well-known equation of photosynthesis is,

$$6CO_2 + 6H_2O \overset{hv}{\Rightarrow} 6C_6H_{12}O_6 + O_2 + heat$$

The necessary factor for photosynthesis is light and the visible light is

absorbed by phytoplankton, which covers 400 – 700 nm spectrums. Others including macronutrients (NO_3^-, PO_3^- and SiO_3^{2-}), carbon dioxide, essential trace metals (such as Fe, Zn, Mn) and vitamins (B_{12}) in seawater are essential factors for photosynthesis (Sakshaug, 2005).

1.4.1 Organic matters produced by phytoplankton

The amounts of organic ligands are produced by microorganisms which are dominated by bacterial and phytoplankton (Hirose, 2006). Both living and non-living marine microorganisms have strong affinity with trace metals (Pribil, 1979), because of their biochemical properties, which includes metal ions adsorption, chemical forms transformation by redox reaction or biomineralization, chemical substances transportation (Sakaguchi, 1991, Francis, 1999). According to previous studies, the metal ions could be complexed in the specific binding sites with ligands supported by microorganism, such as carboxylates. The most bioactive binding sites are located on the cell surface (Koval, 1999).

There are three pathways for organic ligands production by marine microorganisms. Firstly, the intracellular chelators are induced by exposure to metals (Grill, 1985). Then, synthesis and release of extracellular chelators can enhance metal assimilation (Trick, 1989). Finally, cell-surface chelators can complex metal-ion on surface complexation sites (Anderson, 1982). Fisher

(1993) indicated that not only for marine microorganisms have metal-reactive cell surface, but phytoplankton, diatoms and dinoflagellate. These chelators are significant for marine organisms adapting to an environment with extremely low level of bio-active elements (Hirose, 2006).

1.4.2 The mechanisms of metal toxicity on phytoplankton

The interaction between phytoplankton and trace metals have been studies extensively (Sunda and Huntsman, 1998, Miao and Wang, 2006). In general, trace metals are uptaken by organisms from surrounding solutions by three steps: (1) metals diffuse to the cell membrane surface from solution, (2) metals sorb or complex with ligands at binding sites on the cell membrane surface, (3) metals are uptaken into the organisms through the cell membrane (Wang, 2010). So far, there are three models describing the mechanisms of metal toxicity on phytoplankton.

1) Free ion activity model (FIAM)

Free ion activity model (FIAM) is a simplified model for estimating the trace metal bioavailability (Morel, 1983). Morel (1983) suggested that the metals uptake rate and their toxicity are determined by active free metal in the environment rather than the concentration of total metals. However, FIAM cannot correctly estimate the bioavailability and toxicity of trace metals that are comprehensively contributed by the whole metal species instead of only free metal concentration (Wang, 2010).

2) Biotic ligand model (BLM)

Biotic ligand model (BLM) described the mechanism of trace metals toxicity which is due to the interaction between dissolved metals and the proposed biotic ligand on the cell surface (Di Toro, et al., 2001). The most advantage of BLM compared to FIAM is that the complexation between metals and ligands is considered. However, BLM does not take into account the competition effects of different types of metals (such as the synergistic effect and additive effect), and cannot predict the effects of macronutrient uptake on metals' toxicity (Hassler, et al., 2004, Wang and Rainbow, 2006).

3) Subcellular partitioning model (SPM)

Intracellular metal concentration has been preferred as indicator of metal toxicity on marine organisms (De Schamphelaere, et al., 2005). Subcellular partitioning model (SPM) is aiming to determine the relationship between toxicity of trace metals and their subcellular distribution and accumulated concentration in specific subcellular pool (Wang and Rainbow, 2006). However, the application of SPM for marine phytoplankton is rare.

1.4.3 The interaction between Cd and macronutrients

Increasing Cd discharges into aquatic environments caused the negative biological responses (Wang, 2010). Meanwhile the large amount of macronutrients, especially NH_4 released to the environment due to aquaculture developments can potentially lead to eutrophication. The primary

ecosystem response to the increased NH_4 concentration is that the biomass of phytoplankton significantly increases. The interactions between the uptake of macronutrients and metals by phytoplankton populations have been studies recently (Wang, 2010). The assimilation of macronutrients by phytoplankton can be limited during high metal concentration exposure conditions (Mosulen, et al., 2003, Miao and Wang, 2006). Additionally, Wang and Dei (2001) suggested that the metal toxicity only depends on the specific type of macronutrient rather than the total ambient nutrient concentrations or the ratio of ambient nutrient composition. Miao and Wang (2006) have shown that nitrogen influence the Cd toxicity, while the effects of other nutrients (i.e. P and Si) on Cd accumulation have not been found. Although this results have been confirmed by single species cultured in laboratory as well as field phytoplankton community, it has not been observed whether the Cd toxicity on phytoplankton is affect by the total nitrogen amounts or the specific type of nitrogen (such as NO_2^-, NO_3^-, NH_4^+).

2. Hypotheses

Based on previous studies of the interaction between Cd and Nitrogen sources, there were two main hypotheses in this thesis to be addressed and clarify the relationship of nitrogen (ammonia in this case) and Cd toxicity on phytoplankton in marine system.

H1: If Cd toxicity on phytoplankton is directly affected by the ambient ammonia concentrations, then increasing ammonia released due to aquaculture activity may modify Cd toxicity on phytoplankton growth.

H2: NH_4 releasing from aquaculture can increase growth rate and biomass of phytoplankton. Enhanced phytoplankton growth releases more dissolved organic matters (DOM) in seawater. Moreover increasing phytoplankton biomass due to excess NH_4 may also significantly change the molecular structure of DOM (unpublished data, Ardelan, Rosel, Irriarte, et al., personal communication Murat Van Ardelan). Therefore, enhanced DOM and variations in the molecular structures of DOM may affect Cd complexes with organic matters and Cd toxicity on phytoplankton.

3. Objectives

The main objective of this thesis was to examine the Cd toxicity on marine phytoplankton community under different artificially regulated ammonia flux. The specific objectives were (1) to determine the effects of ammonia flux on Cd toxicity to phytoplankton biomass, (2) to determine the effects of ammonia flux on DGT labile Cd concentration after high level Cd exposure, (3) to compare the difference of Cd complexation capacity in natural seawater and Cd complexation capacity in high level Cd seawater, (4) to determine how ammonia flux impacts Cd complexation capacity under high Cd condition.

4. Materials and methods

4.1 Studied area

The mesocosm experiments were carried out in Hopavågen (at 61° 41'' N and 10° 51'' E) (Figure 5), where is a landlocked coastal embayment in central Norway with surface area of 275,000 m^2, total volume of 5.5 million m^3 and a maximum depth of 32 m (Ozturk, et al., 2002). The experimental period was in whole September, 2011, with temperature and salinity ranging between 15-16 °C and 31 psu, respectively (Olsen, et al., 2006).

Figure 5 The location of studied area was in Hopavågen, Norway, marked as a cross.

4.2 Experimental design

Water samples were pre-prepared in mesocosm polyethylene bags (depth 10 m, diameter 2 m, volume 30 m^3, Figure 6). In the mesocosm experiment, the inorganic nutrients were added every second day (daily concentrations in

Table 1), and delivered to about 1-2 m above the bottom of the bag by a plastic tube (length 10-15 m), followed by filling of assumed nutrients solution by lifting it from the bottom to the surface. Until the biological activities responses reached stable in mesocosm bag, water samples were taken from mesocosm bags into 10 L high density plastic barrels. The barrels experiments were the main containers used in this thesis. These barrels experimental period was 14 days from 12.09.2011-28.09.2011. There were two parallel groups including control (without Cd) and Cd treatment (with Cd 2 $\mu mol \cdot L^{-1}$) samples. There were five different ammonia (NH_4) levels with given increasing flux in each parallel group. The nutrients (NO_3^-, NH_4^+, PO_3^- and Si^+) were added every second day and mixed manually. The nutrients flux for each sample was presented in Table 1. Then barrels were attached to 'weight' (stones) linking with the rope which was tight on the surface of the seawater, in order to keep the environmental parameters as same as real surface condition (such as temperature, pressure, irradiance). The scheme of the experimental design is presented in Figure 7.

In general, there were biological and chemical parameters were measured throughout the whole experimental period. The phytoplankton biomass parameters (instantaneous chlorophyll fluorescence, *in vivo* fluorescence and Chlorophyll *a*) were immediately measured by Aquapen, flurometer and flurometer, respectively. In addition, the chemical parameters included pH, ASV labile Cd concentration measured anodic stripping voltammetry (ASV),

DGT labile Cd concentration measured by DGT sampler, and Cd complexation capacity determined by ASV.

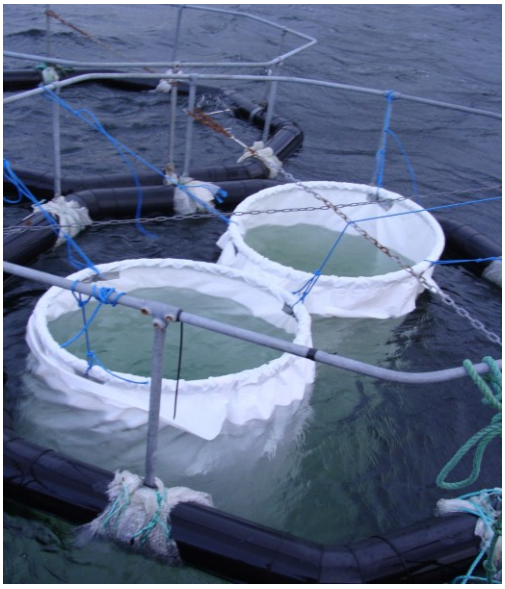

Figure 6 Picture of mesocosm bags in Hopavågen, Norway (depth 10 m, diameter 2 m, volume 30 m^3). Until the biological response reached stable, the water samples were taken from mesocosm bags into the barrels (10 L) for second step experiment. The barrels experiments were the main containers used in this thesis. (Photo by Xixi LIU)

Table 1 The setting of inorganic nutrients flux in barrels (µmol·D^{-1}·L^{-1}) used for Control and Cd treatments during experimental period in Hopavågen, Norway

	NO_3^-	NH_4^+	PO_3^-	Si^+
1	0.125	0.125	0.016	0.25
2	0.125	1.105	0.062	0.25
3	0.125	1.965	0.100	0.25
4	0.125	3.425	0.169	0.25
5	0.125	4.555	0.213	0.25

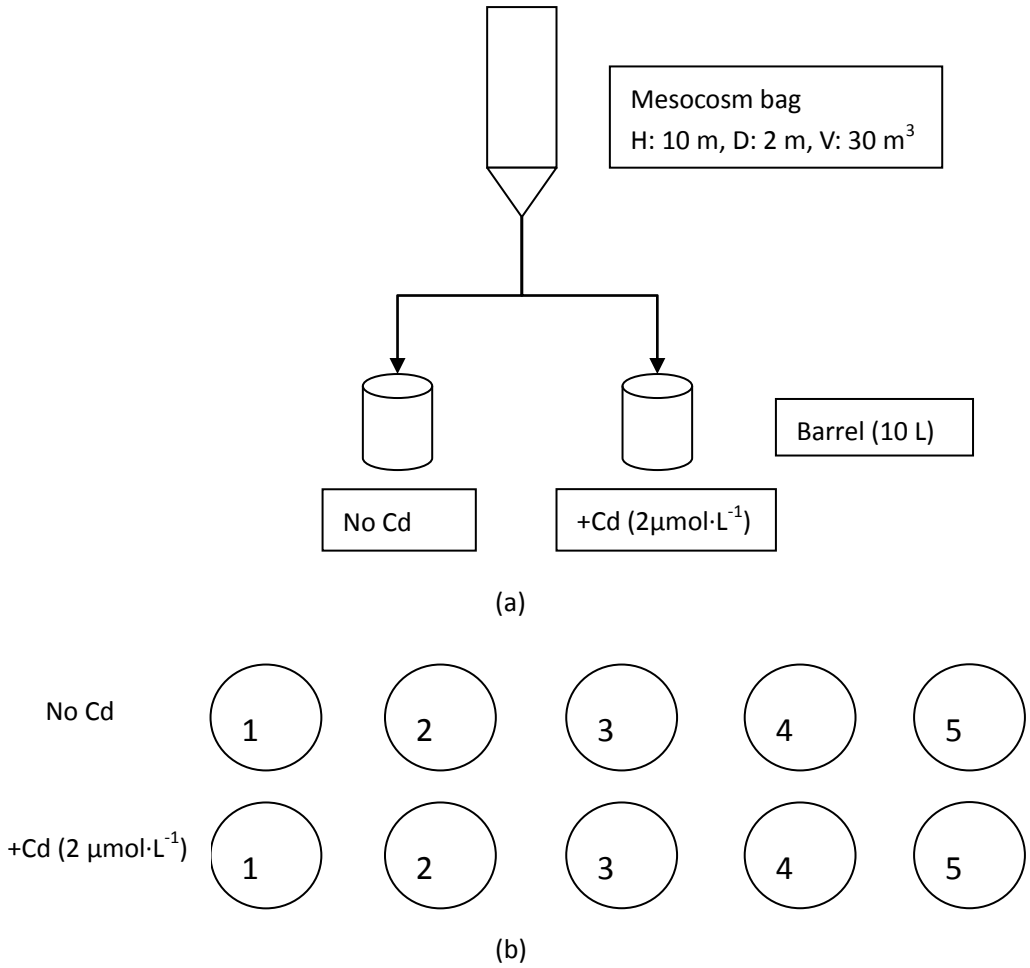

Figure 7 Scheme of setup experiment in Hopavågen, Norway was presented above. The seawater was directly taken from pre-prepared mesocosm bag into barrel. There were two parallel treatments in barrel experiment, including control (without Cd) and treatment (with Cd). (a) Seawater was taken from pre-treated mesocosm bags (b) simplified that samples were with five different nutrient fluxes, the detailed nutrients concentration was presented in Table 1.

4.3 Washing equipment

All sampling bottles and all other plastic equipment were acid washed before the experiments. Here, it has to be noted that DGT washing procedure is different other equipment acid washing. Firstly, DGT samplers were washed with approximately 1 M ultrapure (UP) HNO_3 (Scan-pure, Chem. Scan AS) at

the shaker (IKA Labortechnick KS501 digital) with 65-80 rpm for couple of hours, following by rinsing four times with Milli-Q water (18.2 MΩ, Millipore). DGT units were washed finally with 0.25 M UP HNO_3 after rinsing with MQ water, DGTs were shaking in ammonium hydroxide (UP NH_4OH 0.5 M) for two hour, in order to convert the Chelex-100 to NH_4 forms, Chelex-100 with NH_4 forms is most stable and effective forms for trace metal pre-concentration in seawater (Öztürk, 2002). Washed and conditioned DGTs were triple-bagged in plastics and storage in refrigerator until utilization.

4.4 pH

A combined glass electrode with an Ag/AgCl reference electrode (Titralab 860 Radiometer Analytical SAS) was used for the determination of pH. The pH electrode was calibrated by NBS buffer solutions (pH=7.0 and pH=10.0) at room temperature (about 18 °C). For the conversion of the measured pH (pH_{NBS}) to pH_{total} , the apparent activity coefficient of H^+ (f_{H^+}) was determined by four-point titration of 50 mL seawater by 15 mL standard acid with normalities in the range of 0.008–0.014N HCl, and calculations were done as described in Öztürk et al (2003).

4.5 Instantaneous Chlorophyll Fluorescence (Ft)

Instantaneous chlorophyll fluorescence (Ft), as an indirect indicator of phytoplankton biomass, was measured by Aquapen-C AP-C 100 (Photon Systems Instruments, Czech Republic) (Figure 8). Aquapen-C AP-C 100 is a new cuvette version of the FluorPen fluorometer. It contains a blue and red LED emitter, optically filtered and precisely focused to emit light intensities of up to 3 000 µmol·photon^{-1}·m^{-2}·s^{-1} to measure suspensions. Blue excitation light (455 nm) is intended for chlorophyll excitation. Red-orange excitation light (620 nm) is intended for excitation through phycobilins and is suitable for measuring in cyanobacteria. AquaPen-C is so sensitive that can measure water samples containing low concentrations of phytoplankton (the detection limit is 0.5 µg Chl·L^{-1}). The measurement process are described in AquaPen-P operation manual (Photon Systems Instruments, 2010).

Figure 8 The overview of AquaPen-C AP-C 100 (Photon Systems Instruments, 2010)

4.6 *In vivo* fluorescence

In vivo fluorescence, as an indirect indicator of phytoplankton production, was measured by fluorometer (10AU™ Field and Laboratory Fluorometer, TURNER DESIGNS, USA) (Figure 9). The calculated detection limit (DL) was 0.45 $\mu gChl \cdot L^{-1}$. In living phytoplankton cells, 1-5 % absorbed light is re-emitted as Chlorophyll *a* (Chl-*a*) fluorescence from reaction centers (RC) of photosystem II (PS II), and *in vivo* fluorescence covers approximately 95 % of Chl-*a* fluorescence (Govindjee, 1995). Chl-*a* fluorescence is an indicator of light harvesting and light utilization conditions. In living phytoplankton, Chl-*a* emits red light after absorbs blue light, thus Chl-*a* fluorescence is peaked in the range of red light. Therefore, *in vivo* fluorescence was measured at 685 nm wavelength. The sample was transferred to a fluorometer cuvette. Before measuring, the samples were slightly shacked manually until complete mixture, in order to avoid phytoplankton sinking.

Figure 9 The overview of fluorometer (10AU™ Field and Laboratory Fluorometer, TURNER DESIGNS, USA). (Photo by Xixi LIU)

4.7 Extracted Chlorophyll *a*

The extracted chlorophyll *a* (Chl-*a*) fluorescence was measured by fluorometer (10AU™ Field and Laboratory Fluorometer, TURNER DESIGNS, USA) (Figure 9). The procedure of Chl-*a* extraction and extracted Chlorophyll *a* fluorescence measurement has been described by (Bain, 1969). The concentration of extracted chlorophyll *a* was calculated by equation as follow (Vollenweider, 1969),

$$\mu g\ Chl\ a/L = (FL \times f \times E \times 1000 \times K)/(Fs \times S \times V) \quad (1)$$

where, FL is the fluorescence result reading on the lower scale; f is calibration factor, general equal 0.29; E is the extraction volume (usually 10 mL); K is ratio between the whole filter area and the small pieces; Fs is the slit automatically chosen by instrument (either 1.00 3.16 10.0 or 31.6); S is the sensitivity (either 1 or 100); and V is the filtered volume (mL).

4.8 DGT

Diffusive gradient in thin films (DGT) is the passive sampler in situ monitoring accumulated dissolved substances in water, soils and sediments (Zhang, 2007). The properties of DGT are associated with the type of sample media. In this thesis DGT only determined Cd labile concentration in seawater.

DGT samplers were purchased from Analytica AB (Sweden). DGT unit consists of a 0.4 µm pore-size cellulose acetate filter, a polyacrylamide hydrogel diffusion layer, and a Chelex-100 impregnated binding phase (Figure 10). Chelex-100 is a strong complexing resin with immunodiacetic acid functional ligands. The pore size within the polyacrylamide hydrogel depends on the amount and type of the cross-linker used, and varies in the range 2–20 nm (Sangi, et al., 2002, Ardelan, et al., 2009). DGT units were to collect the DGT labile Cd fraction in seawater samples, which have affinity to the Chelex-100 resin (Öztürk, 2002). The DGT labile Cd fractions include the free cation, inorganic complexes, and weak Cd-organic complexes with relatively fast dissociation kinetics (Zhang, 2007, Ardelan, et al., 2009, Scally, et al., 2003).

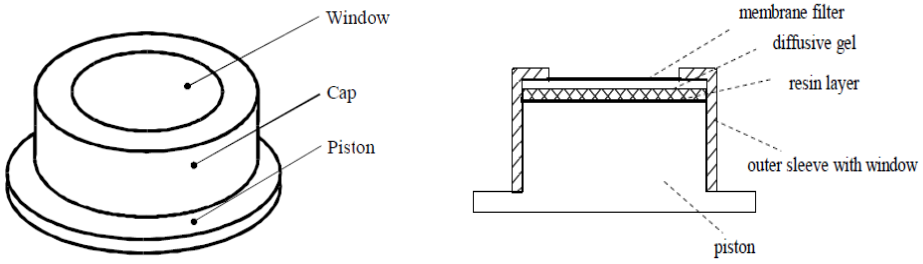

(a) (b)

Figure 10 the structure of DGT deployment moulding (a), and the vertical view of DGT water sampler (b)

The measurement procedure of DGT labile metal concentration is simplified showing in Figure 11. DGT devices were deployed in the acid washed plastic containers filling with about 1 L water sample, and kept in the shaker within 65-80 rpm for 3 days. Because the aim of deployment was to keep samples

stably moving rather than causing turbulence and/or bubbles. After shaking, DGTs were removed immediately to a clean plastic bag sealing with minimum air, following stored in a refrigerator until metal extraction.

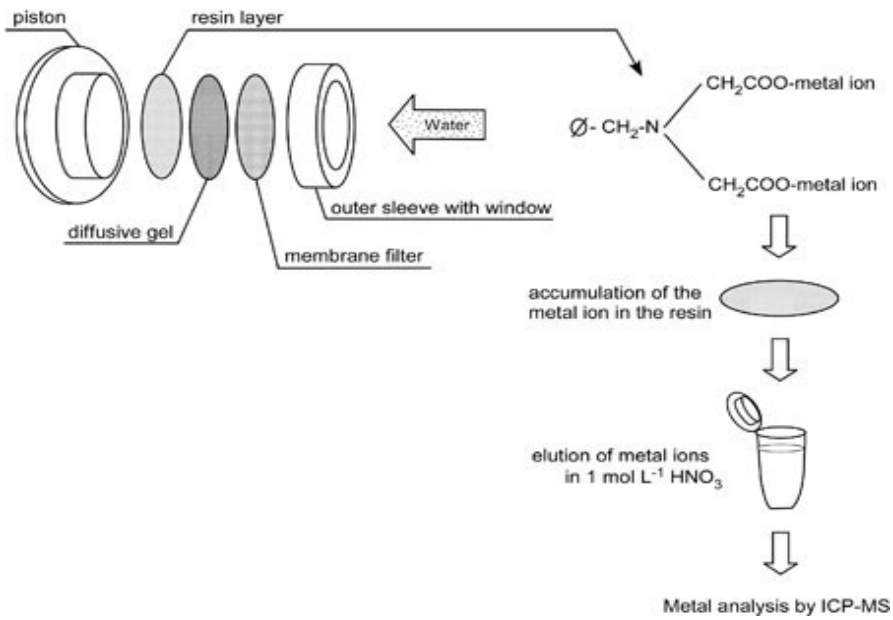

Figure 11 DGT labile metals measurement procedure. The resin layer which accumulated metal ions was taken out, eluted in UP HNO3 solution, and measured DGT labile metals amount/concentration by ICP-MS.

The accumulated Cd in Chelex-100 had to be extracted. Firstly, the Chelex-100 layer was peeled off into a clean sample tube (PE, 11 mL) without filter membrane and diffusive layers. The tube with Chelex-100 added 2 M UP HNO_3 (1 mL) was shaked at 65-80 rpm over one night. After that, the shacked acid solutions were transferred into a new clean tube (PE, 11 mL) with 4 mL rinsed solutions (UP HNO_3 0.25 M). Finally, the extracted Cd in 5 mL solution (HNO_3 0.6 M) was measured by HR-ICP-MS (Thermo Finnigan Element 2, GASS EXPANSION, Australia) performed by Syverin Lierhagen (Dept. Chemistry, NTNU).

The time-averaged DGT-labile concentrations can be calculated by equation:

$$C_{DGT} = \frac{m \cdot L}{t \cdot D \cdot A} \quad (2)$$

Where m is the mass collected by Chelex-100 in the DGT unit; L is the total thickness of the diffusion gel layer, assumption as 0.1 cm; t is the total deployment time, in this case it was chosen as 3 Days (259,200 s); D is the diffusion coefficient for Cd at room temperature ($5.30 \times 10^{-6}\ cm^{-2} \cdot s^{-1}$ at $20.0\ ℃$); A is the cross-sectional area of the active surface of the DGT units ($3.14\ cm^2$) (Ardelan, et al., 2009, Zhang, 2007).

Table 2 Comparison of certified Cd concentration in CASS-4 and NASS-5 with measured DGT labile Cd concentration. Method blank (average of 8 blanks) and detection limits (=3×Standard deviation of instrumental blank) of DGT method.

	Certified value (μmol·L^{-1})	**Measured (μmol·L^{-1})**
CASS-4	0.026 ± 0.003	0.029 ± 0.011
NASS-5	0.023 ± 0.003	0.018 ± 0.005
	Blank (μmol·L^{-1})	**DL (μmol·L^{-1})**
DGT method	0.003 ± 0.001	0.001

The accuracy of the determination of Cd dissolved and DGT labile fraction were verified by regular analysis of the standard reference material NASS-5 (Seawater Reference Material for Trace Metals) and CASS-4 (Nearshore Seawater Reference Material for Trace Metals) (Table 2). Both NASS-5 and CASS-4 were purchased from National Research Council Canada.

4.9 Anodic stripping voltammetry

Anodic stripping voltammetry (ASV) has become one of the most popular techniques of stripping electroanalysis for measuring trace metals (Skogerboe, 1974, Wang, 1985). ASV consists of two steps: deposition and dissolution. Deposition step involves that the target metals are preconcentrated into mercury electrode. The cathodic deposition potential is required generally 0.3 – 0.5 V more negative than E^o, in order to reduce metal ions easier. The metal ions are preconcentrated on the surface of mercury electrode by diffusion and convection, which can be termed as amalgamations (Wang, 2000):

$$M^{n+} + ne^- + Hg \rightarrow M\,(Hg)$$

The duration of deposition is associated with the concentration of metal ions in samples. It requires less than 30 s for relatively high concentration (10^{-7} M), whereas about 20 min for low concentration (10^{-10} M).

Dissolution step or stripping step involves that the amalgamated metals are reoxidized, stripped out of the electrodes following in an order of each metal standard potential:

$$M\,(Hg) \rightarrow M^{n+} + ne^- + Hg$$

The voltammetric peak presents the time-dependent gradient concentration of the metal in the mercury electrode during the anodic scan (Wang, 2000). Meanwhile, the type of metals can be identified by the corresponding peak

potentials. The peak current is correlated with several parameters during deposition and stripping procedure, the characteristics of the analytes metals and the geometric functions of electrodes. In this thesis, the peak height is the relative peak height which means the current peak difference between the original and the top of peak from the base line. Because relative peak height has better linearity in calibration curve compared to peak height from baseline directly or peak area (Mikkelsen, et al., 2006).

Figure 12 The hardware of PalmSens PC, which is connecting with personal computer to display the measurement results. (IVIUM TECHNOLOGIES, 2009)

The voltammetric procedure for the simultaneous determination of Cd in seawater samples was described in (Truzzi, 2002). PalmSens PC (IVIUM TECHNOLOGIES, Netherland) was used as an electrochemical sensor during ASV measurement (Figure 12). PalmSens PC connected with personal computer that can specify the parameters of the measurement, and display the results of the measurements by curves and data. And PalmSens PC connected with three electrodes: working electrode, reference electrode and counter electrode (Figure 13).

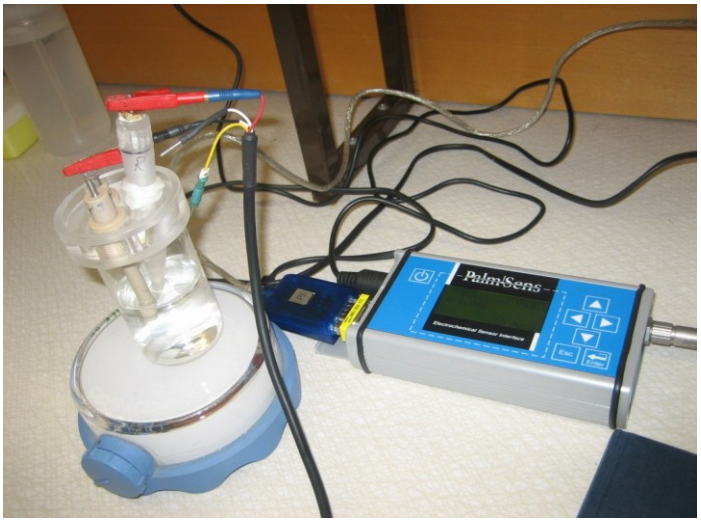

Figure 13 The overview of PalmSens PC connecting with three electrodes: reference electrode, counter electrode and working electrode respectively. (Photo by Xixi LIU)

During ASV experiments, the deposition potential was ranged from -1.1 V to -0.3 V, and the deposition time was 900 s for control samples (without Cd) and 60 s/120 s for Cd treatment samples (with Cd), respectively. Sample was kept 15 min in between each Cd addition, in order to ensure that added Cd was able to complex with organic ligands presenting in the sample. The detection limit of ASV was 0.25 $\mu mol \cdot L^{-1}$ (Manivannan, et al., 2004).

4.10 Cd complexation capacity

Cd complexation capacity in seawater of control and Cd treatment was determined by ASV. Cd complexation capacity of control (without Cd) was graphically determined following the procedure described by Buffle (1990). Cd complexation capacity of Cd (with Cd) was mathematically determined as

follow.

In this thesis, we assume that only 1:1 complex formed might be happened, thus the complex equilibrium is

$$Cd + L = CdL$$

And, the apparent stability constant (K) is presented as follows,

$$\mathrm{K} = \frac{[\mathrm{CdL}]}{[\mathrm{Cd}][\mathrm{L}]} \tag{3}$$

Thus, Cd complexation capacity can be mathematically determined from such relationship

$$\frac{[\mathrm{Cd}]_\mathrm{F}}{[\mathrm{Cd}]_\mathrm{T} - [\mathrm{Cd}]_\mathrm{F}} = \frac{1}{\mathrm{K} \cdot \mathrm{CC}} + \frac{[\mathrm{Cd}]_\mathrm{F}}{\mathrm{CC}} \tag{4}$$

where, CC is the complexation capacity and is equal to the ligand concentration, K is the apparent stability constant. $[Cd]_T$ is the total metal concentration which equal the added Cd plus detected Cd by ASV. $[Cd]_F$ is the concentation of free metal ion determined, and in fact it is ASV labile concentration in this case. The complexation capacity is the reciprocal of the slope, while the apparent stability constant is equal slope over intercept. (Zhang, 1990)

4.11 Statistical analysis

All data estimation (descriptive statistics) and statistical analysis were used by Microsoft Excel 2010. Two unpaired samples (*t*-Test) evaluated significant means differences between control (without Cd) and Cd treatment (with Cd) samples. A parametric analysis of variance (*ANOVA*) was statistically evaluated the difference of multiple comparisons (different ammonia flux) (Miller, 1993). Significant difference was accepted when $p<0.05$.

5. Results and Discussion

In situ experiments were carried out during September 2011, and the remaining samples measurements were done in a Class 100 trace metal clean laboratory and finished in January 2012.

5.1 pH

Since experimental pH is dependence to sample temperature, it is necessary to correct measured pH to room temperature (18 °C). pH temperature corrected data were presented in Appendix A. Each sample was measured two duplicates on each sampling day.

pH is used as an indirect variable of the growth rate of phytoplankton, which is positively related to photosynthetic activity (Sakshaug, 2005, Olsen, 2006). During photosynthesis, plants take up CO_2 and pH increases. Contrarily, pH decreases during respiration processes.

pH of Cd treatment (with Cd) were significantly lower (p<0.0001) than control treatment (without Cd) during the whole experimental period, which indicated that Cd depressed phytoplankton photosynthesis and results to biomass decreased (Figure 14). Furthermore, pH of Cd treatments were significantly different at different ammonia flux on each sampling day (p value was shown in Table 3), which indicated ammonia flux somehow affected the

phytoplankton production under high Cd exposure. pH has been widely used as an indirectly indicator for the growth of phytoplankton due to its simple and fast measurement procedures(Hirn, et al., 1980, Olsen, 2006). However in this case, it was extremely hard to identify the pH trend with different ammonia flux after high level Cd exposure on each sampling day (Figure 15). Thus, pH is not a good indicator to predict whether ammonia flux has positive or negative effects to Cd toxicity on phytoplankton. There might be some unknown mechanisms of excreting inorganic or organic components from phytoplankton controlled by ammonia under high Cd exposure, and these components may adjust pH in seawater, although seawater has buffering pH capability.

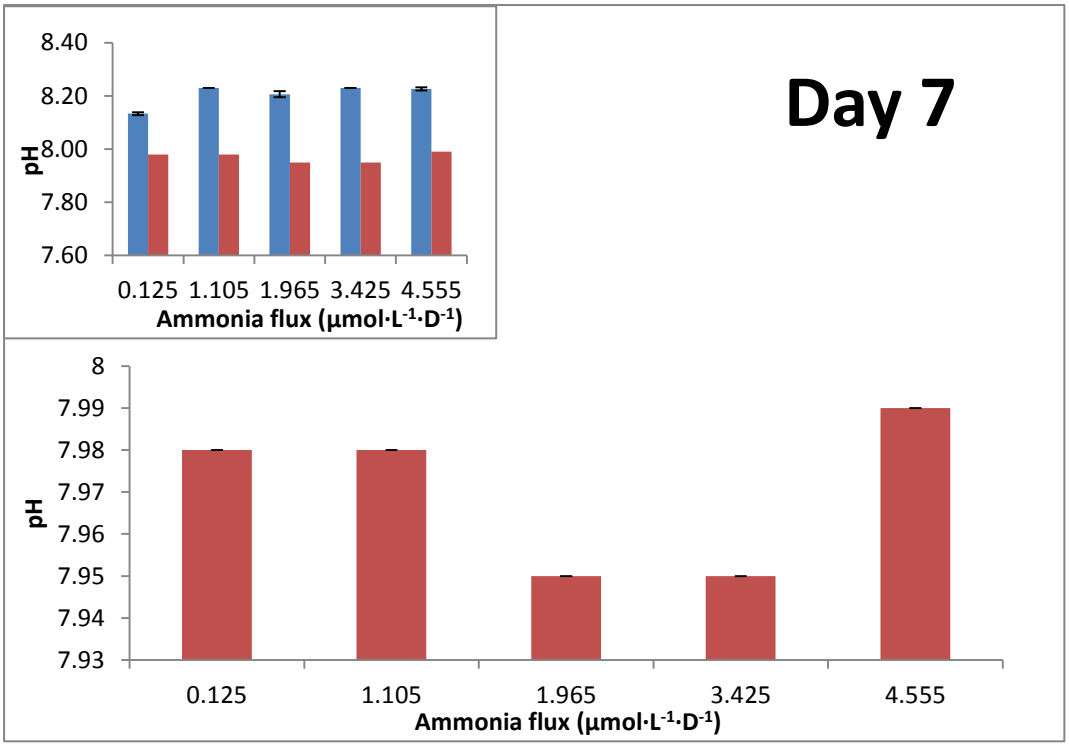

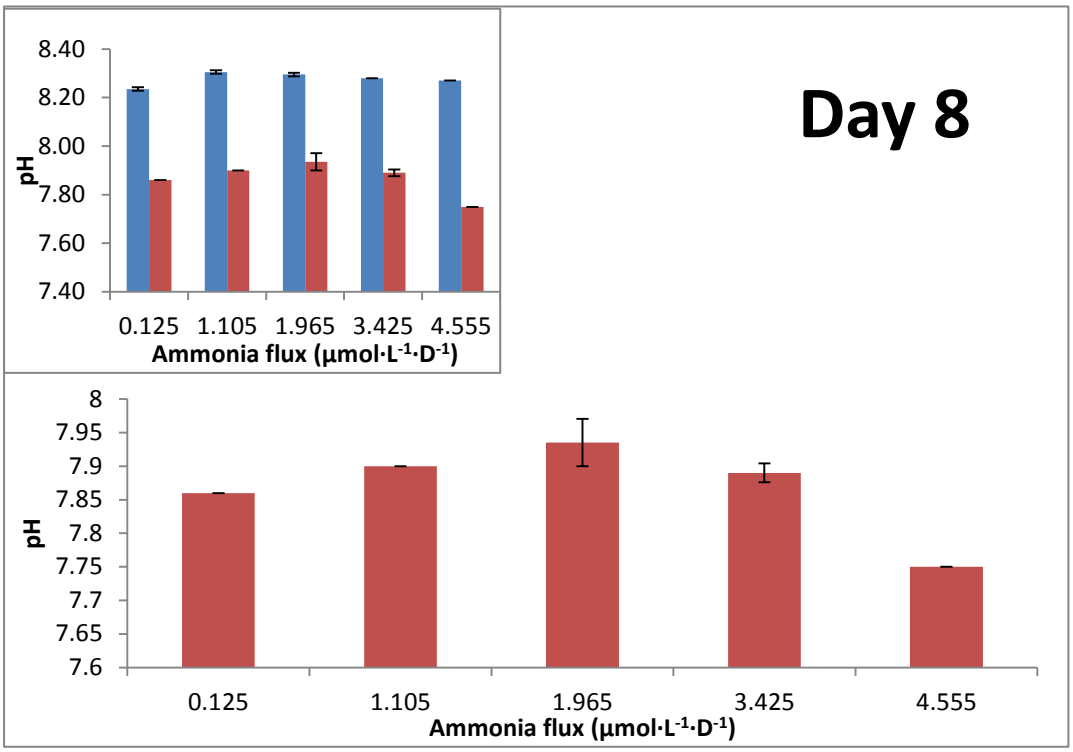
Day 8
8.40
8.20
8.00
7.80
7.60
7.40
pH
0.125
1.105
1.965
3.425
4.555
Ammonia flux (µmol·L-1·D-1)
8
7.95
7.9
7.85
7.8
7.75
7.7
7.65
7.6
pH
0.125
1.105
1.965
3.425
4.555
Ammonia flux (µmol·L-1·D-1)

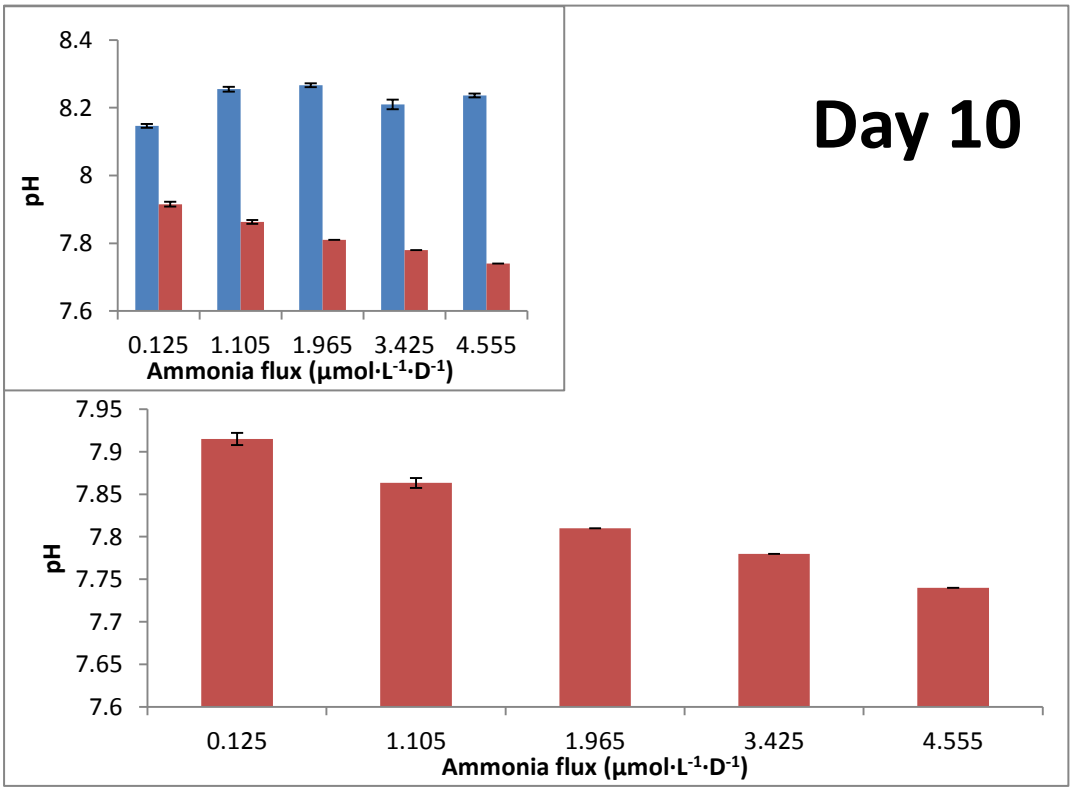
Day 10
8.4
8.2
8
7.8
7.6
pH
0.125
1.105
1.965
3.425
4.555
Ammonia flux (µmol·L-1·D-1)
7.95
7.9
7.85
7.8
7.75
7.7
7.65
7.6
pH
0.125
1.105
1.965
3.425
4.555
Ammonia flux (µmol·L-1·D-1)

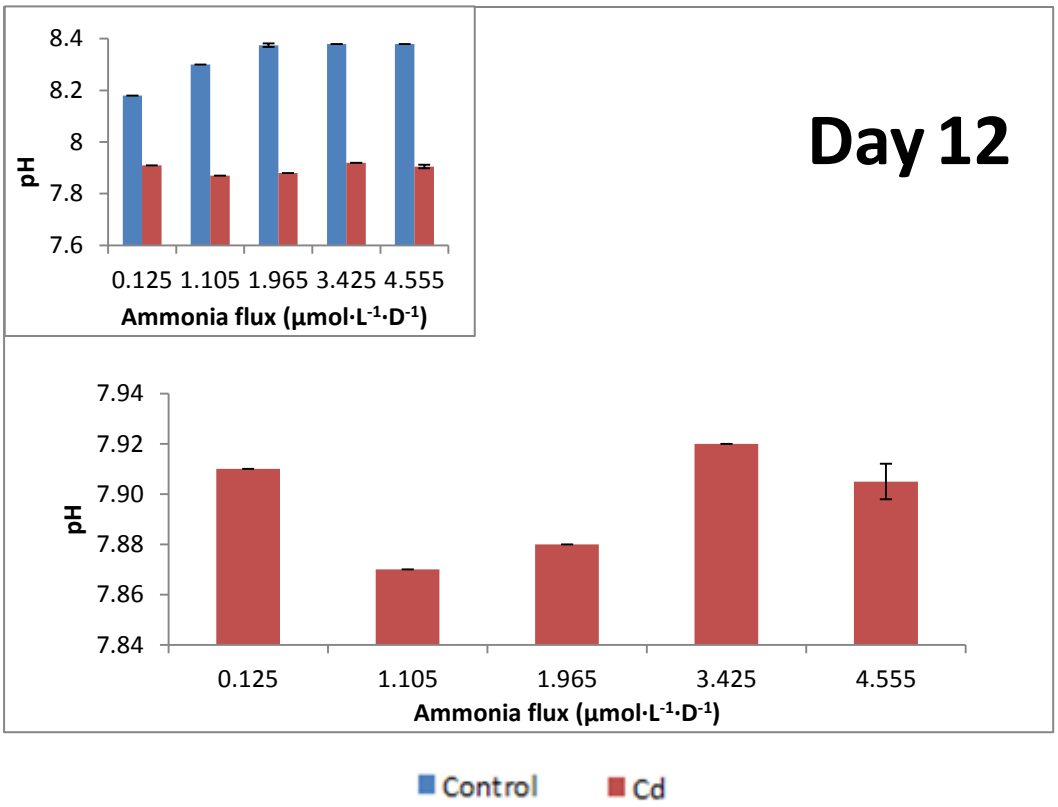

Figure 14 Mean pH of Cd treatment samples (with Cd) at given ammonia flux. The upper left figure illustrates pH mean values compared between control (without Cd) and treatment (with Cd) samples at given ammonia flux. The blue column represents control samples, whereas the red column shows Cd treatment samples. The given days expresses the experimental days accounting from Cd addition. Standard deviation range of each sample was presented (N=2).

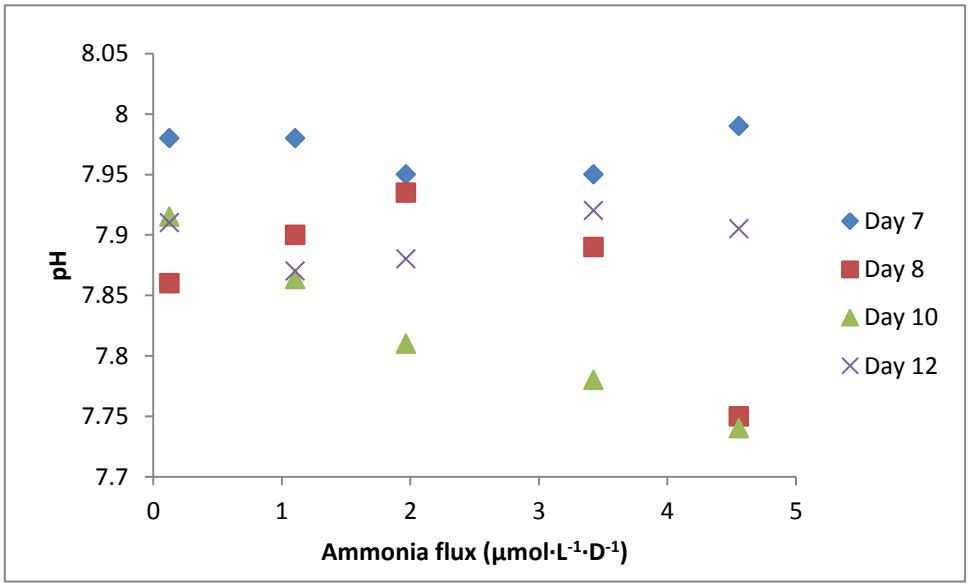

Figure 15 Summary of mean pH trend of Cd treatment at given ammonia flux on each sampling day. The given days expresses the experimental days accounting from Cd addition.

Table 3 Statistical evaluation of pH mean value compared among each ammonia flux on experimental day 7, 8, 10 and 12 (Parametric *ANOVA* test).

	P	**Evaluation**
Day 7	0.0001	Significant difference
Day 8	0.0007	Significant difference
Day 10	1.21E-06	Significant difference
Day 12	7.82E-5	Significant difference

5.2 *In vivo* fluorescence

In vivo fluorescence experimental data was presented in Appendix B. Each sample was measured three duplicates on each sampling day (N=3).

I*n vivo* fluorescence of control treatment (without Cd) was significantly higher than Cd treatment (with Cd) on each sampling day (*p* values equaled 0.003, 0.002, 0.012 and 0.011 for day 7, day 8, day 10 and day 12, respectively) (Figure 16). These results indicated that Cd had toxicity to inhibit phytoplankton production. *In vivo* fluorescence of Cd treatment significantly differenced in comparison among different ammonia flux on each sampling day (*p* value was shown in

Table 4). In addition, *in vivo* fluorescence of Cd treatment samples with kept stable in low ammonia flux, while there was a considerable increase at the

highest ammonia flux on each sampling day (Figure 17).

In vivo fluorescence of Cd treatment results shown that ammonia is one of the main factors to affect the phytoplankton growth. The results indicate phytoplankton biomass after high Cd exposure was restricted in low ammonia flux, while it was surprisingly stimulated due to high ammonia level in the environment. Besides, *in vivo* fluorescence results proved the interaction between ammonia flux and Cd toxicity on phytoplankton. The increasing of phytoplankton biomass at the highest ammonia flux regardless high Cd level, which indicated that high ammonia positively modify (decrease) Cd toxicity.

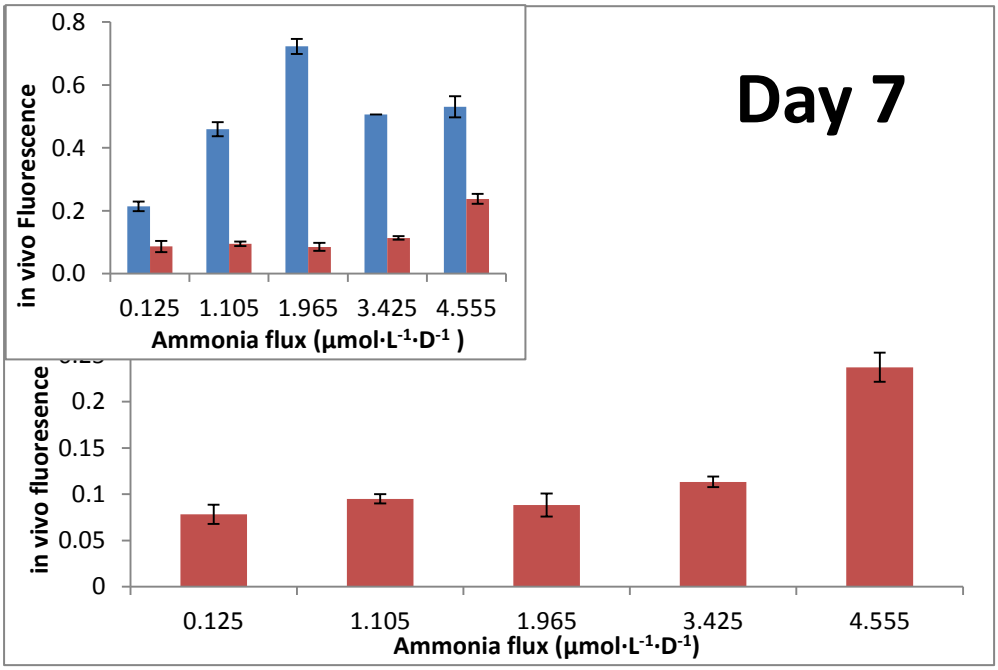

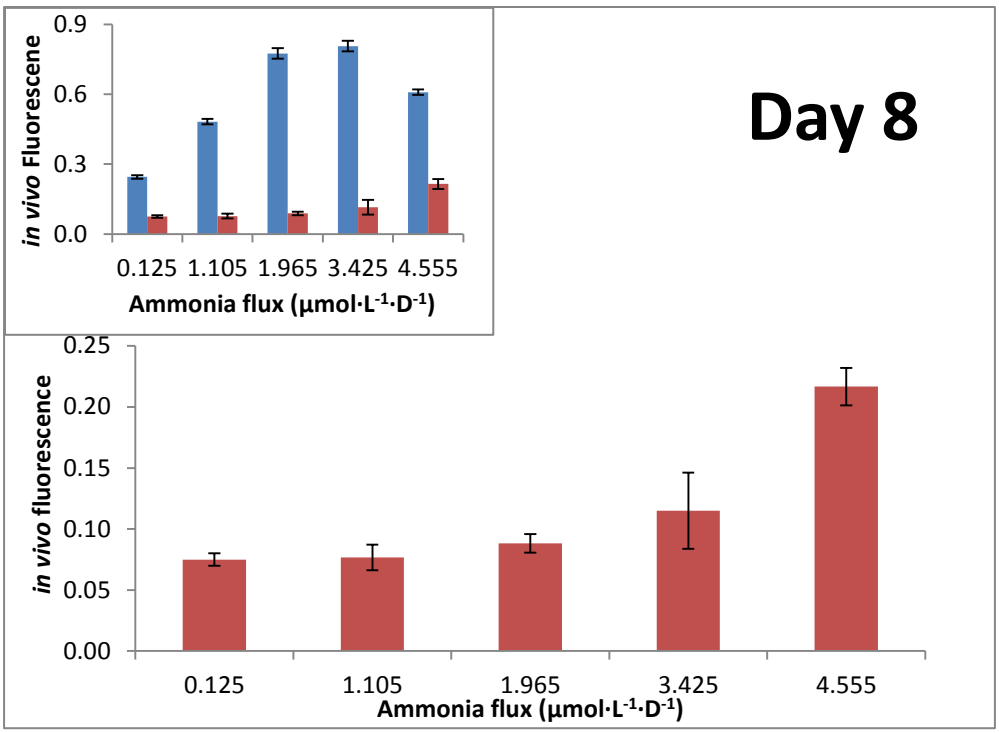
Day 8
in vivo Fluorescene
0.9
0.6
0.3
0.0
0.125 1.105 1.965 3.425 4.555
Ammonia flux (µmol·L-1·D-1)
in vivo fluorescence
0.25
0.20
0.15
0.10
0.05
0.00
0.125 1.105 1.965 3.425 4.555
Ammonia flux (µmol·L-1·D-1)

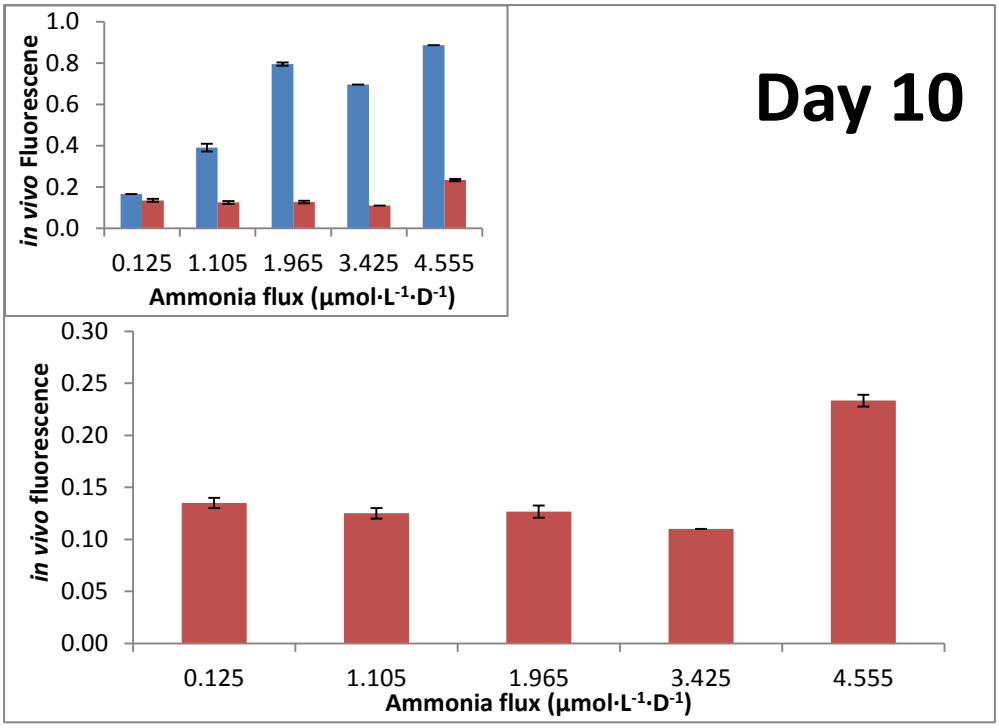
Day 10
in vivo Fluorescene
1.0
0.8
0.6
0.4
0.2
0.0
0.125 1.105 1.965 3.425 4.555
Ammonia flux (µmol·L-1·D-1)
in vivo fluorescence
0.30
0.25
0.20
0.15
0.10
0.05
0.00
0.125 1.105 1.965 3.425 4.555
Ammonia flux (µmol·L-1·D-1)

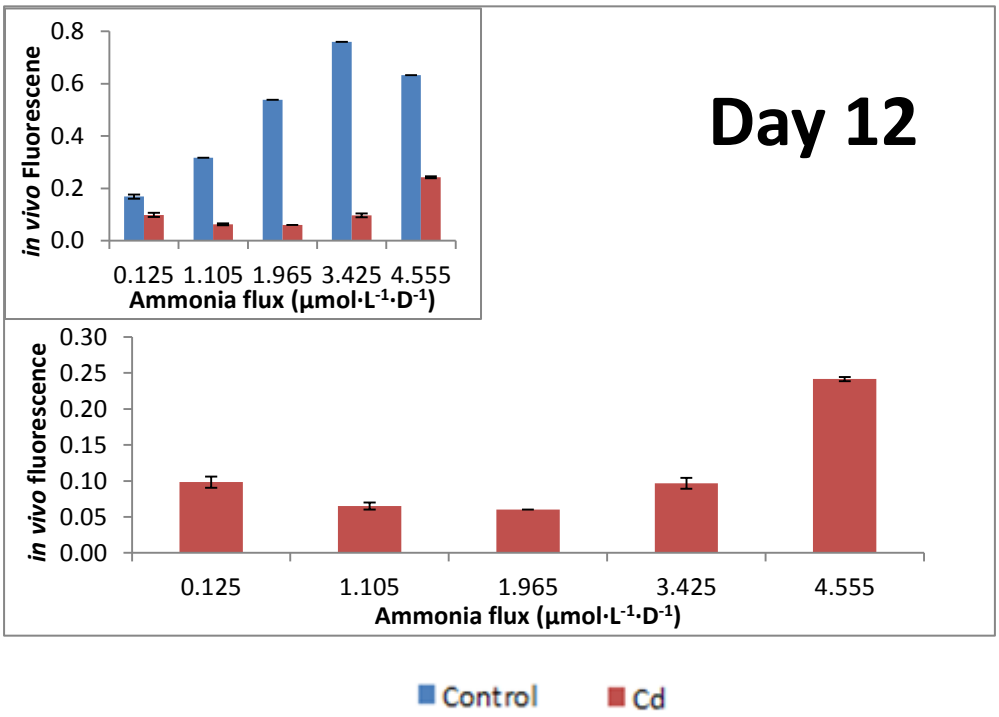

Figure 16 Mean *in vivo* fluorescence of Cd treatment samples (with Cd) at given ammonia flux. The upper left figure illustrates mean *in vivo* fluorescence in comparison between control (without Cd) and Cd treatment (with Cd) samples at given ammonia flux. The blue column represents control samples, whereas the red column shows Cd treatment samples. The given days expresses the experimental days accounting from Cd addition. Standard deviation range of each sample was presented (N=3).

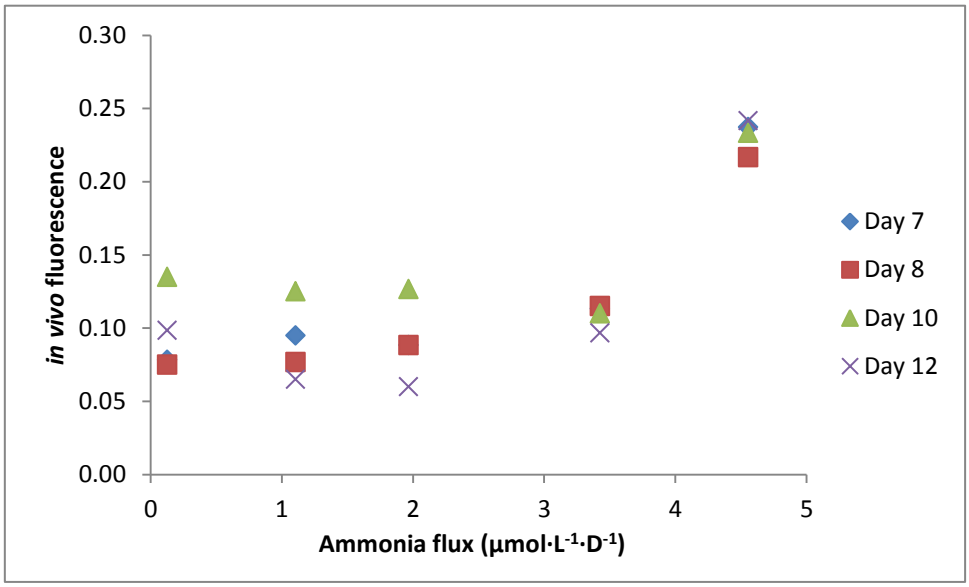

Figure 17 Summary of mean *in vivo* fluorescence value of treatment samples (with Cd) at given ammonia flux on each sampling day. The given days expresses the experimental days accounting from Cd addition.

Table 4 Statistical evaluation of in vivo fluorescence mean value compared among each ammonia flux on experimental day 7, 8, 10 and 12. (Parametric *ANOVA* test)

	P	**Evaluation**
Day 7	2.95E-8	Significant difference
Day 8	5.22E-6	Significant difference
Day 10	1.75E-10	Significant difference
Day 12	1.1E-11	Significant difference

5.3 Instantaneous chlorophyll fluorescence

Instantaneous chlorophyll fluorescence (Ft) results were presented in Appendix C. There was no duplicate during Ft measurement.

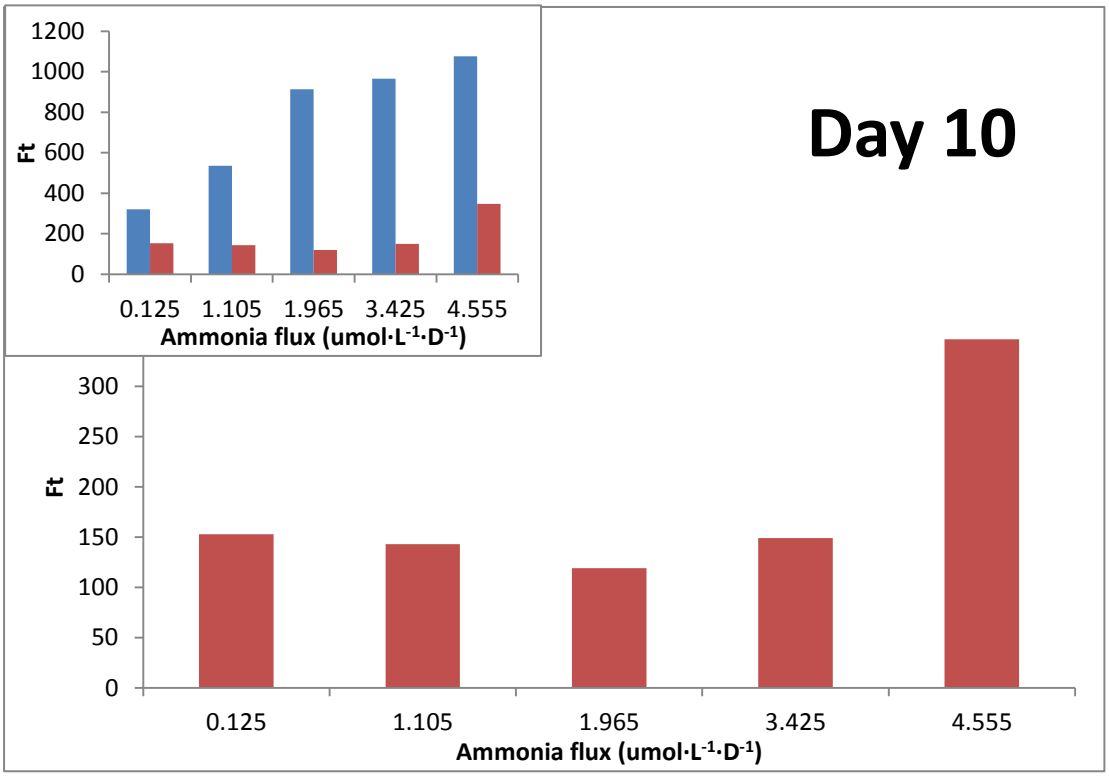

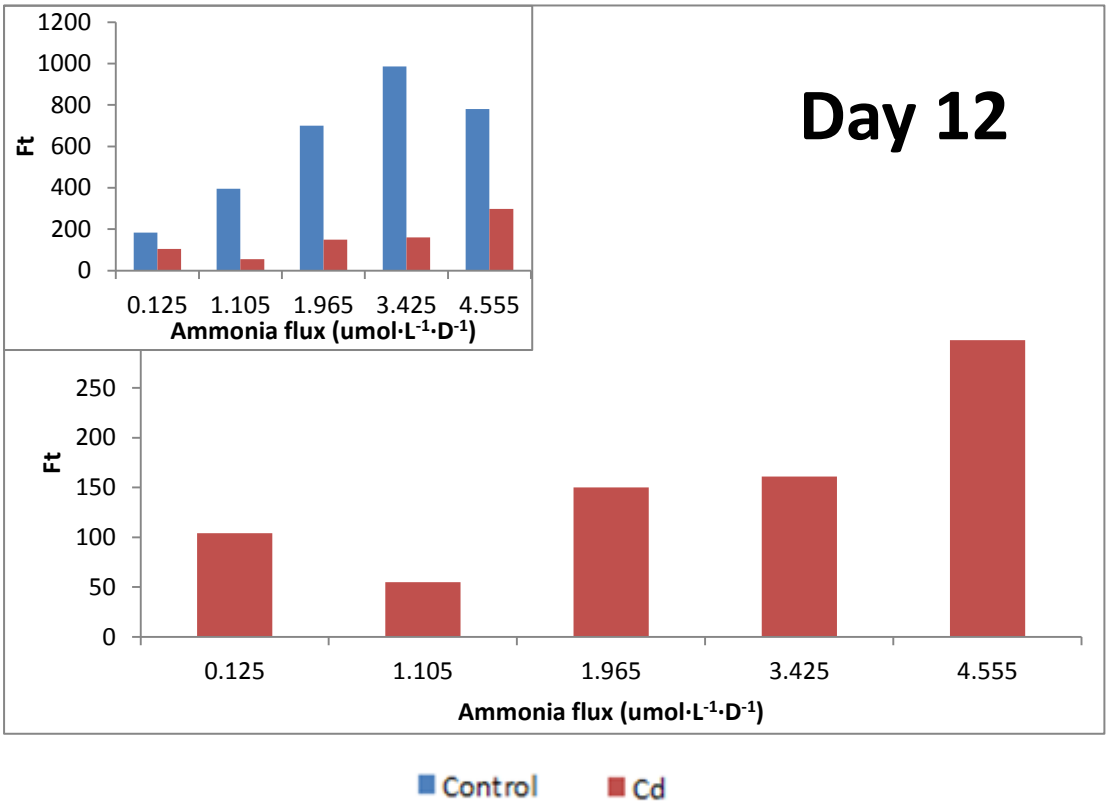

Figure 18 Instantaneous chlorophyll fluorescence (Ft) of treatment samples (with Cd) at given ammonia flux. The upper left figure illustrates Ft values compared between control (without Cd) and treatment (with Cd) samples at given ammonia flux. The blue column represents control samples, whereas the red column shows Cd treatment samples. The given days expresses the experimental days accounting from Cd addition.

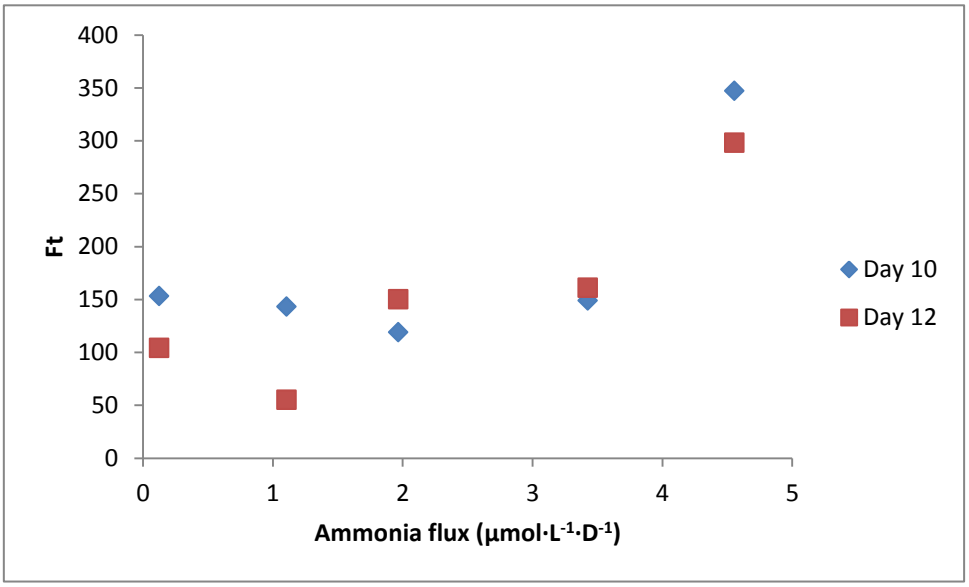

Figure 19 Summary of instantaneous chlorophyll fluorescence (Ft) values of treatment samples (with Cd) at given ammonia flux on each sampling day. The given days expresses the experimental days accounting from Cd addition.

Ft of control treatment (without Cd) was significant higher than Cd treatment (with Cd) on each sampling day (*p* value equaled 0.0046 and 0.0152 in day 10 and day 12, respectively) (Figure 18). Ft of Cd treatment samples did not show considerably changes with ammonia increase at low ammonia flux, whereas Ft was dramatically increased at the highest ammonia flux (Figure 19). Ft of Cd treatment was reduced about two third when ammonia flux was 1.105 $\mu mol \cdot L^{-1} \cdot D^{-1}$ in day 12. Since quantum yield (QY) of this sample was below instrument detection limit, the sample had to be calculated after concentration rather directly measured. This point could be assumed as error due to instrument or personal performance errors.

The changing trend of Ft of Cd treatment with ammonia flux was match to *in vivo* fluorescence results. Therefore phytoplankton production of Cd treatment was stimulated at high ammonia flux, which indicated Cd had less toxic at high ammonia flux compared to low ammonia flux.

5.4 Chlorophyll *a*

Chlorophyll-*a* concentration was calculated from extracted chl-*a* fluorescence equation (1). The extracted chl-*a* concentration data was presented in Appendix D. Every sample was taken two duplicates.

Chl-*a* concentration of control treatment (without Cd) were significant higher than Cd treatment samples (p = 0.039) (Figure 20). Chl-*a* concentration of Cd treatment significantly differenced in comparison among different ammonia flux (p = 2.45E-06, see Table 5). The samples contained lower Chl-*a* concentration at lower ammonia flux, and it was obviously increased at higher ammonia flux.

Table 5 Statistical evaluation of Chlorophyll-a mean value compared among each ammonia flux in experimental Day 12. (Parametric ANOVA test)

	P	**Evaluation**
Day 12	2.45E-6	Significant difference

Chl-*a* concentration values of Cd treatment showed the same trend as *in vivo* fluorescence and Ft results, especially the increasing trend of biological parameters was the most obvious in the last sampling day (day 12). These results indicated that high ammonia flux positively reduce Cd toxicity on phytoplankton.

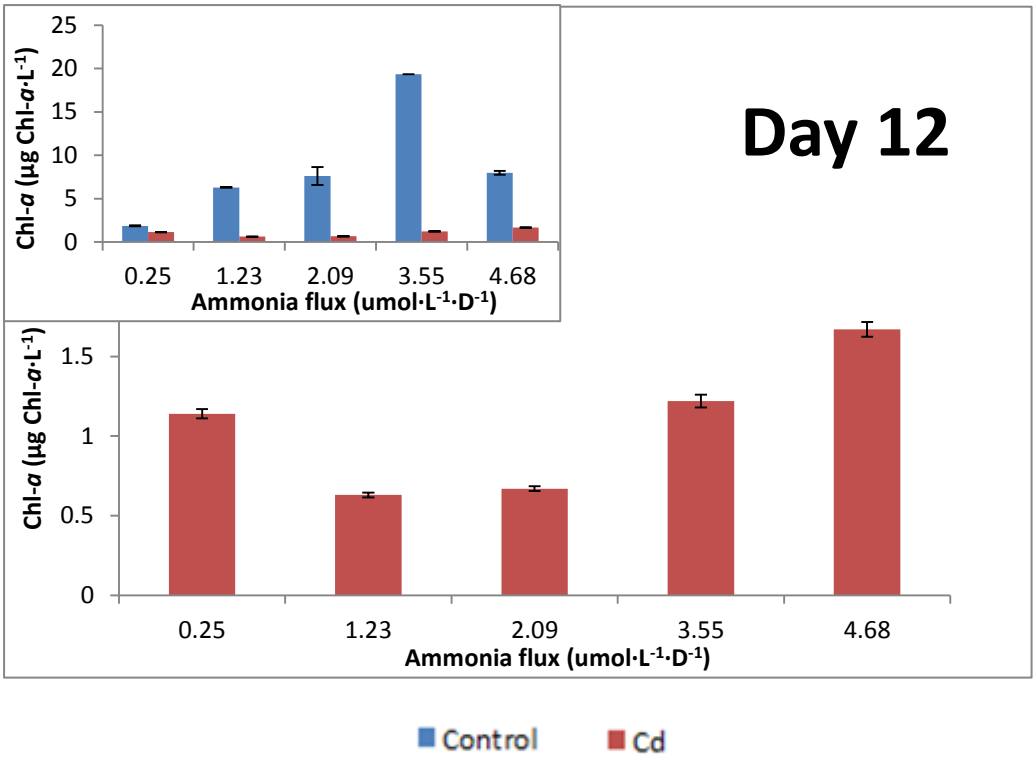

Figure 20 Mean Chlorophyll *a* (Chl-*a*) of Cd treatment samples (with Cd) at given ammonia flux. The upper left figure illustrates Chl-*a* mean values compared between control (without Cd) and treatment (with Cd) samples at given ammonia flux. The blue column represents control samples, whereas the red column shows Cd treatment samples. The given days expresses the experimental days accounting from Cd addition. Standard deviation range of each sample was presented (N=2).

5.5 Cd calibration curve of ASV

The ASV results including voltammetric scans figures and scanned peaks data were presented in Appendix E. The calibration curves were derived by plotting known added Cd concentration (µmol·L^{-1}) against measured ASV peak height (µA).

The calibration curve of control treatment (without Cd) contained completely two different slopes compared low and high Cd concentration addition. The

peak height was slightly increased with low Cd concentration addition, while it was significantly increased with high Cd concentration addition. Such nonlinear increase of calibration curve slopes of control treatment (without Cd) indicated that the ASV labile Cd in high Cd concentration addition was higher than in low Cd concentration addition. It could be explained as either organic complexation or colloidal cadmium-hydroxide formation adsorbed by voltammetric cell, or mixture (Mikkelsen, et al., 2006). Once the whole available dissolved ligands were complexed by added Cd, the ASV labile Cd was detectable and the peak heights were linear increased with Cd addition.

The calibration curve of Cd treatment (with Cd) was completely different with control treatment. The peak heights were linear increased with Cd concentration addition. Those results illustrated that the whole available organic ligands were complexed by existed Cd in samples due to previous treatment addition (added 2 $\mu mol \cdot L^{-1}$ Cd in first experimental day).

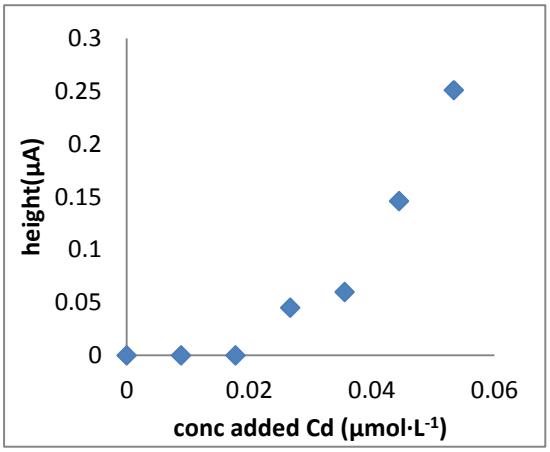

(a1)

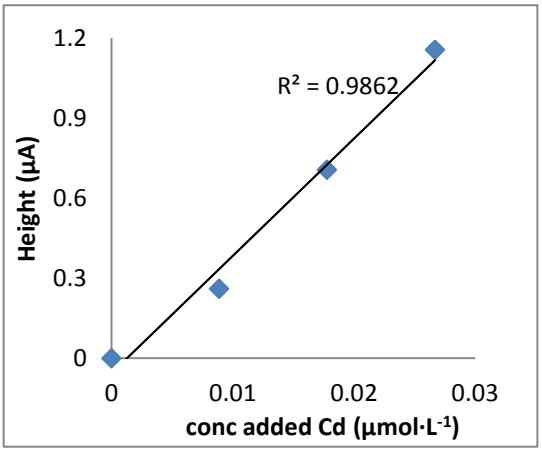

(a2)

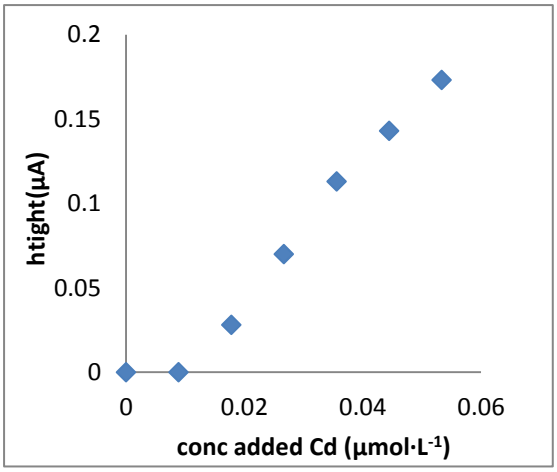

(b1)

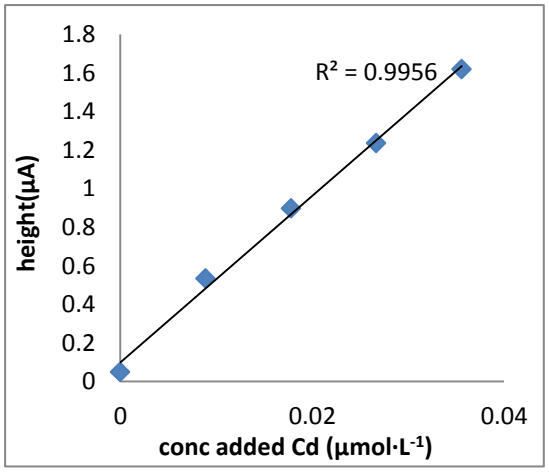

(b2)

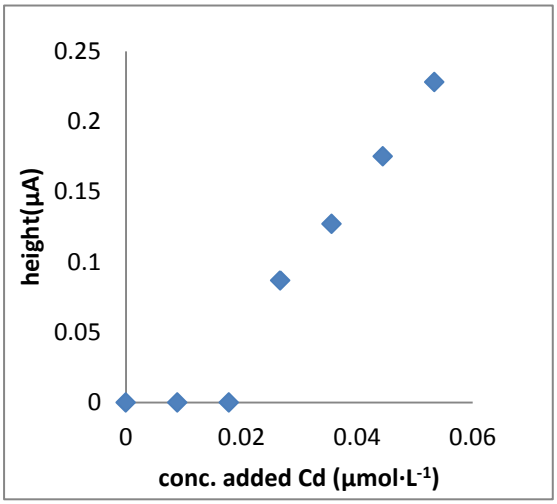

(c1)

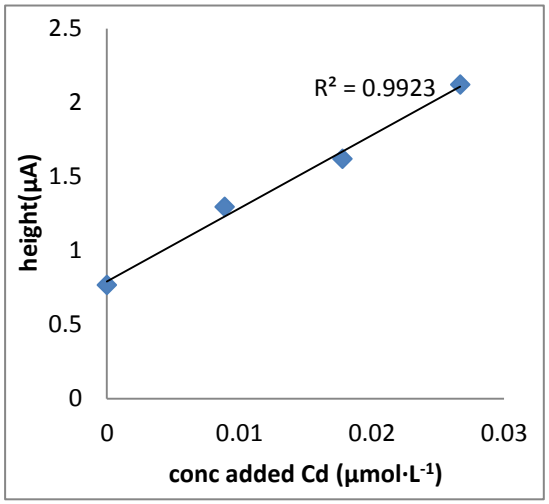

(c2)

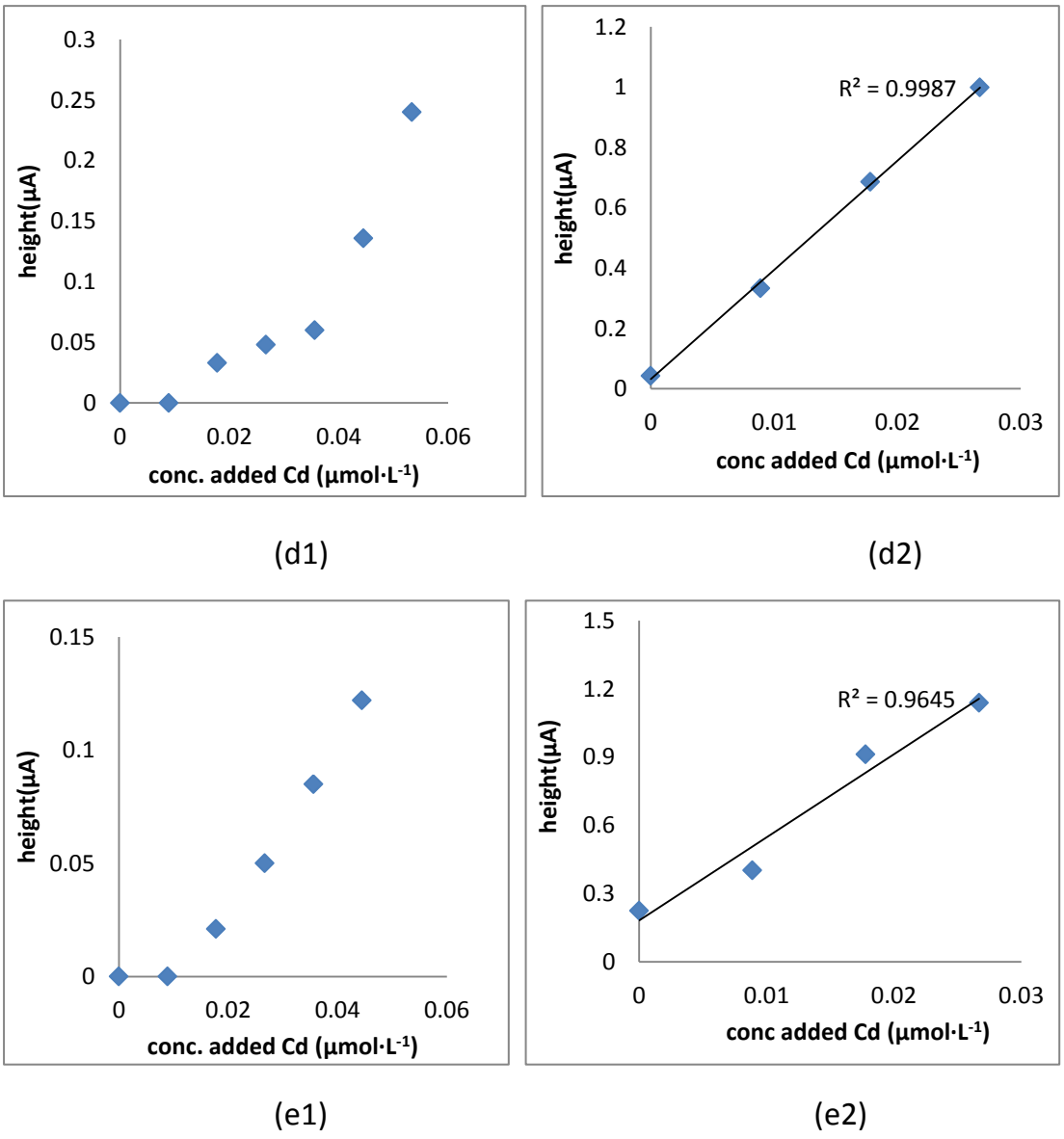

Figure 21 Calibration curve of Cd in control (without Cd) and Cd treatment (with Cd) samples in experimental day 5. Figures with subtitle 1 (left column) represented control samples (deposition time 900 s), whereas figures with subtitle 2 (right column) represented Cd treatment sample (deposition time 60 s). Subtitles a, b, c, d, e were presented ammonia flux at 0.125, 1.105, 1.965, 3.425, 4.555 µmol·L^{-1}·D^{-1}, respectively. The height (relative peak height) is the current difference between the original and the top of peak form the base line. The height was assumed as 0 if there was no peak appeared during voltammetric scan.

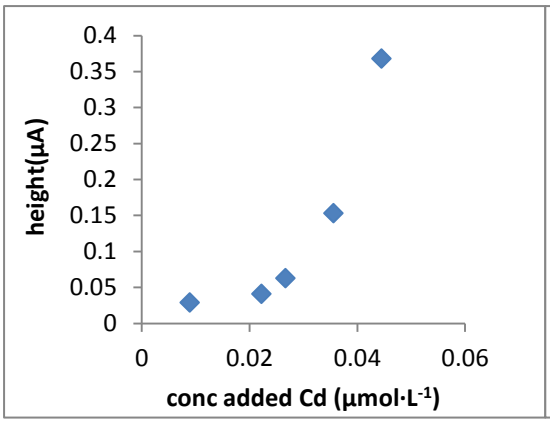

(a1)

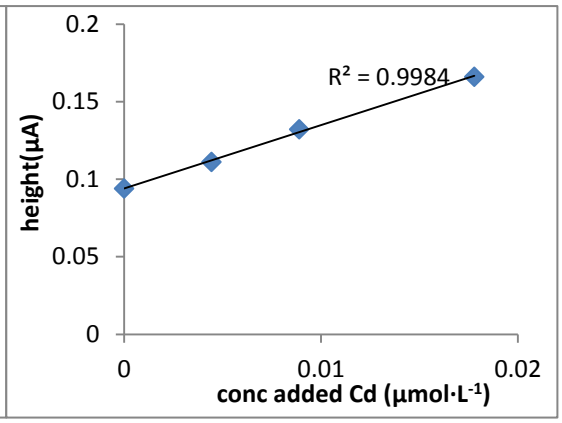

(a2)

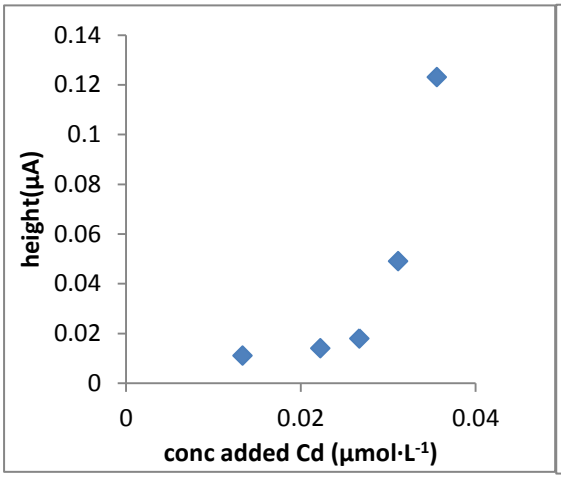

(b1)

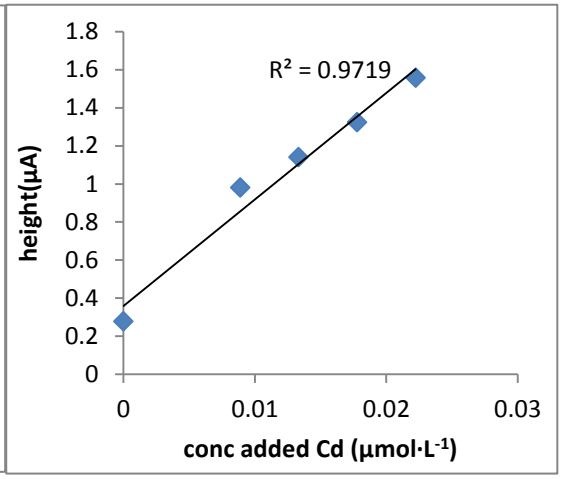

(b2)

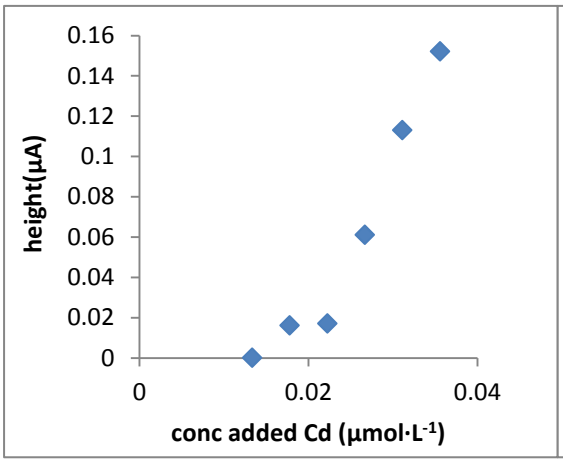

(c1)

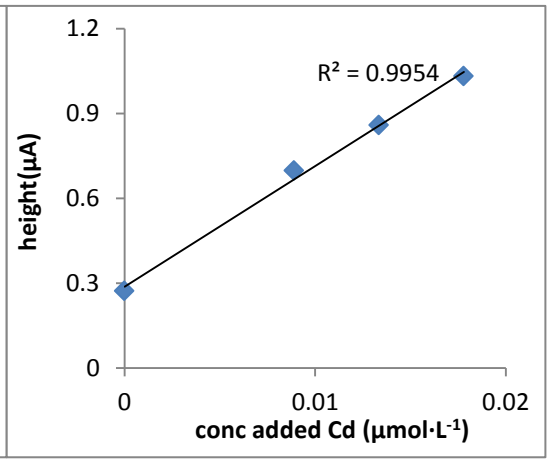

(c2)

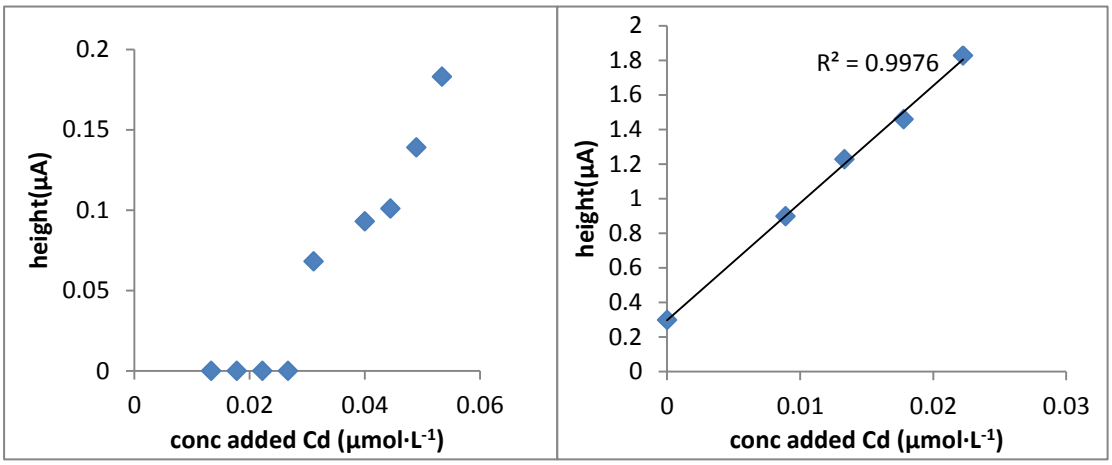

(d1) (d2)

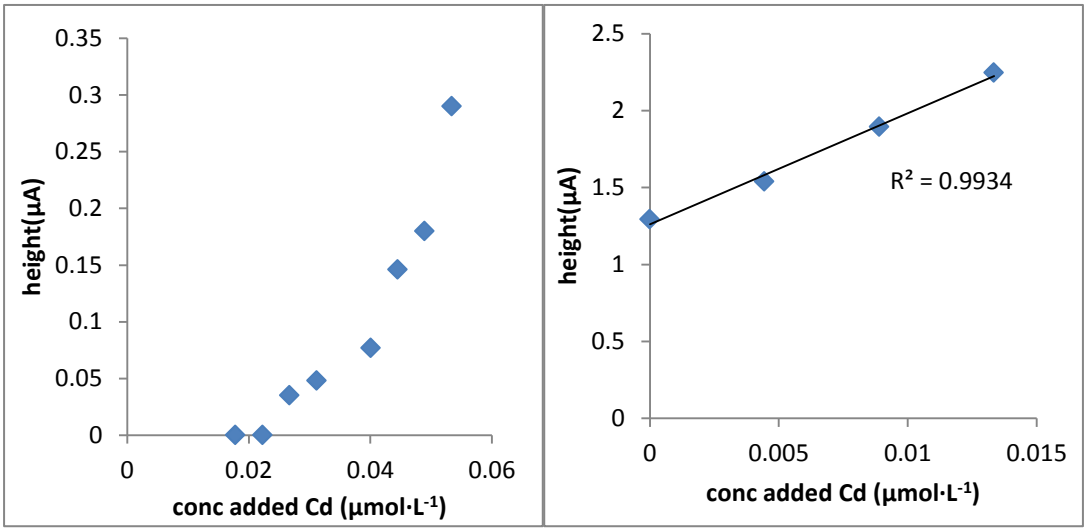

(e1) (e2)

Figure 22 Calibration curve of Cd in control (without Cd) and Cd treatment (with Cd) samples in experimental day 12. Figures with subtitle 1 (left column) represented control samples (deposition time 900 s), whereas figures with subtitle 2 (right column) represented Cd treatment sample (deposition time 120 s). Subtitles a, b, c, d, e were presented ammonia flux at 0.125, 1.105, 1.965, 3.425, 4.555 µmol·L^{-1}·D^{-1}, respectively. The height (relative peak height) is the current difference between the original and the top of peak form the base line. The height was assumed as 0 if there was no peak appeared during voltammetric scan.

5.6 DGT labile Cd concentration

The calculated results of time-average DGT labile Cd concentration are presented in appendix F. There were two duplicates in day 8 and three duplicates in day 12.

DGT labile Cd concentration of control treatment (without Cd) was lower approximately 1000 times than Cd treatment (with Cd). The units of time-average DGT labile Cd concentration of control treatment was $nmol \cdot L^{-1}$, whereas the units of Cd treatment was $\mu mol \cdot L^{-1}$ (Figure 23 and Figure 24). The trend of DGT labile Cd concentration of control treatment with ammonia flux in day 8 was obviously unlike as day 12 (Figure 23 and Figure 24). Additionally, the DGT labile Cd concentration of control samples in day 8 was up to approximately 12 $nmol \cdot L^{-1}$, while it was only up to 1.2 $nmol \cdot L^{-1}$ in day 12. Those approximately 10 times differences of DGT labile Cd concentration of control samples between day 8 and day 12, might be due to contamination was happened during experimental process. The huge standard deviation also illustrated that contamination was the main reason resulting such irregular trend of DGT Cd labile concentration of control treatment.

DGT Cd labile concentration of Cd treatment in day 8 was linear (R^2=0.974) decreased with ammonia flux increasing (Figure 23). Regarding the definition of DGT labile metals, this result indicated that free Cd cation and

Cd-organic/inorganic ligands complexes in seawater was linear reduced due to high ammonia. Since the mass balance of Cd, Cd was either accumulated by phytoplankton or existing in seawater as free Cd cation and complexes. Thus we could assume that there was more Cd uptake by phytoplankton at high ammonia level. Wang and Dei (2001) have reported that Cd uptake by marine phytoplankton community could be stimulated by high ambient nitrogen concentration(Wang and Dei, 2001a, Wang and Dei, 2001b).

However, DGT labile Cd concentration in day 12 was decreased at lower ammonia flux, while DGT labile Cd concentration was raised at the highest ammonia flux (Figure 24). These results demonstrated that the Cd accumulation by phytoplankton was increased at lower ammonia flux, while accumulated Cd was decreased at higher ammonia flux. And such regulations have been proved by Hunnestad from another WAFOW experiment (unpublished master thesis, Hunnestad, 2012). She found Cd amount per particular organic carbon (POC) reached the peak at the medial ammonia level.

The difference profile of DGT labile Cd concentration between day 8 and day 12 indicated that exposure time might be another factor affecting Cd toxicity on phytoplankton at high ammonia flux, since our finding from day 8 was not as same as day 12. It might be due to either phytoplankton may require longer

time to detoxify the accumulated Cd, or phytoplankton community in Hopavågen, Norway, has less tolerance to high Cd concentration.

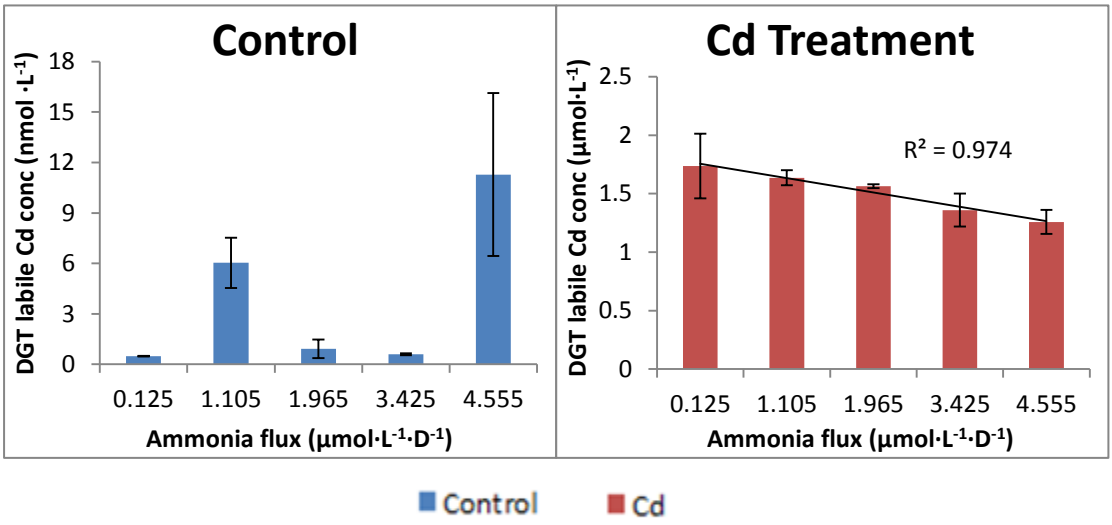

Figure 23 Time average DGT labile Cd concentration at gradient increasing ammonia flux of control (without Cd) and Cd treatment (with Cd) samples in the first sampling day (Day 8).

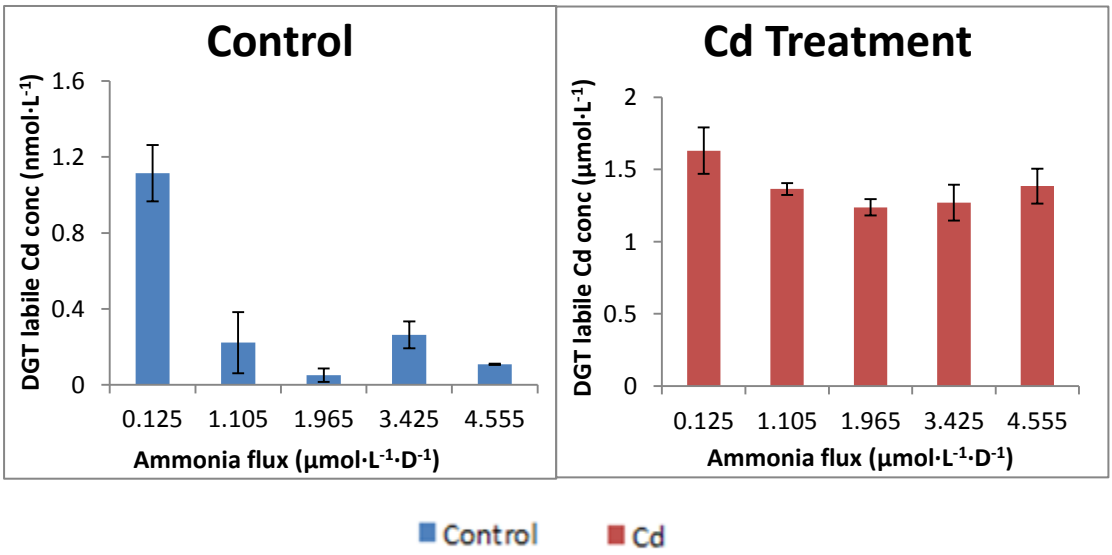

Figure 24 Time average DGT labile Cd concentration at gradient increasing ammonia flux of control (without Cd) and Cd treatment (with Cd) samples in the second sampling day (Day 12).

5.7 Cd complexation capacity

Cd complexation capacity determination consisted of Cd complexation capacity of control treatment (without Cd) and Cd treatment (with Cd). The results were presented in Appendix G.

5.7.1 The effects of ammonia to Cd complexation capacity of natural seawater

Cd complexation capacity of control treatment (without Cd) was graphically determined from ASV calibration curve, and it ranged from 0.01 to 0.035 $\mu mol \cdot L^{-1}$ (Figure 25). Determined Cd complexation capacity in surface seawater in Hopavågen, Norway, was as similar as previous studies in other geophysical sites. For instance, Zhang (1990) determined Cd complexation capacity of surface seawater in the South China Sea, and it ranged from 0.01-0.09 $\mu mol \cdot L^{-1}$. Omanovic, et al. (1996) also studies Cd complexation capacity in Pacific Ocean, and it was around 0.05 $\mu mol \cdot L^{-1}$. Different physiochemical factors might dominate such small difference between our result and previous data, such as temperature and biota amounts.

Besides, the interactions between ammonia flux and Cd complexation capacity of control treatment (without Cd) have been studied (Figure 25). There was no considerable difference of Cd complexation capacity at lower ammonia flux, whereas it was increased at higher ammonia flux. Additionally, Cd complexation capacity was reached the maximum at the second highest

ammonia flux. There was a slight reduction at the highest ammonia flux compared to the second highest. Therefore, these results illustrated the amount of organic ligands released by phytoplankton was increased at high ammonia flux. Moreover, Ardelan et al. found high ammonia level even can modify the molecular structure of DOM. The production N and S contained in DOM molecules significantly increased from 7 and 3 % in the initial water to 47.4 and 15.5 % in the treatment with highest ammonia flux, respectively (unpublished data, Ardelan, et al.).

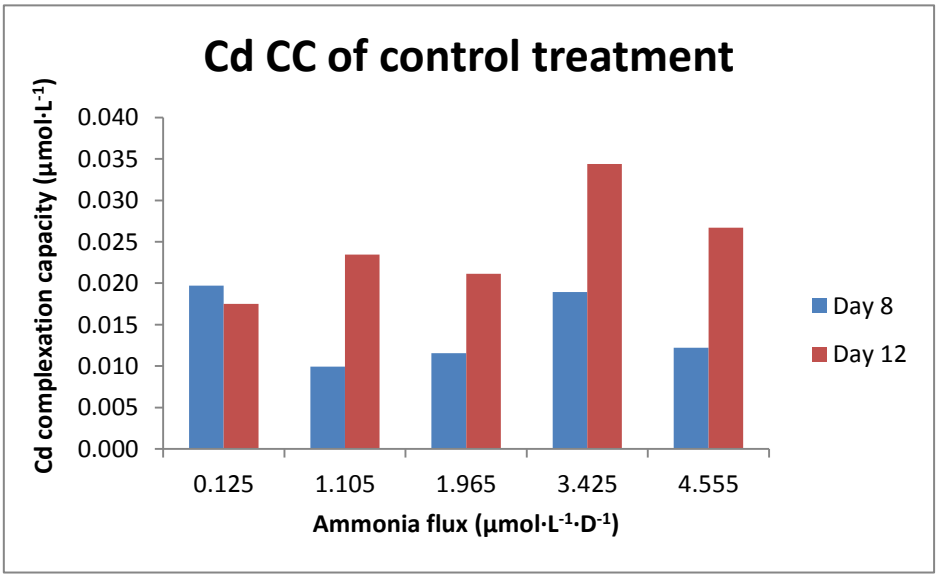

Figure 25 Cd complexiation capacity of control treatment (without Cd) at given ammonia flux on each sampling day. The given days expresses the experimental days accounting from Cd addition.

5.7.2 Cd complexiation capacity after high Cd exposure

Cd complexation capacity of Cd treatment (with Cd) in surface seawater was graphically determined according to the equation (4). And the calculated data and the determination figures were presented in Appendix G.

Cd complexation capacity of surface seawater after high Cd level exposure ranged from 1.96 to 2.04 µmol·L-1 (Figure 26), which was approximately 100-fold higher than Cd complexation capacity of control treatment (without Cd) (Figure 25). Cd complexation capacity indeed illustrates the available ligands concentration in seawater which can complex with free Cd. That is to say, the amount of bioavailable organic ligands released by phytoplankton was significantly increased due to high Cd level exposure. The metal complexation with organic ligands in seawater is able to affect the bioavailable metal concentration (Guan, 2006). Such spontaneous biological response from phytoplankton is to adapt toxic surroundings (Scharek, et al., 1997).

There was obvious difference of Cd complexation capacity and stability constant of Cd treatment with different ammonia flux in day 8 and day 12 (Figure 26). It appeared that there were more organic ligands released by phytoplankton at higher ammonia flux in day 8. Regarding to the equilibrium expression of stability constant, K should be expected to decrease at high ammonia flux due to increasing organic ligand concentration, if we do not consider the contributions from Cd-organic complexes and free Cd cation.

However in this case, stability constant of Cd at higher ammonia flux was surprisingly increased. Then the only explanation to achieve such results is that Cd-organic complexes concentration was increased or the free Cd cation was decreased or mixture.

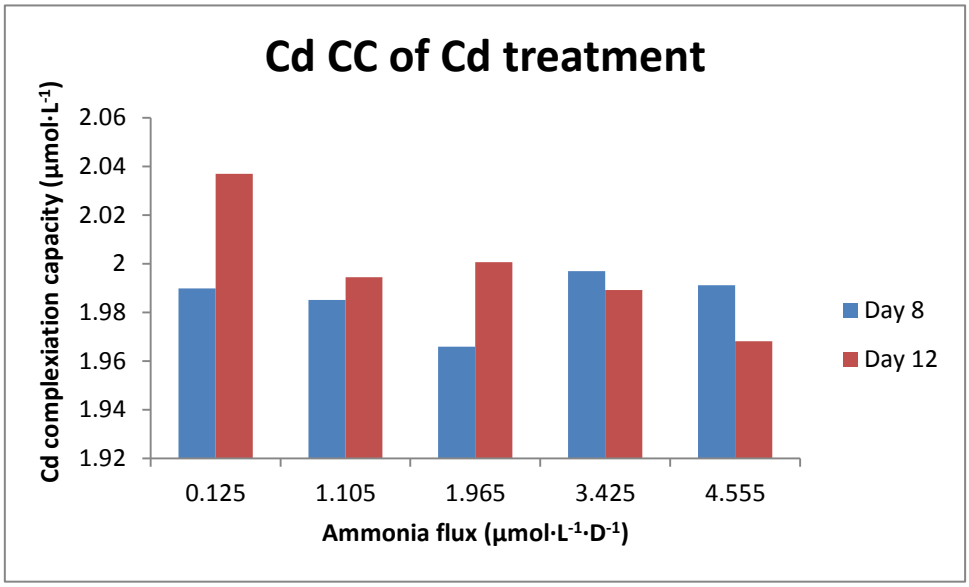

Figure 26 Cd complexation capacity of Cd treatment (with Cd) at different ammonia flux on each sampling day.

Cd complexation capacity of Cd treatment in day 12 was decreased with increasing ammonia flux. Moreover, DGT results in day 12 shown the Cd-organic complexes and free Cd cation was decreased at low ammonia flux. Thus, it was hard to predict K according to the definition of stability constant. Our results shown that K was increased at low ammonia flux, which indicated the reduction of organic ligands dominated the chemical reaction. Additionally, K was decreased at high ammonia flux, which could be mathematically explained by the equilibrium expression of stability constant, since DGT labile

Cd concentration was increased and organic ligands was decreased at high ammonia flux.

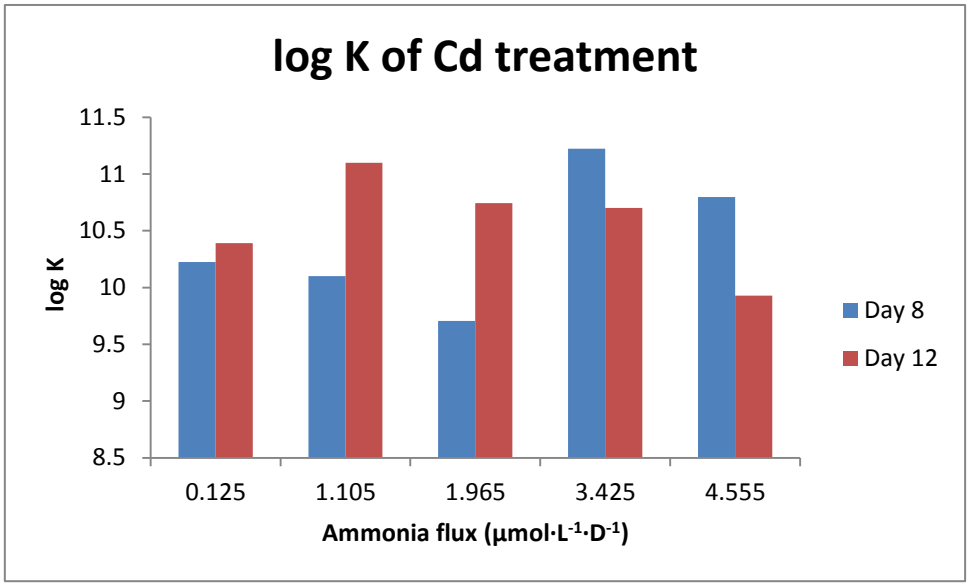

Figure 27 Stability constant (log K) of Cd treatment (with Cd) at different ammonia flux on each sampling day.

5.8 The interactions between ammonia and Cd toxicity on phytoplankton

Strong interactions between ammonia and Cd toxicity on phytoplankton have been studied in this thesis (Figure 28). The results of *in vivo* fluorescence, Ft and Chlorophyll-*a* indicated that the biomass of phytoplankton was decreased at lower ammonia flux, and it was significantly increased at higher ammonia flux, although the samples were exposed under high Cd concentration. Therefore, high ammonia flux may positively affect (decrease) Cd toxicity on phytoplankton in marine system. In addition, Miao and Wang (2006) studied the interaction between Cd uptake and nitrite (NO_3^-) by specific phytoplankton

species in laboratory. And the same conclusions had been proved by diatom *T. weissfloggi* and the dinoflagellate *P. minimum* (Miao and Wang, 2006). And this thesis found ammonia might be another nitrogen source to affect Cd uptake by marine phytoplankton.

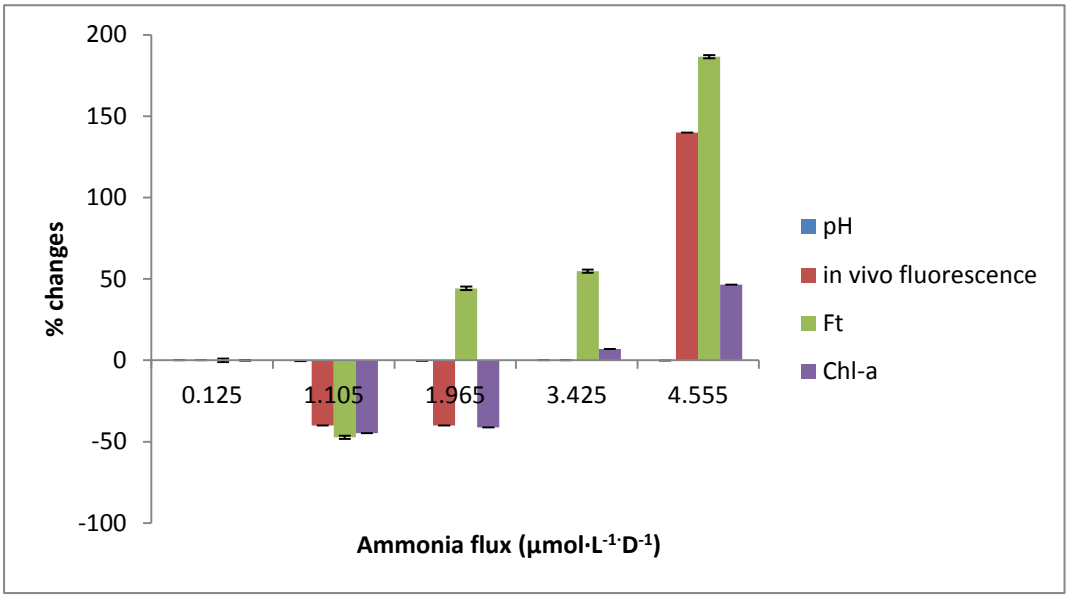

Figure 28 The change percentage of phytoplankton biomass parameters of Cd treatment (with Cd) at different ammonia flux on the last sampling day (Day 12). The result of parameters at 0.125 µmol·L^{-1}·D^{-1} ammonia flux was the base line.

It is surprise that Cd had less toxicity at high ammonia flux, although there were more accumulated Cd in phytoplankton cells. There might be some unclear detoxify mechanisms. For instance, the phytochelatins might play an important role in Cd detoxification by phytoplankton (Wang, 2010). However the phytochelatin data is rarely and its understandings are still unknown. Since N is the essential component for protein, phytoplankton might stimulate protein synthesis to somehow generate specific enzymes which can either

adjust Cd existing form or change the molecular functions. Accumulated Cd might be directly or indirectly redox or complex by enzyme to form non-toxic or less toxic molecules. It is also possible that Cd is able to continue acting nutrient-like characteristics even under high Cd exposure.

So far, the mechanisms of how ammonia affects Cd toxicity on phytoplankton (such as the Cd uptake pathway and the Cd detoxification) are not clear. Throughout the results of this thesis, the Cd complexation with organic ligands and Cd complexation capacity were modified by high ammonia. Therefore, the reduction of Cd toxicity on phytoplankton by high ammonia might be due to either unknown intercellular/subcellular detoxification processes can be somehow stimulated by high ammonia, or DOM released from phytoplankton can be affected. The molecular structure of DOM in seawater is able to shift from carbon-dominated to N- and S-dominated by high ammonia discharge (unpublished data, Ardelan, Rosel, Irriarte, et al.). Then the molecular structure changing of DOM may continually influence the metal organic complexation, which probably affects the bioavailability and toxicity of metals in seawater (Murat V. Ardelan, personal communication).

6. Conclusions

The interaction between ambient ammonia and Cd toxicity on phytoplankton has been studied in this thesis. Phytoplankton production decreased after high Cd exposure at low ammonia flux, while the Cd toxicity on phytoplankton was decreased at high ammonia flux.

Cd complexation capacity in surface seawater after high Cd exposure was significantly increased than normal seawater. Therefore, phytoplankton produced significant large amount of DOM in high Cd level.

Ammonia also impact Cd complexation capacity after high Cd exposure. However whether ammonia positively or negatively affect Cd complexation capacity was not clear in this thesis

7. Future work

DOM is important to predict Cd toxicity on marine system. Although the effects of ammonia on the molecular structure of DOM have been studied, the structural character and composition of Cd-complexing organic ligands are still not clear. And whether Cd toxicity is affected by the some specific DOM species should also be listed in the future work.

Cd toxicity on phytoplankton can be decreased by high NH_4 has been proved in this thesis. And the interaction between NH_4 and Cd accumulation has been studied by another relevant WOFOW project. However, although the accumulated Cd amount is affected by NH_4, whether NH_4 affect Cd accumulation pathway by phytoplankton is still unclear. Since we found the Cd was less toxic to phytoplankton even through accumulated Cd was still increasing. Such conflicts demonstrated there might be some subcellular detoxification mechanisms which are still unknown.

The influences of NH_4 on Cd accumulation, bioavailability or toxicity are highly biological species specific. My thesis only generally estimated the effects on field marine phytoplankton communities. Therefore, it is still necessary to certain the influences on specific phytoplankton species.

Reference

Anderson, M. A. and F.M.M. Morel. *Limnol. Oceanogr.* 1982.

Ardelan, M. V., E. Steinnes, S. Lierhagen, and S. O. Linde. "Effects of Experimental Co2 Leakage on Solubility and Transport of Seven Trace Metals in Seawater and Sediment." [In eng]. *Sci Total Environ* 407, no. 24 (Dec 1 2009): 6255-66.

Badger, M. "The Roles of Carbonic Anhydrases in Photosynthetic Co2 Concentrating Mechanisms." *Photosynth. Res.* 77 (2003): 83-94.

Bain, R. C. "Algal Growth Assessments by Fluorescence Techniques." Paper presented at the Proc. Eutrophication-Biostimulation Assessment Workshop, Corvallis, OR, 1969.

Bruland, K. W., Knauer, G. A., Martin, J. H. "Cadmium in Northest Pacific Waters." *Limnol. Oceanogr.* 23 (1978): 618-25.

Buffle, J., R. S. Altmann, M. Filella. "Complexaion by Natural Heterogeneous Compounds: Site Occupation Distribution Functions." *Geochemical et Cosmochimca Acta* 54 (1990): 1535-53.

Cox, E. H. "The Active Site Structure of Thalassiosira Weissflogii Carbonic Anhydrase ". *Biochemistry* 39, no. 12128-12130 (2000).

De Schamphelaere, K. A. C., J. L. Stauber, K. L. Wilde, S. J. Markich, P. L. Brown, N. M. Franklin, N. M. Creighton, and C. R. Janssen. "Toward a Biotic Ligand Model for Freshwater Green Algae: Surface-Bound and Internal Copper Are Better Predictors of Toxicity Than Free Cu2+-Ion Activity When Ph Is Varied." *Environmental Science & Technology* 39, no. 7 (Apr 1 2005): 2067-72.

Di Toro, D. M., H. E. Allen, H. L. Bergman, J. S. Meyer, P. R. Paquin, and R. C. Santore. "Biotic Ligand Model of the Acute Toxicity of Metals. 1. Technical Basis." *Environmental Toxicology and Chemistry* 20, no. 10 (Oct 2001): 2383-96.

Falkowski, P. G. "The Evolution of Modern Eukaryotic Phytoplankton." *Science* 305, no. 354-360 (2004).

Field, C. B., M. J. Behrenfeld, J. T. Randerson, and P. Falkowski. "Primary Production of the Biosphere: Integrating Terrestrial and Oceanic Components." *Science* 281, no. 5374 (Jul 1998): 237-40.

Francis, A.J. "Biomediation of Contaminated Soil." *Agronomy Monograph* 37, USA, 239 (1999).

Govindjee. "Sixty-Three Years since Kautsky : Chlorophyll a Fluorescence." *Aust. J. Plant. Physiol* 22 (1995): 131-60.

Gowen, R. J. "Managing Eutrophication Associated with Aquaculture Development." [In English]. *Journal of Applied Ichthyology-Zeitschrift Fur Angewandte Ichthyologie* 10, no. 4 (Dec 1994): 242-57.

Grill, E., E.L. Winnacker, M. H. Zenk. "Science." 230 (1985): 674.

Guan, R. "Bioavailability and Toxicity of Trace Metals to the Cladoceran Daphnia Magna in Relation to Cd Exposure History." Hong Kong University of Science and Technology, 2006.

Hassler, C. S., V. I. Slaveykova, and K. J. Wilkinson. "Some Fundamental (and Often Overlooked) Considerations Underlying the Free Ion Activity and Biotic Ligand Models." *Environmental Toxicology and Chemistry* 23, no. 2 (Feb 2004): 283-91.

Hirn, J., H. Viljamaa, and M. Raevuori. "Effect of Physicochemical, Phytoplankton and Seasonal Factors on Fecal Indicator Bacteria in Northern Brackish Water." [In English]. *Water Research* 14, no. 3 (1980): 279-85.

Hirose, Katsumi. "Chemical Speciation of Trace Metals in Seawater: A Review." *Analytical Sciences* 22 (2006): 1055-63.

IVIUM TECHNOLOGIES. "Http://Www.Ivium.Nl/Welcome."

Kasuya, M., Terainisha, H., Aoshima, K., Katon, T., Horiguchi, H., Morikawa, Y, Nishijo, M. and Iwata, K. "Water Pollution by Cadmium and the Onset of 'Itai-Itai' Disease." *Water and Science and Technology* 26 (1992): 149-56.

Koval, S. F. and T. J. Beveridge. *Encyclopedia of Microbiology*. edited by J. Lederberg San Diego: Academic Press, 1999.

Lane, T. W. "A Cadmium Enzyme from a Marine Diatom." *Nature* 435 (2005): 42.

Lane, T. W, Morel, F. M. M. "A Biological Function for Cadmium in Marine Diatoms." *Proc. Natl Acad. Sci. USA* 97 (2000): 4627-31.

Manivannan, A., R. Kawasaki, D. A. Tryk, and A. Fujishima. "Interaction of Pb and Cd During Anodic Stripping Voltammetric Analysis at Boron-Doped Diamond Electrodes." [In English]. *Electrochimica Acta* 49, no. 20 (Aug 30 2004): 3313-18.

Mantoura, R. F. C. *Marine Organic Chemistry*. Amsterdan: Elsevier, 1981.

Miao, A. J., and W. X. Wang. "Cadmium Toxicity to Two Marine Phytoplankton under Different Nutrient Conditions." [In English]. *Aquatic Toxicology* 78, no. 2 (Jun 15 2006): 114-26.

Mikkelsen, O., C. M. G. van den Berg, and K. H. Schroder. "Determination of Labile Iron at Low Nmol L-1 Levels in Estuarine and Coastal Waters by Anodic Stripping Voltammetry." [In English]. *Electroanalysis* 18, no. 1 (Jan 2006): 35-43.

Miller, J. N., J. N. Miller. *Statistic for Analytical Chemistry*. New York: Ellis Horwood PTR Prentice Hall, 1993.

Morel, F. M. M. *Principles of Aquatic Chemistry*. New York: Wiley, 1983.

Morel, F. M. M., and N. M. Price. "The Biogeochemical Cycles of Trace Metals in the Oceans." *Science* 300, no. 5621 (May 2003): 944-47.

Morel, F.M. M. "Zinc and Carbon Co-Limitation of Marine Phytoplankton." *Nature* 344 (1994): 658-60.

Mosulen, S., M. J. Dominguez, J. Vigara, C. Vilchez, A. Guiraum, and J. M. Vega. "Metal Toxicity in Chlamydomonas Reinhardtii. Effect on Sulfate and Nitrate Assimilation." [In English]. *Biomolecular Engineering* 20, no. 4-6 (Jul 2003): 199-203.

Olsen, S. Agusti, T. Andersen, C. M. Duarte, J. M. Gasol, I. Gismervik, A. S. Heiskanen*, et al.* "A Comparative Study of Responses in Planktonic Food Web Structure and Function in Contrasting European Coastal Waters Exposed to Experimental Nutrient Addition." *Limnology and Oceanography* 51, no. 1 (Jan 2006): 488-503.

Olsen, L. M., Ozturk, M., Sakshaug, E., Johnsen, G. "Photosynthesis-Induced Phosphate Precipitation in Seawater: Ecological Implications for Phytoplankton." [In English]. *Marine Ecology-Progress Series* 319 (2006): 103-10.

Olsen, Y., Olsen L. M. . "Environmental Impact of Aquaculture on Coastal Planktonic Ecosystems." In *Fisheries for Global Welfare and Environment, 5th World Fisheries Congress* edited by T. Kawamura K. Tsukamoto, T. Takeuchi, T. D. Beard, Jr. and M. J. Kaiser. 181–96, 2008.

Ozturk, M., E. Steinnes, and E. Sakshaug. "Iron Speciation in the Trondheim Fjord from the Perspective of Iron Limitation for Phytoplankton." [In English]. *Estuarine Coastal and Shelf Science* 55, no. 2 (Aug 2002): 197-212.

Photon Systems Instruments. "Aquapen-P Operation Manual."

Porrello, S., M. Lenzi, E. Persia, P. Tomassetti, and M. G. Finoia. "Reduction of Aquaculture Wastewater Eutrophication by Phytotreatment Ponds System I. Dissolved and Particulate Nitrogen and Phosphorus." [In English].

Aquaculture 219, no. 1-4 (Apr 2 2003): 515-29.

Pribil, S. and P. Marvan. "Hydrobiol. Suppl.". *Algological Studies* 49, no. 15 (1979): 214.

Rue, E. L., and K. W. Bruland. "Complexation of Iron(Iii) by Natural Organic-Ligands in the Central North Pacific as Determined by a New Competitive Ligand Equilibration Adsorptive Cathodic Stripping Voltammetric Method." [In English]. *Marine Chemistry* 50, no. 1-4 (Aug 1995): 117-38.

Saito, M. A., and J. W. Moffett. "Temporal and Spatial Variability of Cobalt in the Atlantic Ocean." [In English]. *Geochimica Et Cosmochimica Acta* 66, no. 11 (Jun 2002): 1943-53.

Sakaguchi, T. and A. Nakajima. "Mineral Bioprocessing." In *The Minerals, Metals & Materials Society*, edited by M.Misra R.W Smith. 309, 1991.

Sakshaug, E. , Ray, F. , and Ardelan, M. V. . "Seawater, Its Constituents and Chemistry." Chap. 4 In *Ecosystem Barents Sea*, edited by Egil Sakshaug. 83-116. Trondheim: Tapir Academic Press, 2005.

Sangi, M. R., M. J. Halstead, and K. A. Hunter. "Use of the Diffusion Gradient Thin Film Method to Measure Trace Metals in Fresh Waters at Low Ionic Strength." [In English]. *Analytica Chimica Acta* 456, no. 2 (Apr 8 2002): 241-51.

Scally, S., W. Davison, and H. Zhang. "In Situ Measurements of Dissociation Kinetics and Labilities of Metal Complexes in Solution Using Dgt." [In English]. *Environmental Science & Technology* 37, no. 7 (Apr 1 2003): 1379-84.

Scharek, R., M. A. VanLeeuwe, and H. J. W. DeBaar. "Responses of Southern Ocean Phytoplankton to the Addition of Trace Metals." [In English]. *Deep-Sea Research Part Ii-Topical Studies in Oceanography* 44, no. 1-2 (1997): 209-27.

Sillen, L. G. *Oceanography*. edited by M. Sears Washington DC: American Association of Advance Sciences, 1961.

Skogerboe, T.R. Copeland and R.K. *Analytical chemistry* 46, no. 1257A (1974).

Stumm, W., and P. A. Brauner. *Chemical Oceanography*. edited by J. P. Riley and G. Skirrow. 2nd ed. Vol. 1, London: Academic Press, 1975.

Sunda, W. G., and S. A. Huntsman. "Processes Regulating Cellular Metal Accumulation and Physiological Effects: Phytoplankton as Model Systems." [In English]. *Science of the Total Environment* 219, no. 2-3 (Aug 28 1998):

165-81.

Templeton, D. M., F. Ariese, R. Cornelis, L. G. Danielsson, H. Muntau, L. P van Leeuwen. "Pure Appl. Chem.". 72 (2000): 1453.

Tessier, A, Turner D. "Metal Sepeciation and Bioavailablity in Aquatic System." *John Wiley and Sons* (1995).

Trick, C. G. *Curr. Microbiol.* 1989.

Truzzi, C., L. Lambertucci, G. Gambini, G. Scarponi. "Optimization of Square Wave Anodic Stripping Voltammetry (Swasv) for the Simultaneous Determination of Cd, Pb, and Cu in Seawater and Comparison with Differential Pulse Anodic Stripping Voltammetry (Dpasv)." *Ann. Chim* 92 (2002): 313-26.

Vasconcelos, M., Leal, M., can den Berg, C. "Influence of the Nature of the Exudates Released by Different Marine Algal on the Growth, Trace Metal Uptake and Exudation of Emiliania Huxleyi in Natural Seawater." *Marine Chemistry* 77 (2002): 187-210.

Vollenweider, R. A. *A Manual on Methods for Measuring Primary Prodcution in Aquatic Environments*. Vol. 12, Oxford: Blackwell Scientific Publications, 1969.

Wang, J. *Stripping Analysis: Principles, Instrumentation and Application*. VCH Publishers, 1985.

Wang, Joseph. *Analytical Electrochemistry*. 2nd ed. Canada: A Jonh Wiley & Sons, INC, 2000.

Wang, Mengjiao. "Prediction of Cadmium Txicity in Marine Phytoplankton." the Hong Kong University of Science and Technology, 2010.

Wang, W. X., and R. C. H. Dei. "Effects of Major Nutrient Additions on Metal Uptake in Phytoplankton." *Environmental Pollution* 111, no. 2 (2001a): 233-40.

Wang, W.X., "Metal Uptake in a Coastal Diatom Influenced by Major Nutrients (N, P, and Si)." *Water Research* 35, no. 1 (Jan 2001b): 315-21.

Wang, W. X., and P. S. Rainbow. "Subcellular Partitioning and the Prediction of Cadmium Toxicity to Aquatic Organisms." [In English]. *Environmental Chemistry* 3, no. 6 (2006): 395-99.

Wells, M. *Marine Colloids and Trace Metals.* . Biogeochemistry of Marine Dissolved Organic Matter. edited by D. Carlson Hansell, C: Academic Press, 2002.

Wen, Liang-Saw, Kuo-Tung Jiann, and Peter H. Santschi. "Physicochemical Speciation of Bioactive Trace Metals (Cd, Cu, Fe, Ni) in the Oligotrophic South China Sea." *Marine Chemistry* 101, no. 1-2 (2006): 104-29.

Xu, Y., L. Feng, P. D. Jeffrey, Y. Shi, and F. M. Morel. "Structure and Metal Exchange in the Cadmium Carbonic Anhydrase of Marine Diatoms." [In eng]. *Nature* 452, no. 7183 (Mar 6 2008): 56-61.

Zhang, H. "Manual for Dgt " DGT Research Ltd.

Zhang, Manping et al. "Heavy Metal Complexation Capacity of the South China Sea Water." *CHIN.J. OCEANOL.LIMNOL.* 8 (1990): 158-66.

Öztürk, M., Steinnes, E., Sakshaug, E. "Iron Speciation in the Trondheim Fjord from the Perspective of Iron Limitation for Phytoplankton ". *Estuarine, Coastal and Shelf Science* 55, no. 2 (2002): 197-212.

Appendix A pH

The measured pH values were shown below. The results were obtained by Titralab 860 (Radiometer Analytical SAS). Each sample was measured two duplicates. Additionally, pH was corrected corresponding to room temperature (18 °C).

Table 6 pH value of each duplicate of control treatment (without Cd) in experimental day 7, 8, 10 and 12, respectively

NH4 ($\mu mol \cdot D^{-1} \cdot L^{-1}$)	0.125	1.105	1.965	3.425	4.555
Day 7	8.13 8.13	8.23 8.23	8.2 8.2	8.23 8.23	8.22 8.23
Day 8	8.24 8.23	8.3 8.31	8.29 8.3	8.28 8.28	8.27 8.27
Day 10	8.15 8.15	8.26 8.25	8.27 8.27	8.22 8.2	8.24 8.24
Day 12	8.18 8.18	8.3 8.3	8.38 8.37	8.38 8.38	8.38 8.38

Table 7 pH value of each duplicate of Cd treatment (with Cd) in experimental day 7, 8, 10 and 12, respectively

NH4 ($\mu mol \cdot D^{-1} \cdot L^{-1}$)	0.125	1.105	1.965	3.425	4.555
Day 7	7.98 7.98	7.98 7.98	7.95 7.95	7.95 7.95	7.99 7.99
Day 8	7.86 7.86	7.9 7.9	7.96 7.91	7.9 7.88	7.75 7.75
Day 10	7.92 7.91	7.87 7.86	7.81 7.81	7.78 7.78	7.74 7.74
Day 12	7.91 7.91	7.87 7.87	7.88 7.88	7.92 7.92	7.9 7.91

Appendix B *In vivo* fluorescence

The measured *in vivo* fluorescence values were shown below. In vivo fluorescence is corresponding with Chlorophyll a (Chl-a), which can indicate phytoplankton biomass. The results were obtained by Turner Design. Each sample was measured three duplicates.

Table 8 *In v*ivo fluorescence of each duplicate of control treatment (without Cd) in experimental day 7, 8, 10 and 12, respectively

NH4 ($\mu mol \cdot D^{-1} \cdot L^{-1}$)	0.125	1.105	1.965	3.425	4.555
Day 7	0.2 0.21 0.23	0.44 0.47 0.46	0.73 0.74 0.7	0.51 0.51 0.51	0.55 0.51 0.54
Day 8	0.25 0.24 0.245	0.49 0.47 0.47	0.76 0.79 0.79	0.79 0.82 0.55	0.60 0.62 0.60
Day 10	0.17 0.17 0.17	0.38 0.41 0.38	0.80 0.79 0.79	0.70 0.70 0.70	0.89 0.89 0.89
Day 12	0.16 0.17 0.18	0.32 0.32 0.32	0.54 0.54 0.54	0.76 0.76 0.76	0.63 0.63 0.63

Table 9 *In vivo* fluorescence of each duplicate of Cd treatment (with Cd) in experimental day 7, 8, 10 and 12, respectively

NH_4 ($\mu mol \cdot D^{-1} \cdot L^{-1}$)	0.125	1.105	1.965	3.425	4.555
Day 7	0.08 0.07 0.08	0.10 0.09 0.10	0.09 0.07 0.08	0.12 0.11 0.11	0.22 0.25 0.24
Day 8	0.08 0.07 0.08	0.08 0.09 0.07	0.09 0.10 0.08	0.14 0.13 0.08	0.20 0.23 0.21
Day 10	0.13 0.14 0.13	0.13 0.12 0.12	0.12 0.13 0.13	0.11 0.11 0.11	0.23 0.23 0.24
Day 12	0.12 0.10 0.11	0.07 0.06 0.06	0.06 0.06 0.06	0.12 0.11 0.10	0.24 0.25 0.25

Appendix C Instantaneous chlorophyll fluorescence

Table 10 Instantaneous chlorophyll fluorescence (Ft) of control treatment (without Cd) in experimental day 10 and day 12

NH_4 ($\mu mol \cdot D^{-1} \cdot L^{-1}$)	0.125	1.105	1.965	3.425	4.555
Day 10	320	535	913	966	1076
Day 12	184	396	700	987	780

Table 11 Instantaneous chlorophyll fluorescence (Ft) of Cd treatment (with Cd) in experimental day 10 and day 12

NH_4 ($\mu mol \cdot D^{-1} \cdot L^{-1}$)	0.125	1.105	1.965	3.425	4.555
Day 10	153	143	119	149	347
Day 12	104	55*	150	161	298

* Ft value of sample (sampling day 12 at 1.105 $\mu mol \cdot D^{-1} \cdot L^{-1}$ NH_4 flux) was inversely calculated from condensate, since the Ft value was below 100 which could not be detected by AquApen.

Appendix D Chlorophyll *a*

Chlorophyll-*a* (Chl-*a*) measurement has become the preferred parameter for investigate phytoplankton biomass. In this thesis, Chl-*a* was extracted by methanol after phytoplankton filtration, and measured by using fluormeter. Extracted Chl-*a* concentration was calculated by the eqµAtion:

$$\mu g\ Chl\ a/L = (FL \times f \times E \times 1000 \times K)/(Fs \times S \times V)$$

Where, FL is the fluorescence result reading on the lower scale; f is calibration factor, general eqµAl 0.29; E is the extraction volume (usµAlly use 10 mL); K is ratio between the whole filter area and the small pieces; Fs is the slit automatically chosen by instrument (either 1.00 3.16 10.0 or 31.6); S is the sensitivity (either 1 or 100); and V is the filtered volume (mL).

Table 12 Chlorophyll a concentration of control treatment (without Cd) and Cd treatment (with Cd) in experimental day 12

NH_4 ($\mu mol \cdot D^{-1} \cdot L^{-1}$)	0.125	1.105	1.965	3.425	4.555
Control	1.84 1.90	6.28 6.31	6.89 8.34	19.33 19.33	8.12 7.83
Cd	1.16 1.12	0.62 0.64	0.66 0.68	1.25 1.19	1.70 1.64

Appendix E Anodic stripping voltammetry

1. Voltammetric scan

The voltammetric scans of control treatment (without Cd) and Cd treatment (with Cd) on experimental day 5 and day 12 were shown as follow.

Control treatment in Day 5

1) NH_4 flux= 0.125 µmol·D^{-1}·L^{-1}

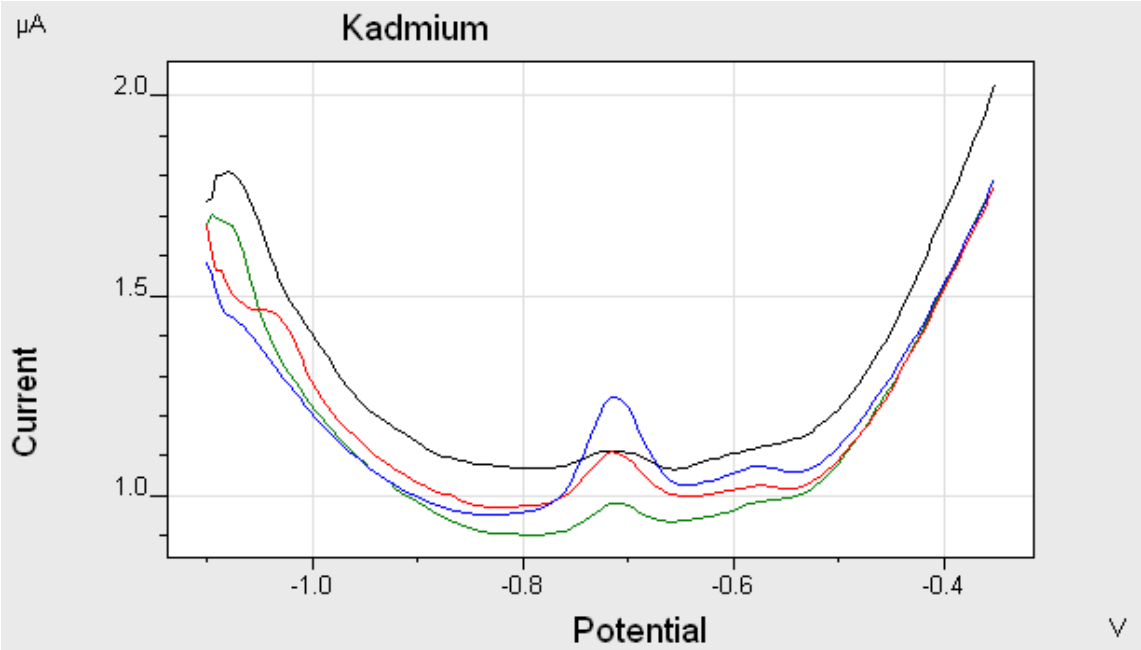

2) NH_4 flux= 1.105 µmol·D^{-1}·L^{-1}

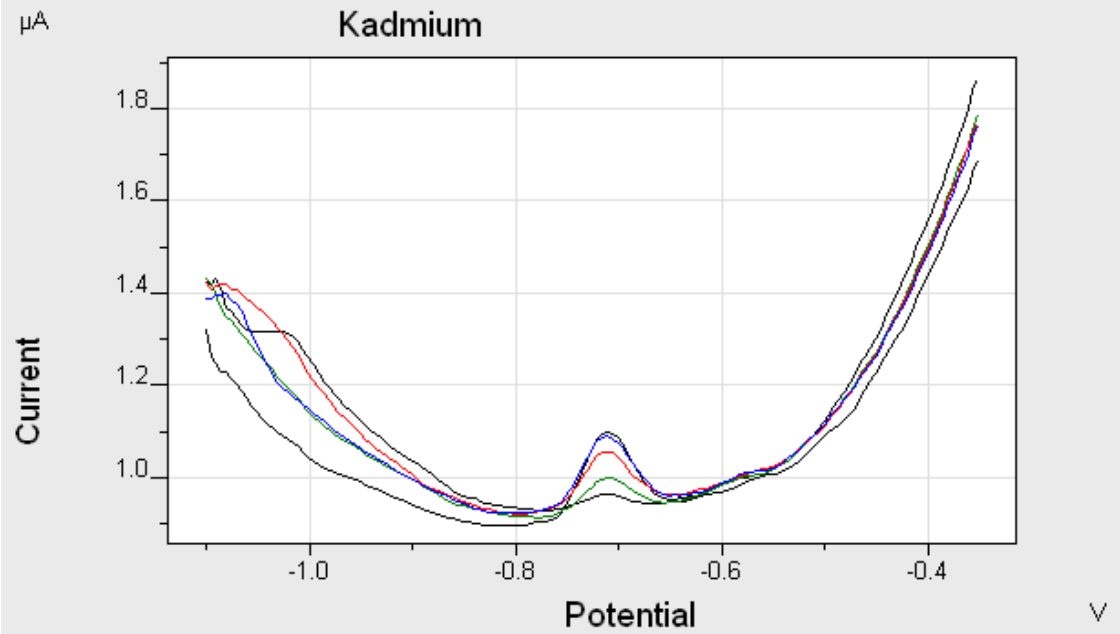

3) NH_4 flux= 1.965 µmol·D^{-1}·L^{-1}

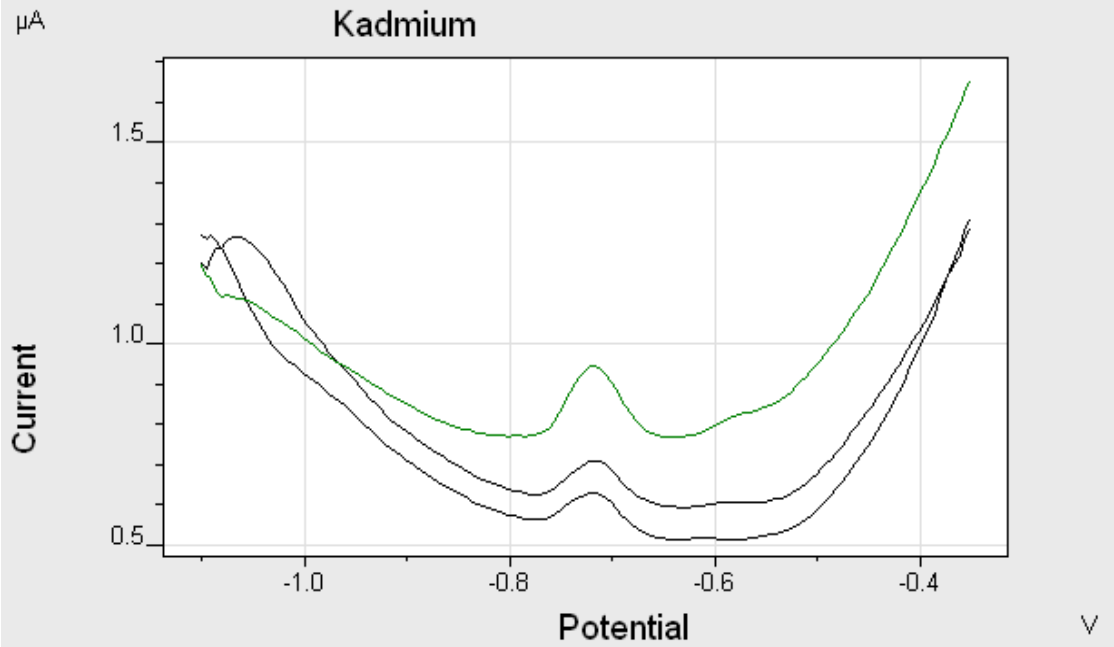

4) NH_4 flux= 3.425 µmol·D^{-1}·L^{-1}

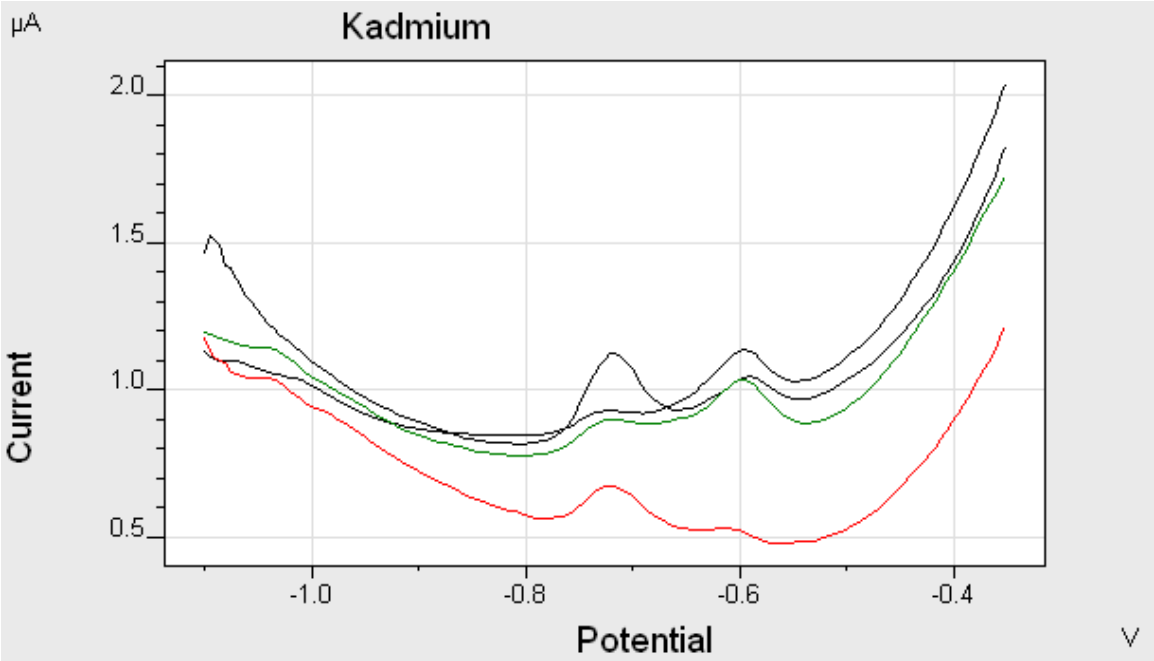

5) NH_4 flux= 4.555 µmol·D^{-1}·L^{-1}

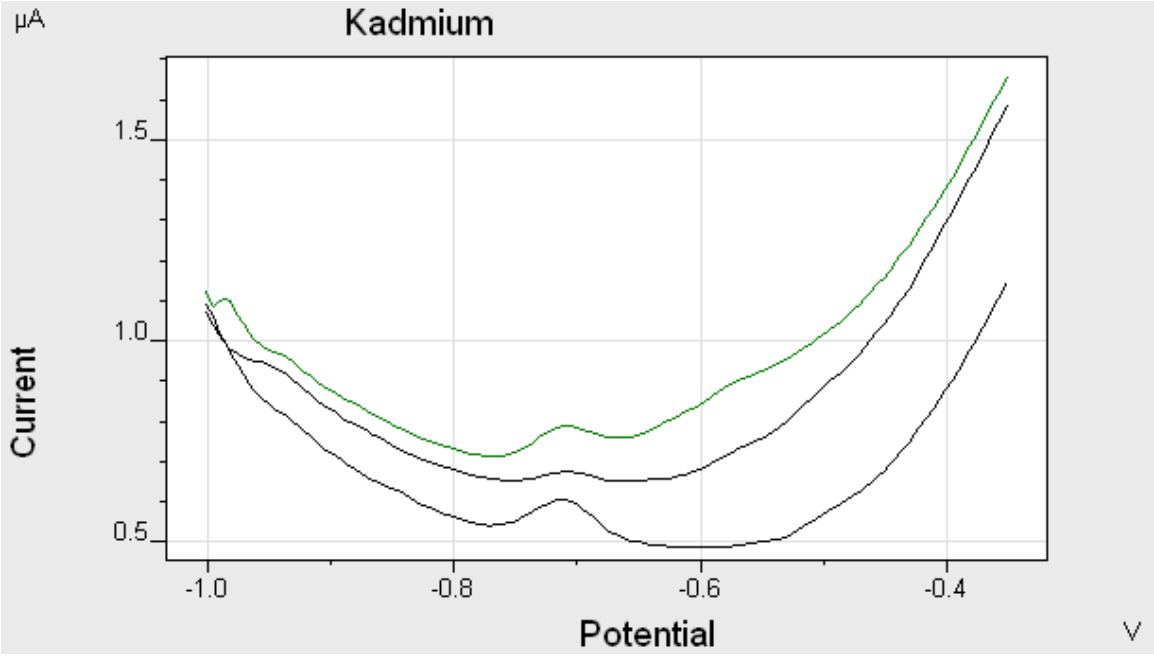

Cd Treatment in day 5

1) NH_4 flux= 0.125 µmol·D^{-1}·L^{-1}

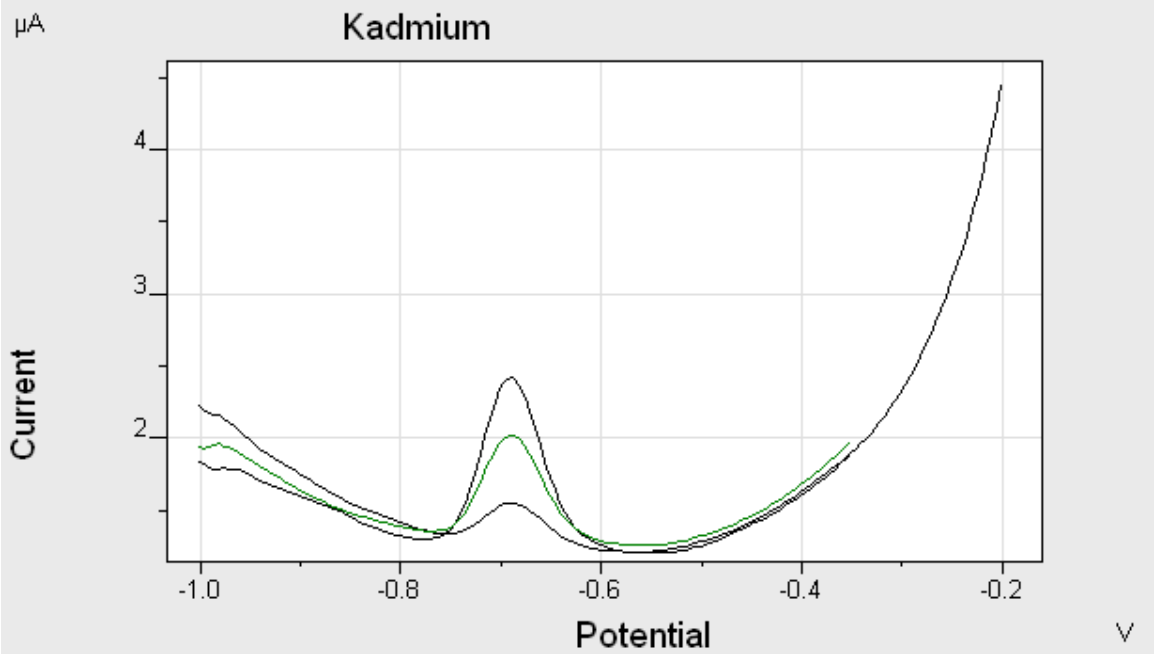

2) NH_4 flux= 1.105 µmol·D^{-1}·L^{-1}

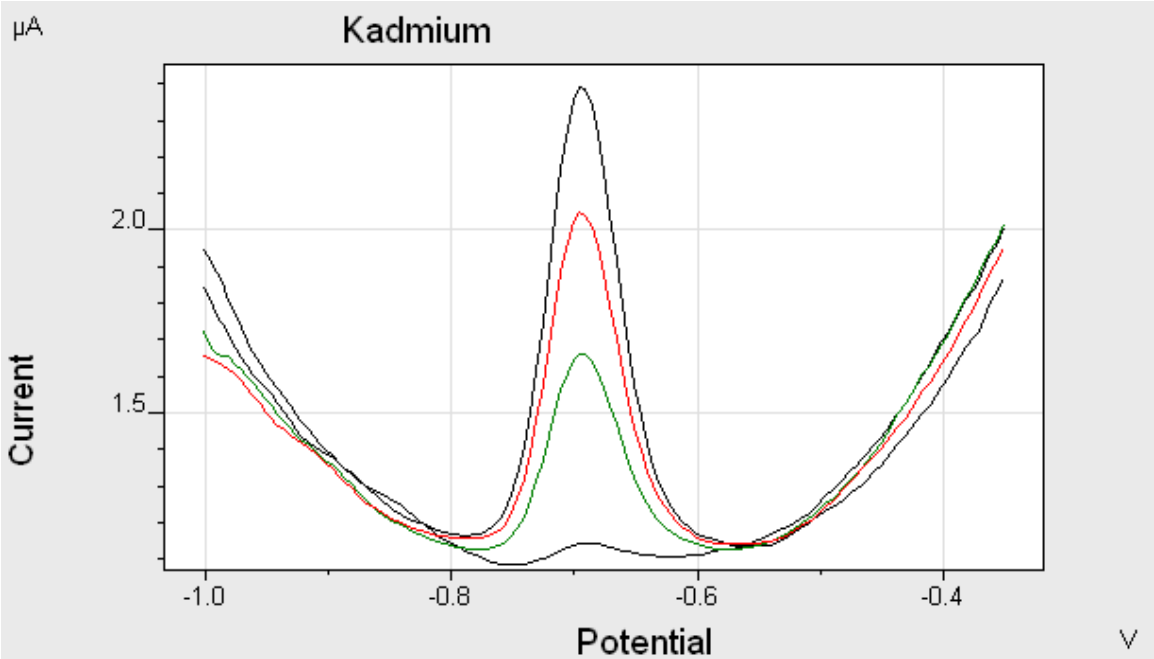

3) NH_4 flux= 1.965 µmol·D^{-1}·L^{-1}

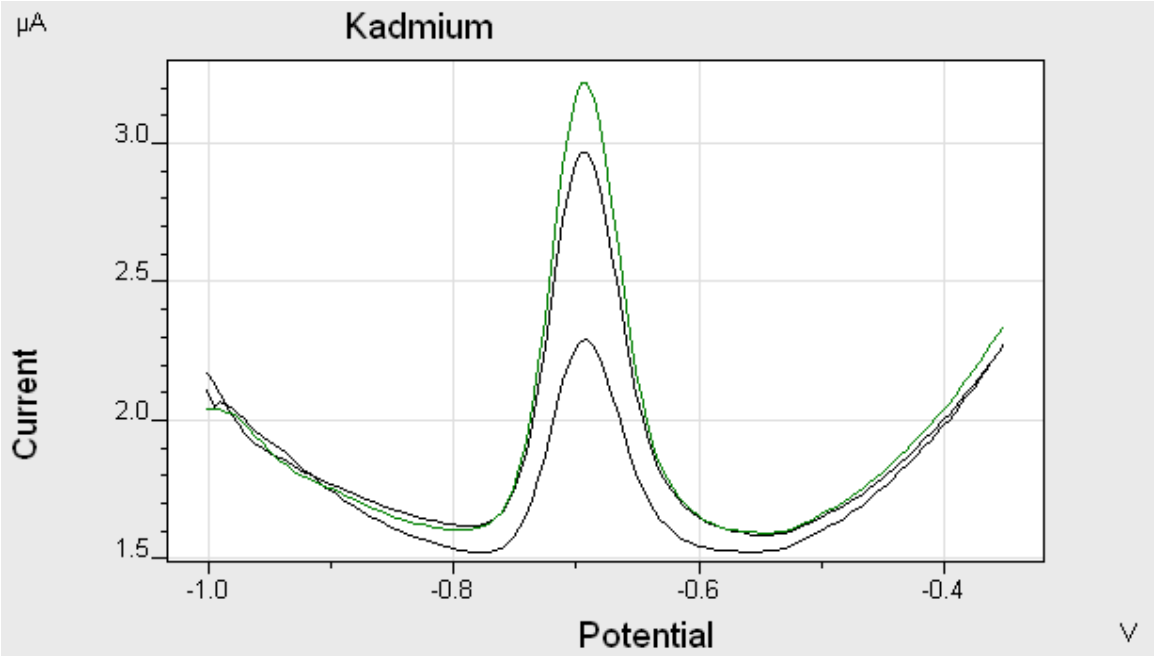

4) NH_4 flux= 3.425 µmol·D^{-1}·L^{-1}

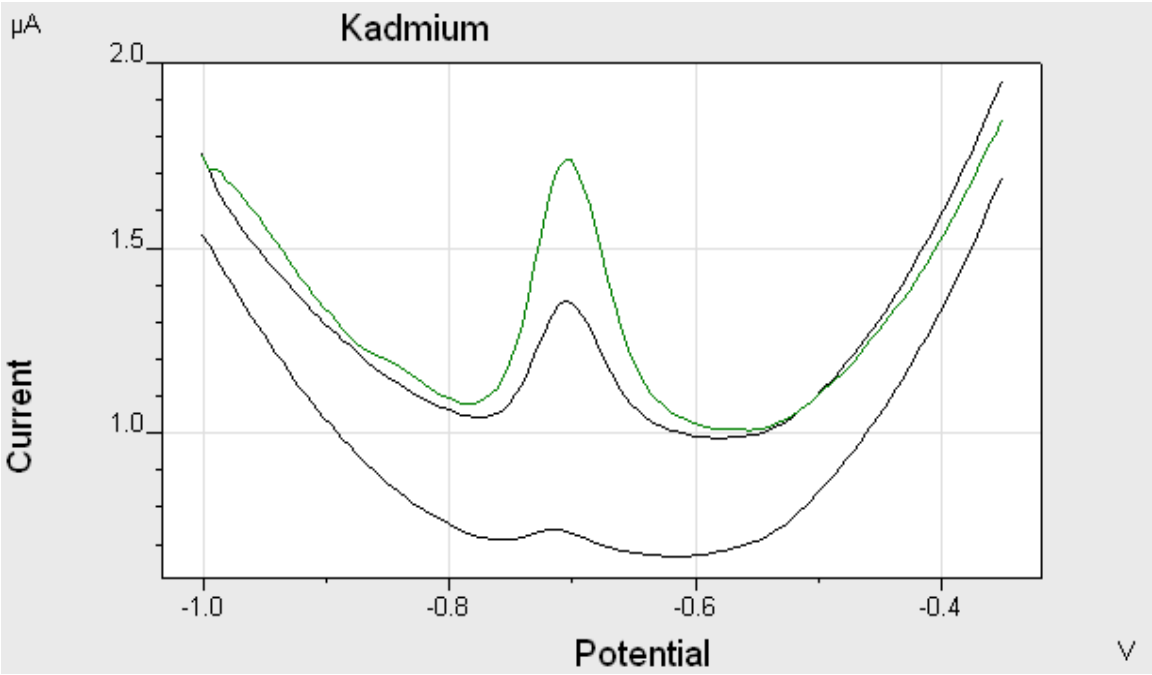

5) NH_4 flux= 4.555 µmol·D^{-1}·L^{-1}

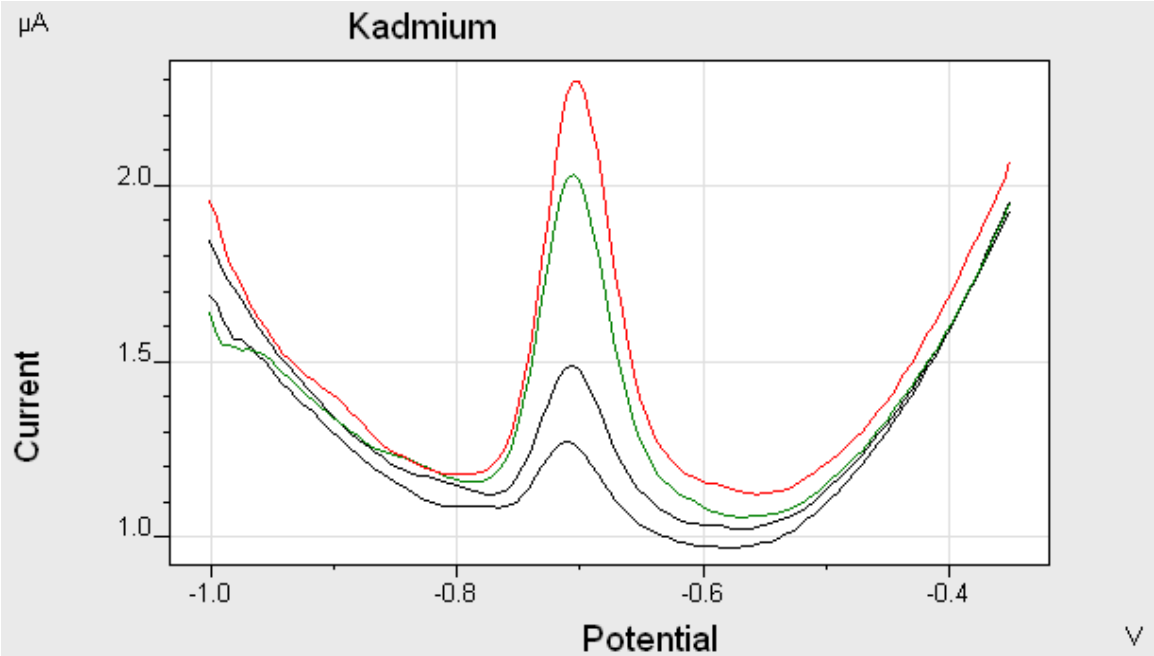

Control treatment on Day 12

1) NH_4 flux= 0.125 µmol·D^{-1}·L^{-1}

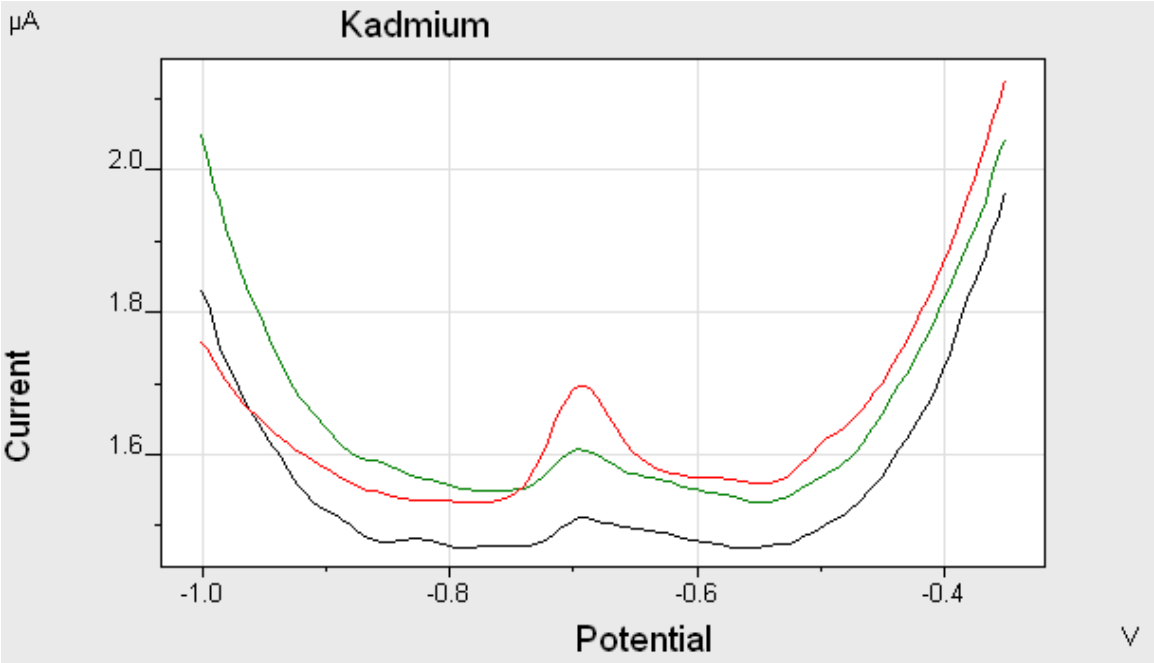

2) NH_4 flux= 1.105 µmol·D^{-1}·L^{-1}

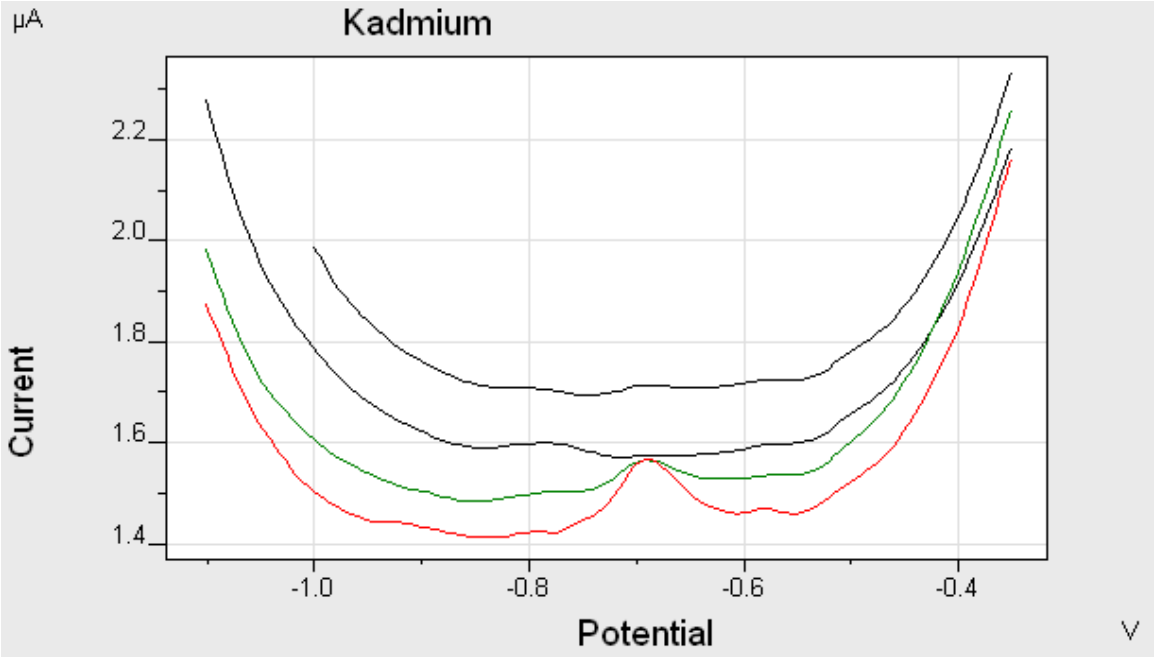

3) NH_4 flux= 1.965 µmol·D^{-1}·L^{-1}

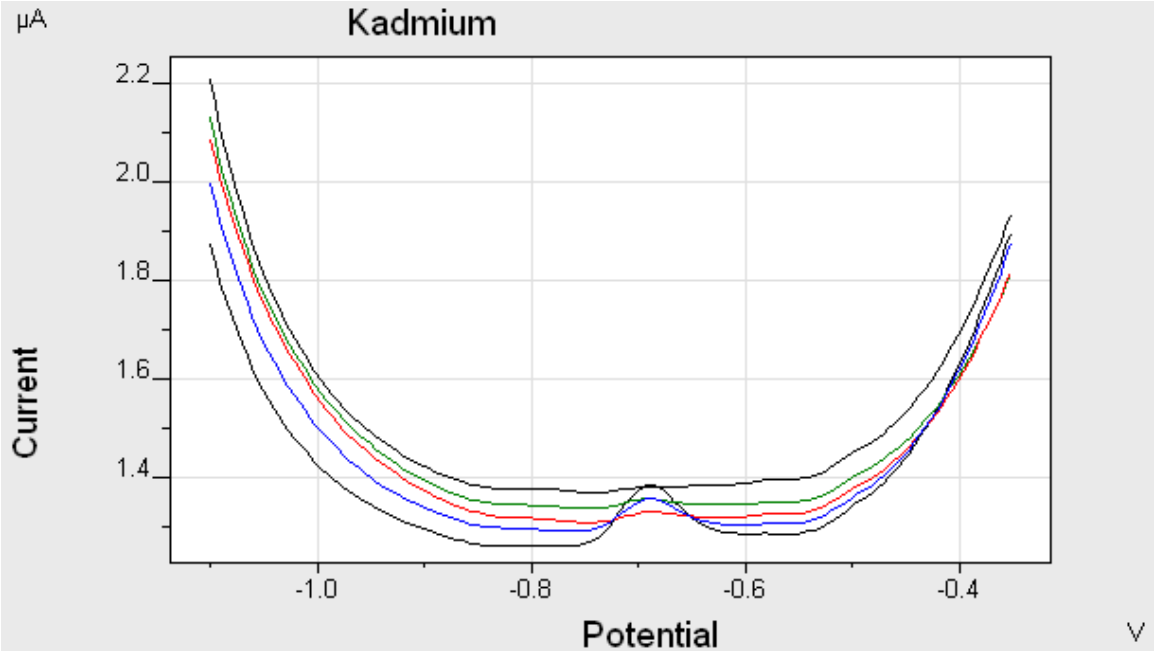

4) NH_4 flux= 3.425 µmol·D^{-1}·L^{-1}

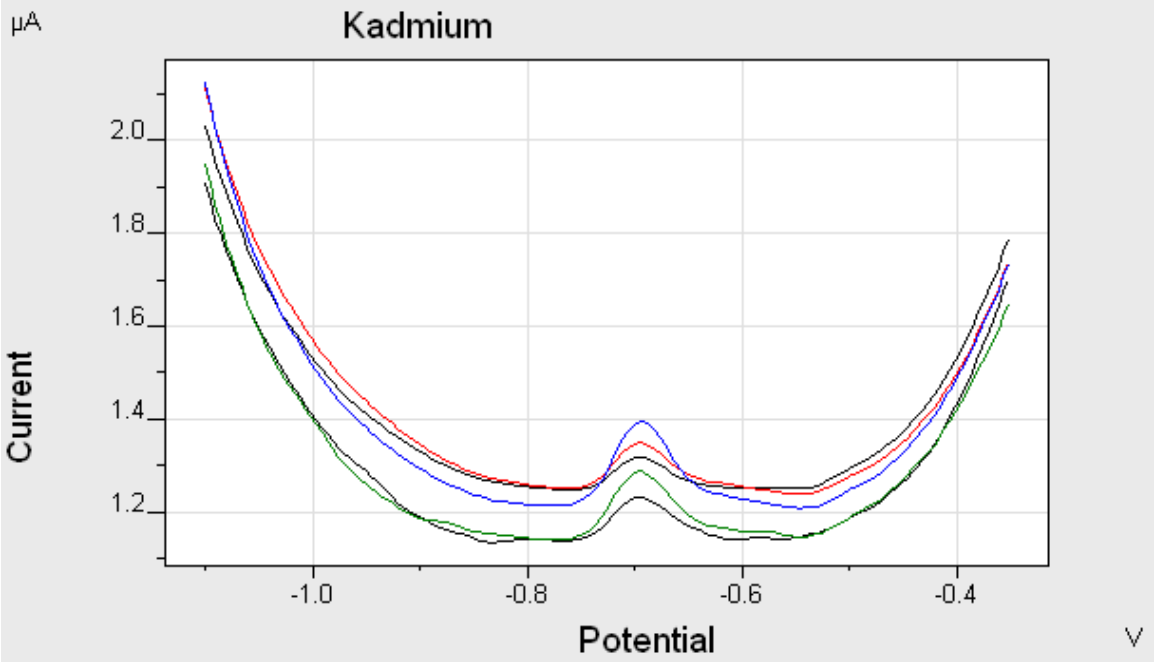

5) NH_4 flux= 4.555 µmol·D^{-1}·L^{-1}

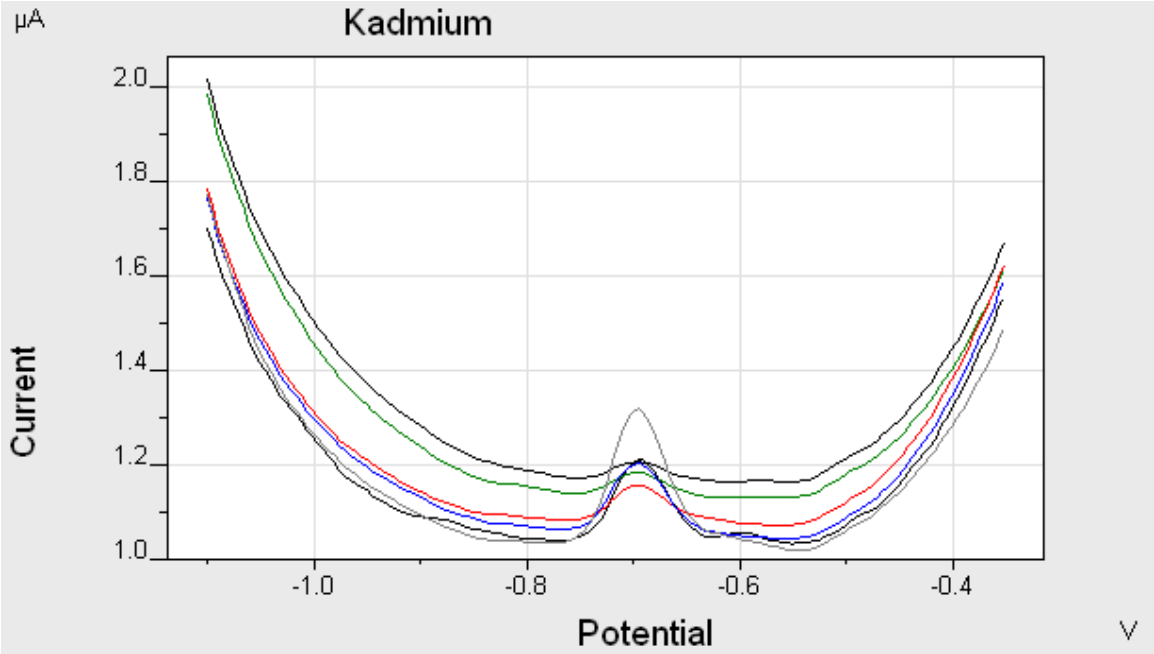

Cd treatment in Day 12

1) NH_4 flux= 0.125 µmol·D^{-1}·L^{-1}

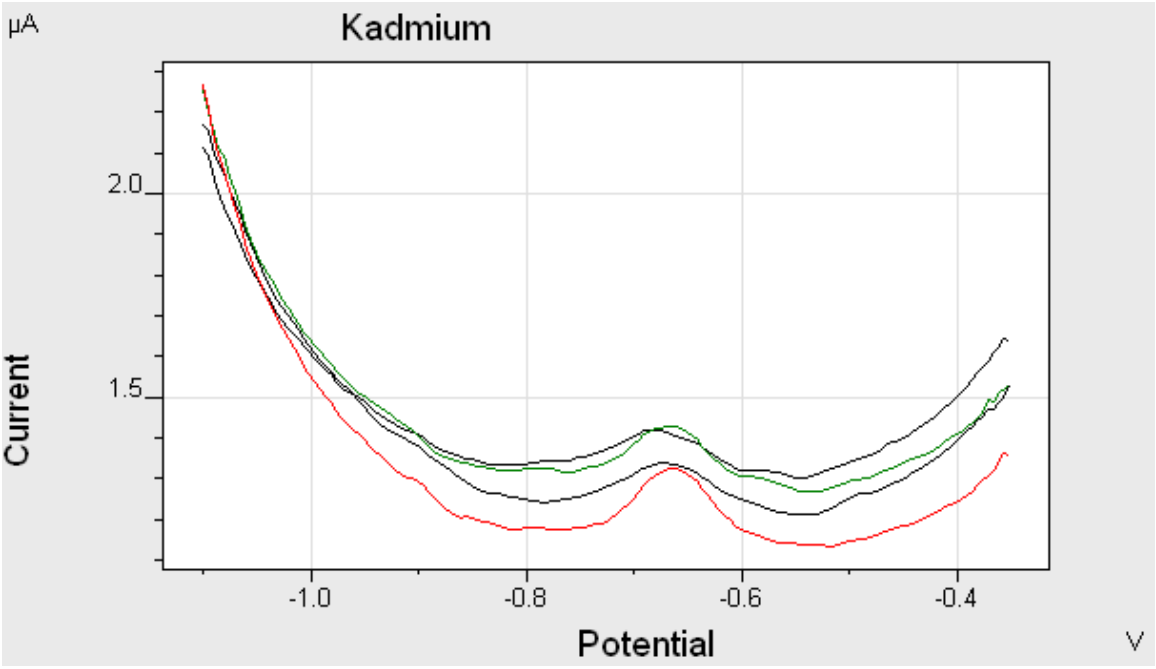

2) NH_4 flux= 1.105 µmol·D^{-1}·L^{-1}

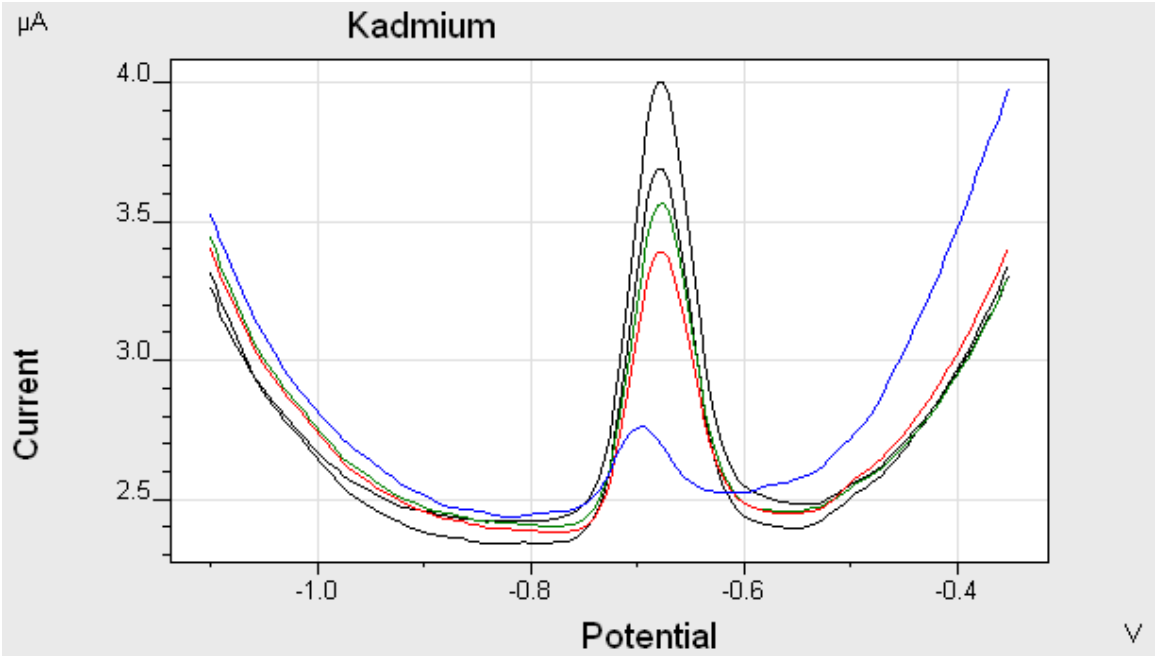

3) NH_4 flux= 1.965 µmol·D^{-1}·L^{-1}

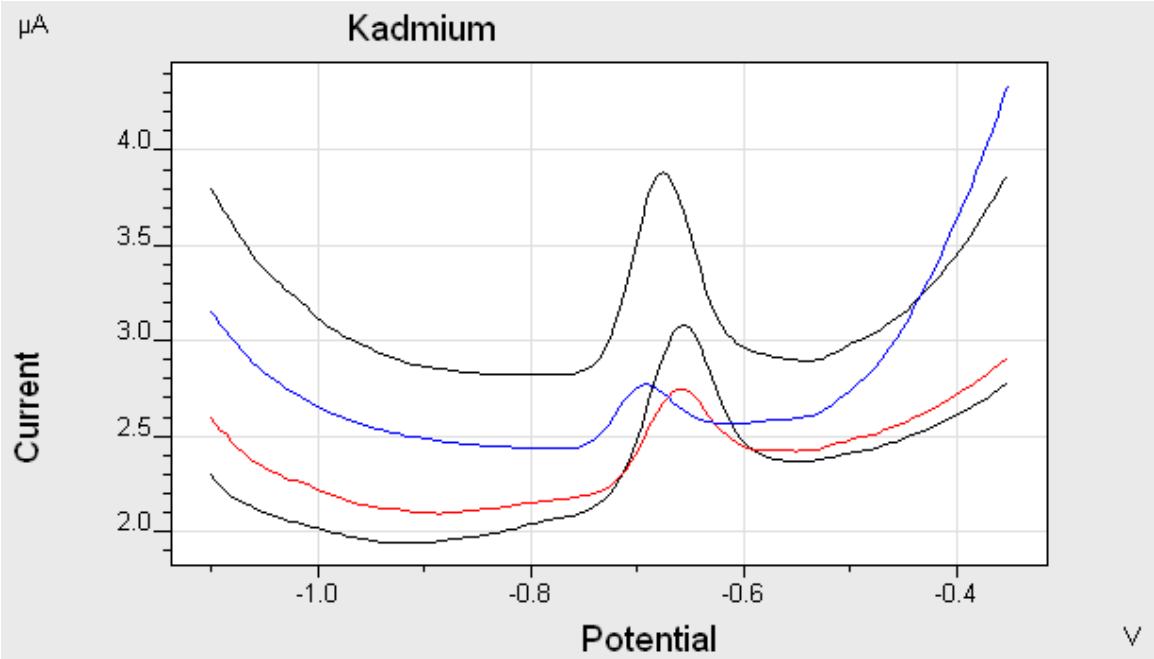

4) NH_4 flux= 3.425 µmol·D^{-1}·L^{-1}

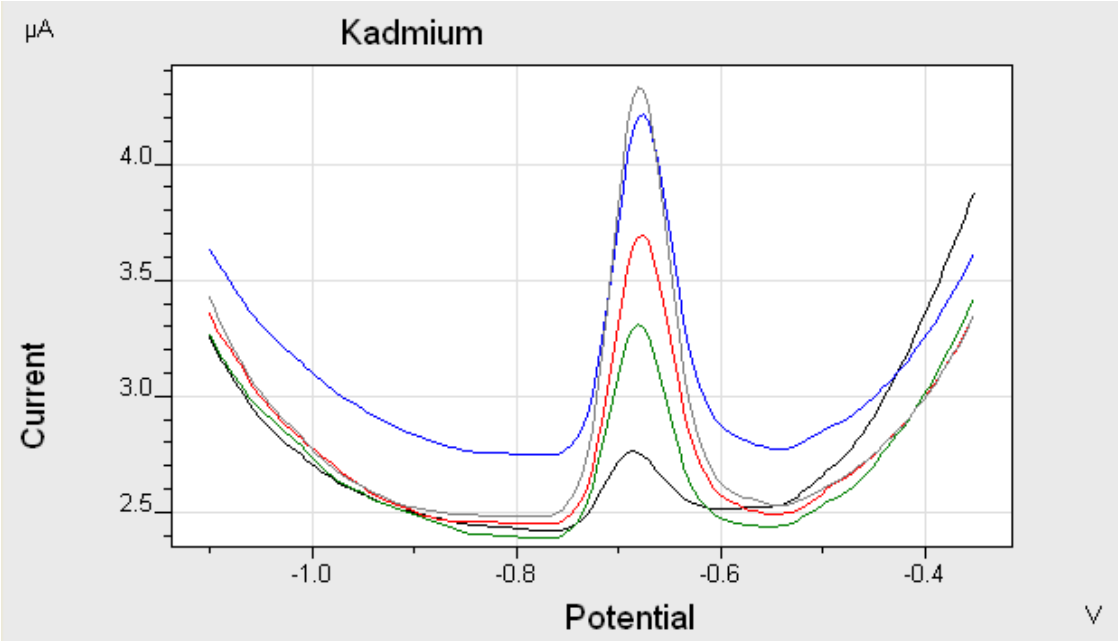

5) NH_4 flux= 4.555 µmol·D^{-1}·L^{-1}

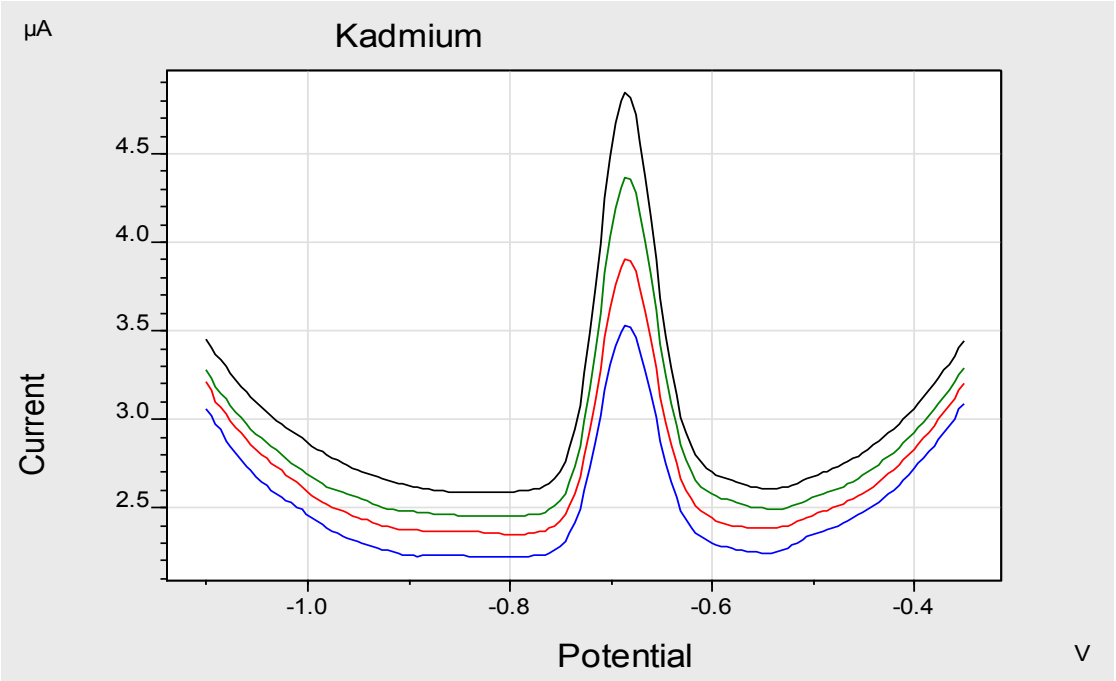

2. Scan peak

The peak data of voltammetric scans of control treatment (without Cd) and Cd treatment (with Cd) on experimental day 5 and day 12 were shown as follow.

Control treatment in Day 5

1) NH_4 flux= 0.125 µmol·D^{-1}·L^{-1}

Cd addition/ ppb	Epeak /V	height /µA	width /V	Area/ nAV
0	0	0	0	0
1	0	0	0	0
2	0	0	0	0
3	-0.716	0.045	0.130	5.656
4	-0.711	0.060	0.130	4.895
5	-0.711	0.146	0.175	5.277
6	-0.711	0.251	0.165	5.570

2) NH_4 flux= 1.105 µmol·D^{-1}·L^{-1}

Cd addition/ppb	Epeak /V	height /µA	width /V	Area /nAV
0	0	0	0	0
1	0	0	0	0
2	-0.711	0.028	0.105	4.962
3	-0.711	0.070	0.125	4.981
4	-0.711	0.113	0.150	5.068
5	-0.711	0.143	0.145	5.158
6	-0.711	0.173	0.155	5.076

3) NH_4 flux= 1.105 µmol·D^{-1}·L^{-1}

Cd addition/ ppb	Epeak /V	height /µA	width /V	Area/ nAV
0	0	0	0	0
1	0	0	0	0
2	0	0	0	0
3	-0.721	0.087	0.125	3.003
4	-0.716	0.127	0.140	3.871
5	-0.716	0.175	0.140	4.346

4) NH_4 flux= 3.425 µmol·D^{-1}·L^{-1}

Cd addition/ ppb	Epeak /V	height /µA	width /V	Area/ nAV
0	0	0	0	0
1	0	0	0	0
2	-0.721	0.033	0.090	4.763
4	-0.716	0.048	0.100	4.523
5	-0.721	0.127	0.140	3.098
6	-0.716	0.240	0.135	5.045

5) NH_4 flux= 4.555 µmol·D^{-1}·L^{-1}

Cd addition/ ppb	Epeak /V	height /µA	width /V	Area/ nAV
0	0	0	0	0
1	0	0	0	0
2	-0.711	0.021	0.090	3.491
3	-0.711	0.050	0.100	3.975
4	-0.711	0.083	0.115	2.920

Cd treatment in day 5

1) NH_4 flux= 0.125 µmol·D^{-1}·L^{-1}

Cd addition/ ppb	Epeak /V	height /µA	width /V	Area/ nAV
0	0	0	0	0
1	-0.691	0.260	0.155	7.183
2	-0.691	0.706	0.185	8.081
3	-0.691	1.156	0.205	8.459

2) NH_4 flux= 1.105 µmol·D^{-1}·L^{-1}

Cd addition/ ppb	Epeak /V	height /µA	width /V	Area/ nAV
0	-0.686	0.049	0.130	5.795
1	-0.696	0.534	0.200	6.719
2	-0.696	0.898	0.205	7.425
3	-0.696	1.236	0.225	7.833

3) NH_4 flux= 1.965 µmol·D^{-1}·L^{-1}

Cd addition/ ppb	Epeak /V	height /µA	width /V	Area/ nAV
0	0	0	0	0
1	-0.691	0.766	0.215	9.066
2	-0.696	1.294	0.235	10.301
3	-0.696	1.618	0.245	10.544

4) NH_4 flux= 3. 425 µmol·D^{-1}·L^{-1}

Cd addition/ ppb	Epeak /V	height /µA	width /V	Area/ nAV
0	-0.716	0.043	0.120	3.701
1	-0.706	0.330	0.160	5.945
2	-0.706	0.686	0.195	6.613

5) NH_4 flux= 4.555 µmol·D^{-1}·L^{-1}

Cd addition/ ppb	Epeak /V	height /µA	width /V	Area/ nAV
0	-0.711	0.224	0.160	5.755
1	-0.706	0.402	0.165	6.354
2	-0.706	0.912	0.205	7.223
3	-0.701	1.139	0.235	7.577

Control treatment in day 12

1) NH_4 flux= 0.125 µmol·D^{-1}·L^{-1}

Cd addition/ ppb	Epeak /V	height /µA	width /V	Area/ nAV
1	-0.701	0.029	0.100	10.275
2.5	-0.691	0.041	0.190	7.634
3	-0.696	0.063	0.215	8.011
4	-0.691	0.153	0.225	8.149

2) NH_4 flux= 1.105 µmol·D^{-1}·L^{-1}

Cd addition/ ppb	Epeak /V	height /µA	width /V	Area/ nAV
1.5	-0.686	0.011	0.095	8.986
2.5	-0.831	0.014	0.105	10.469
3	-0.786	0.018	0.120	8.288
3.5	-0.691	0.049	0.135	7.968
4	-0.686	0.123	0.175	7.661

3) NH_4 flux= 1.965 µmol·D^{-1}·L^{-1}

Cd addition/ ppb	Epeak /V	height /µA	width /V	Area/ nAV
1.5	0	0	0	0
2	-0.691	0.016	0.140	6.968
2.5	-0.686	0.017	0.125	6.861
3	-0.691	0.061	0.160	6.797
3.5	-0.691	0.113	0.175	6.748

4) NH_4 flux= 3.425 µmol·D^{-1}·L^{-1}

Cd addition/ ppb	Epeak /V	height /µA	width /V	Area/ nAV
1.5	0	0	0	0
2	0	0	0	0
2.5	0	0	0	0
3	0	0	0	0
3.5	-0.696	0.068	0.160	6.573
4.5	-0.696	0.093	0.160	6.064
5	-0.696	0.101	0.215	6.542
5.5	-0.696	0.139	0.175	6.174
6	-0.696	0.183	0.230	6.477

5) NH_4 flux= 4.555 µmol·D^{-1}·L^{-1}

Cd addition/ ppb	Epeak /V	height /µA	width /V	Area/ nAV
2.5	0	0	0	0
3	-0.696	0.037	0.130	6.149
3.5	-0.696	0.048	0.135	5.986
4.5	-0.696	0.077	0.170	5.695
5	-0.696	0.146	0.205	5.622
5.5	-0.696	0.168	0.145	5.731
6	-0.696	0.290	0.230	5.670

Cd treatment in day 12

1) NH_4 flux= 0.125 μmol·D^{-1}·L^{-1}

Cd addition/ ppb	Epeak /V	height /μA	width /V	Area/ nAV
0	-0.681	0.094	0.220	6.963
0.5	-0.676	0.111	0.230	6.521
1.0	-0.671	0.132	0.220	6.881
2.0	-0.661	0.166	0.245	6.180

2) NH_4 flux= 1.105 μmol·D^{-1}·L^{-1}

Cd addition/ ppb	Epeak /V	height /μA	width /V	Area/ nAV
0	-0.696	0.276	0.210	13.099
1.0	-0.676	0.980	0.220	13.908
1.5	-0.676	1.140	0.220	14.202
2.0	-0.681	1.323	0.230	14.105
2.5	-0.676	1.556	0.260	14.607

3) NH_4 flux= 1.965 μmol·D^{-1}·L^{-1}

Cd addition/ ppb	Epeak /V	height /μA	width /V	Area/ nAV
0	-0.676	1.031	0.230	16.233
1.0	-0.656	0.858	0.215	12.905
1.5	-0.656	0.698	0.235	12.781
2.0	-0.656	0.448	0.200	12.655

4) NH_4 flux= 3.425 μmol·D^{-1}·L^{-1}

Cd addition/ ppb	Epeak /V	height /μA	width /V	Area/ nAV
0	-0.686	0.298	0.165	13.320
1.0	-0.681	0.898	0.215	13.831
1.5	-0.676	1.227	0.225	14.604
2.0	-0.676	1.458	0.225	16.436
2.5	-0.681	1.828	0.235	15.554

5) NH_4 flux= 4.555 µmol·D^{-1}·L^{-1}

Cd addition/ ppb	Epeak /V	height /µA	width /V	Area/ nAV
0	-0.686	1.293	0.245	13.262
0.5	-0.686	1.539	0.245	14.276
1.0	-0.686	1.894	0.260	15.183
1.5	-0.686	2.246	0.295	15.899

Appendix F DGT labile Cd concentration

Table 13 DGT labile Cd concentration (nmol/L) of control treatment in experimental day 8

NH_4 flux ($\mu mol \cdot D^{-1} \cdot L^{-1}$)	0.125	1.105	1.965	3.425	4.555
DGT labile Cd 1 (nmol/L)	0.50	4.98	0.53	0.55	7.86
DGT labile Cd 2 (nmol/L)	0.48	7.09	1.31	0.63	14.70
mean (nmol/L)	0.49	6.03	0.92	0.59	11.28
STD	0.02	1.50	0.55	0.06	4.84

Table 14 DGT labile Cd concentration (µmol/L) of Cd treatment in experimental day 8

NH_4 flux ($\mu mol \cdot D^{-1} \cdot L^{-1}$)	0.125	1.105	1.965	3.425	4.555
DGT labile Cd 1 (µmol/L)	1.54	1.59	1.55	1.46	1.19
DGT labile Cd 2 (µmol/L)	1.93	1.68	1.57	1.26	1.33
mean (umol/L)	1.74	1.64	1.56	1.36	1.26
STD	0.28	0.06	0.02	0.14	0.10

Table 15 DGT labile Cd concentration (nmol/L) of control treatment in experimental day 12

NH_4 flux ($\mu mol \cdot D^{-1} \cdot L^{-1}$)	0.125	1.105	1.965	3.425	4.555
DGT labile Cd 1 (nmol/L)	1.01	0.11	0.03	0.21	0.11
DGT labile Cd 2 (nmol/L)	1.22	0.34	0.08	0.31	0.11
mean (nmol/L)	1.11	0.22	0.05	0.26	0.11
STD	0.15	0.16	0.04	0.07	0.00

Table 16 DGT labile Cd concentration (µmol/L) of Cd treatment in experimental day 8

NH_4 flux (µmol·D^{-1}·L^{-1})	0.125	1.105	1.965	3.425	4.555
DGT labile Cd 1 (µmol/L)	1.48	1.33	1.26	1.37	1.52
DGT labile Cd 2 (µmol/L)	1.80	1.41	1.28	1.13	1.28
DGT labile Cd 3 (µmol/L)	1.60	1.35	1.17	1.32	1.36
mean (µmol/L)	1.63	1.36	1.24	1.27	1.39
STD	0.16	0.04	0.06	0.12	0.12

Appendix G Cd complexation capacity

Cd complexation capacity determination consisted of Cd complexation capacity of control and Cd treatment. Cd complexation capacity was determined by anodic stripping voltammetry (ASV).

1. Cd compaxation capacity of control treatment

Table 17 Cd complexation capacity of control treatment (without Cd) in experimental day 8 and day 12

NH_4 flux ($\mu mol \cdot D^{-1} \cdot L^{-1}$)	0.125	1.105	1.965	3.425	4.555
Day 8	0.020	0.010	0.012	0.019	0.012
Day 12	0.018	0.023	0.021	0.034	0.027

2. Cd complexation capacity of Cd treatment

Cd complexation capacity of Cd treatment in day 8

Table 18 Cd complexation capacity of Cd treatment (with Cd) at ammonia flux 0.125 µmol·L^{-1}·D^{-1} in day 8

$[Cd]_{ASV}$ (mol·L^{-1})	$[Cd]_T$-$[Cd]_{ASV}$ (mol·L^{-1})	$[Cd]_F/([Cd]_T-[Cd]_F)$
7.71056E-09	2.00119E-06	0.003852993
2.09371E-08	1.99686E-06	0.010485045
3.42823E-08	1.99241E-06	0.017206478

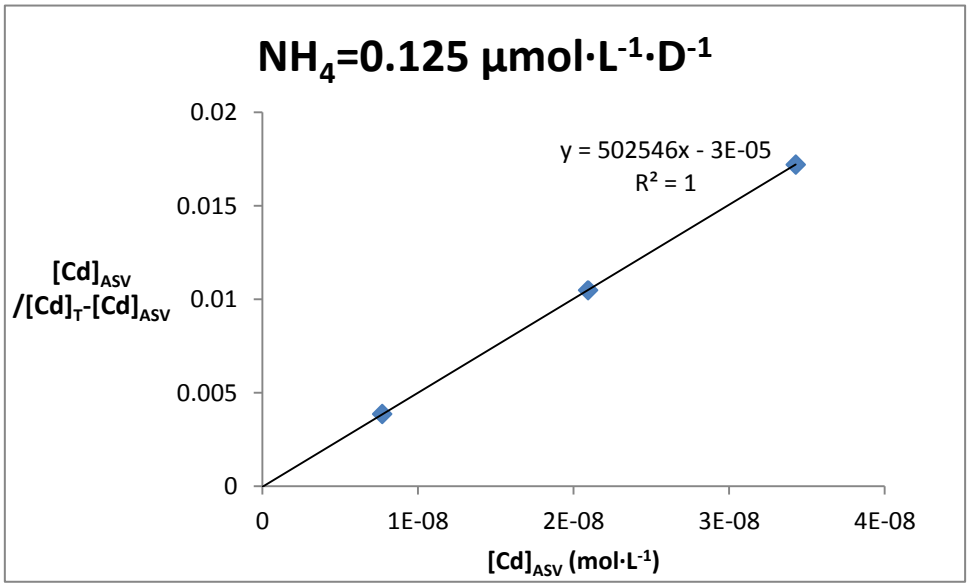

Figure 29 Cd complexation capacity of Cd treatment (with Cd) at ammonia flux 0.125 µmol·L^{-1}·D^{-1} in day 8

Table 19 Cd complexation capacity of Cd treatment (with Cd) at ammonia flux 1.105 µmol·L^{-1}·D^{-1} in day 8

$[Cd]_{ASV}$ (mol·L^{-1})	$[Cd]_T$-$[Cd]_{ASV}$ (mol·L^{-1})	$[Cd]_F/([Cd]_T-[Cd]_F)$
7.71056E-09	2.00119E-06	0.003852993
2.09371E-08	1.99686E-06	0.010485045
3.42823E-08	1.99241E-06	0.017206478

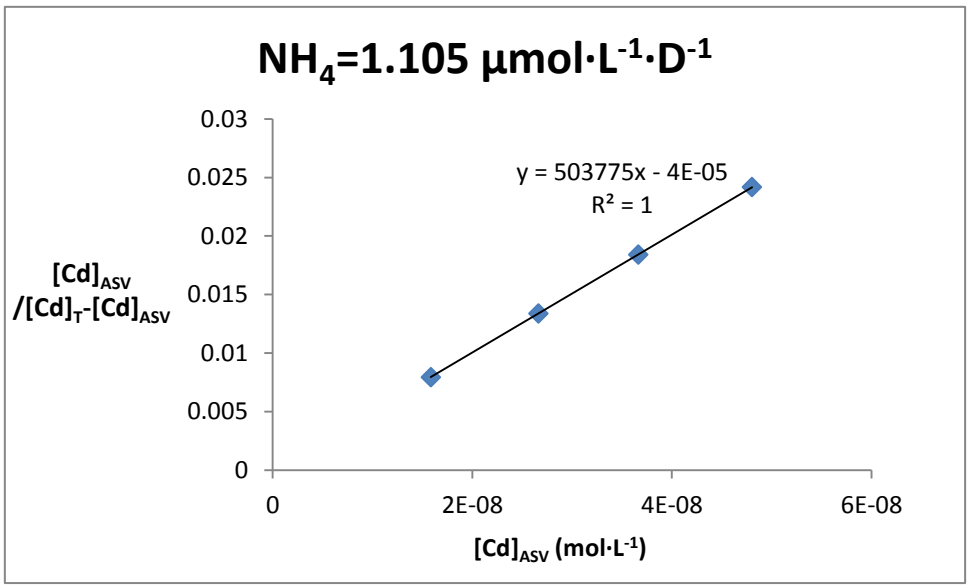

Figure 30 Cd complexation capacity of Cd treatment (with Cd) at ammonia flux 1.105 µmol·L^{-1}·D^{-1} in day 8

Table 20 Cd complexation capacity of Cd treatment (with Cd) at ammonia flux 1.965 µmol·L^{-1}·D^{-1} in day 8

$[Cd]_{ASV}$ (mol·L^{-1})	$[Cd]_T$-$[Cd]_{ASV}$ (mol·L^{-1})	$[Cd]_F/([Cd]_T-[Cd]_F)$
1.58363E-08	1.99306E-06	0.007945719
2.66311E-08	1.99116E-06	0.013374639
3.66548E-08	1.99004E-06	0.01841917

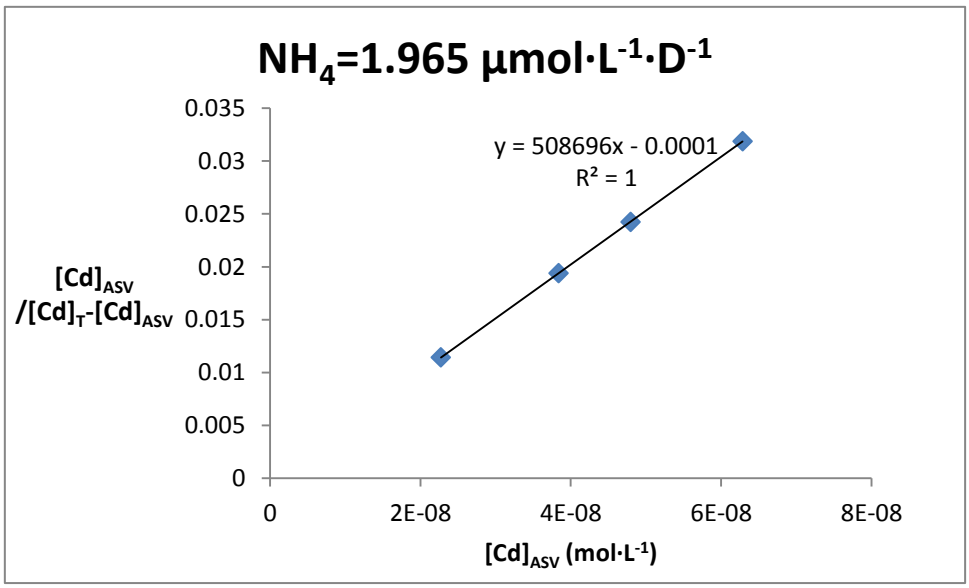

Figure 31 Cd complexation capacity of Cd treatment (with Cd) at ammonia flux 1.965 µmol·L^{-1}·D^{-1} in day 8

Table 21 Cd complexation capacity of Cd treatment (with Cd) at ammonia flux 3.425 µmol·L^{-1}·D^{-1} in day 8

$[Cd]_{ASV}$ (mol·L^{-1})	$[Cd]_T$-$[Cd]_{ASV}$ (mol·L^{-1})	$[Cd]_F/([Cd]_T-[Cd]_F)$
2.27165E-08	1.98618E-06	0.011437274
3.83749E-08	1.97942E-06	0.01938693
4.79834E-08	1.97871E-06	0.024249873
6.28707E-08	1.97272E-06	0.031870114

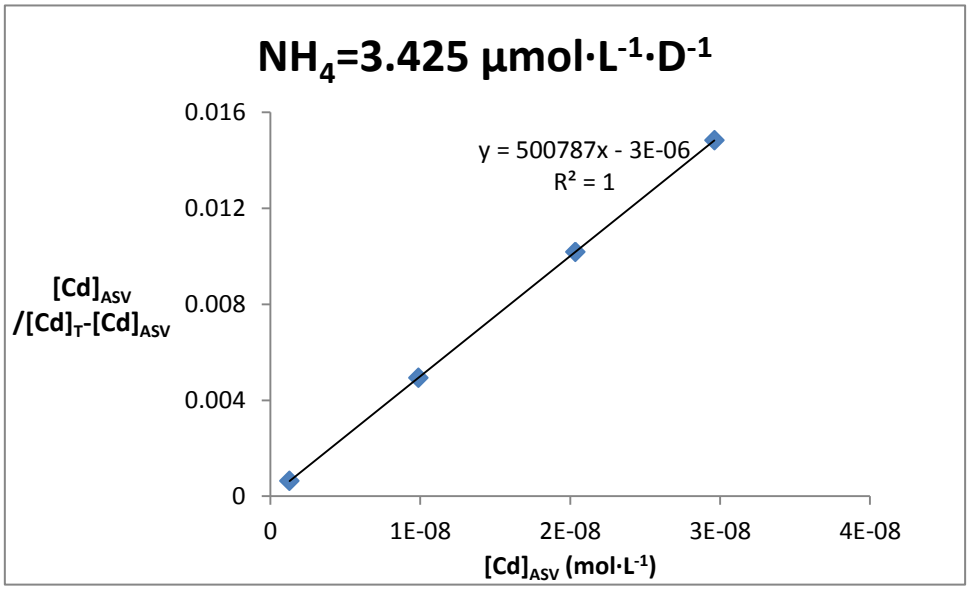

Figure 32 Cd complexation capacity of Cd treatment (with Cd) at ammonia flux 3.425 µmol·L^{-1}·D^{-1} in day 8

Table 22 Cd complexation capacity of Cd treatment (with Cd) at ammonia flux 4.555 µmol·L^{-1}·D^{-1} in day 8

$[Cd]_{ASV}$ (mol·L^{-1})	$[Cd]_T$-$[Cd]_{ASV}$ (mol·L^{-1})	$[Cd]_F/([Cd]_T-[Cd]_F)$
1.27521E-09	1.99872E-06	0.000638011
9.87544E-09	1.99902E-06	0.00494014
2.0344E-08	1.99745E-06	0.010184993
2.96263E-08	1.99706E-06	0.014834945

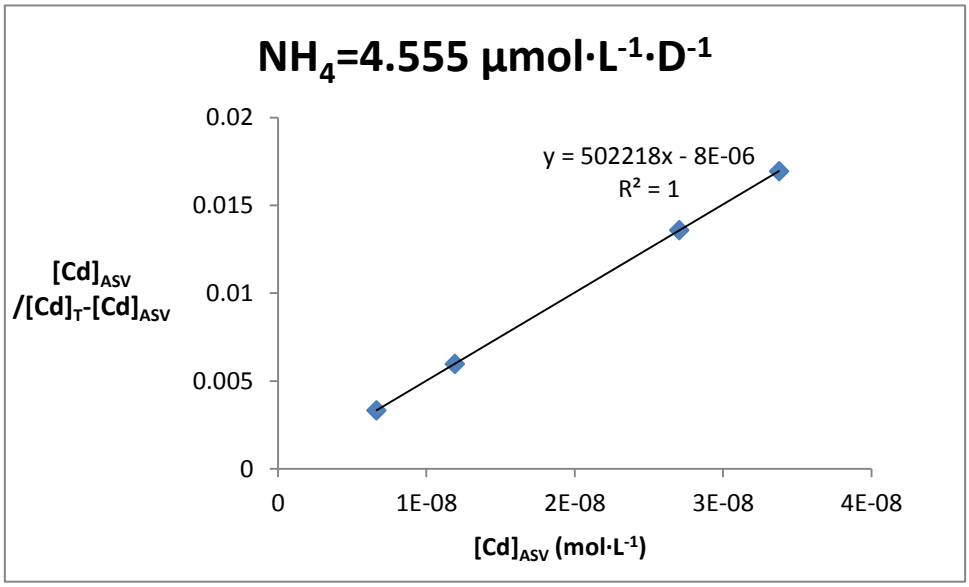

Figure 33 Cd complexation capacity of Cd treatment (with Cd) at ammonia flux 4.555 µmol·L^{-1}·D^{-1} in day 8

Cd complexation capacity of Cd treatment in day 12

Table 23 Cd complexation capacity of Cd treatment (with Cd) at ammonia flux 0.125 µmol·L^{-1}·D^{-1} in day 12

$[Cd]_{ASV}$ (mol·L^{-1})	$[Cd]_T$-$[Cd]_{ASV}$ (mol·L^{-1})	$[Cd]_F/([Cd]_T-[Cd]_F)$
1.6726E-09	1.99833E-06	0.000836999
1.97509E-09	2.00247E-06	0.000986325
2.34875E-09	2.00655E-06	0.001170545
2.95374E-09	2.01484E-06	0.001465991

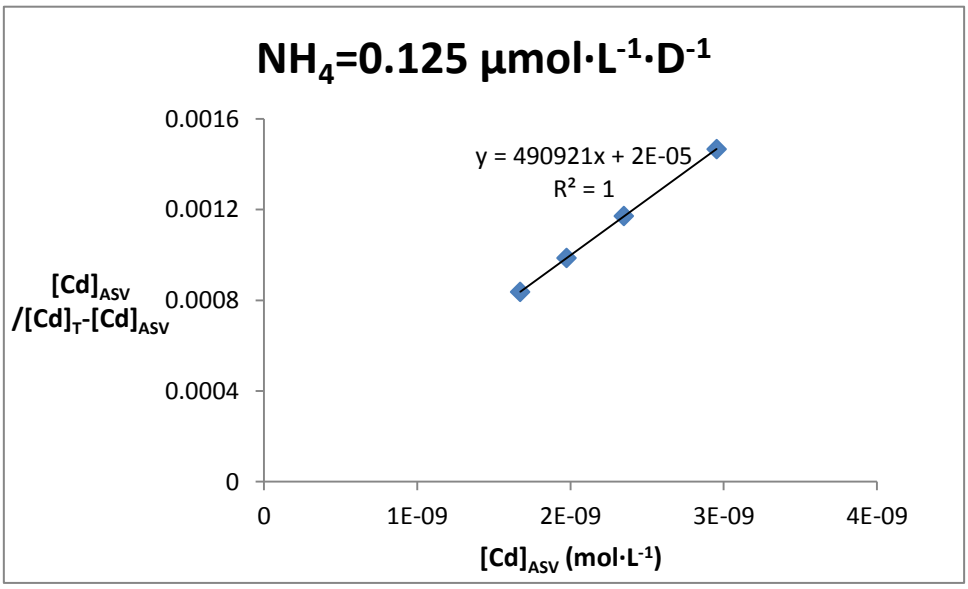

Figure 34 Cd complexation capacity of Cd treatment (with Cd) at ammonia flux 0.125 µmol·L^{-1}·D^{-1} in day 12

Table 24 Cd complexation capacity of Cd treatment (with Cd) at ammonia flux 1.105 µmol·L^{-1}·D^{-1} in day 12

$[Cd]_{ASV}$ (mol·L^{-1})	$[Cd]_T$-$[Cd]_{ASV}$ (mol·L^{-1})	$[Cd]_F/([Cd]_T-[Cd]_F)$
4.91103E-09	1.99509E-06	0.00246156
1.74377E-08	1.99146E-06	0.008756254
2.02847E-08	1.99306E-06	0.010177663
2.35409E-08	1.99425E-06	0.011804384
2.76868E-08	1.99456E-06	0.013881207

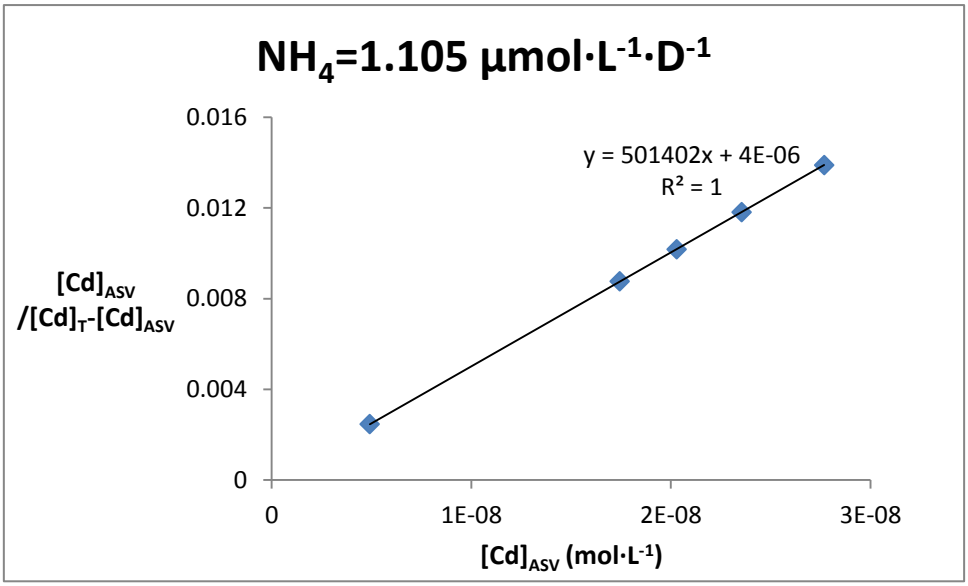

Figure 35 Cd complexation capacity of Cd treatment (with Cd) at ammonia flux 1.105 µmol·L^{-1}·D^{-1} in day 12

Table 25 Cd complexation capacity of Cd treatment (with Cd) at ammonia flux 1.965 µmol·L^{-1}·D^{-1} in day 12

$[Cd]_{ASV}$ (mol·L^{-1})	$[Cd]_T$-$[Cd]_{ASV}$ (mol·L^{-1})	$[Cd]_F/([Cd]_T-[Cd]_F)$
4.83986E-09	1.99516E-06	0.002425799
1.24199E-08	1.99648E-06	0.006220923
1.52669E-08	1.99808E-06	0.007640794
1.83452E-08	1.99945E-06	0.009175128

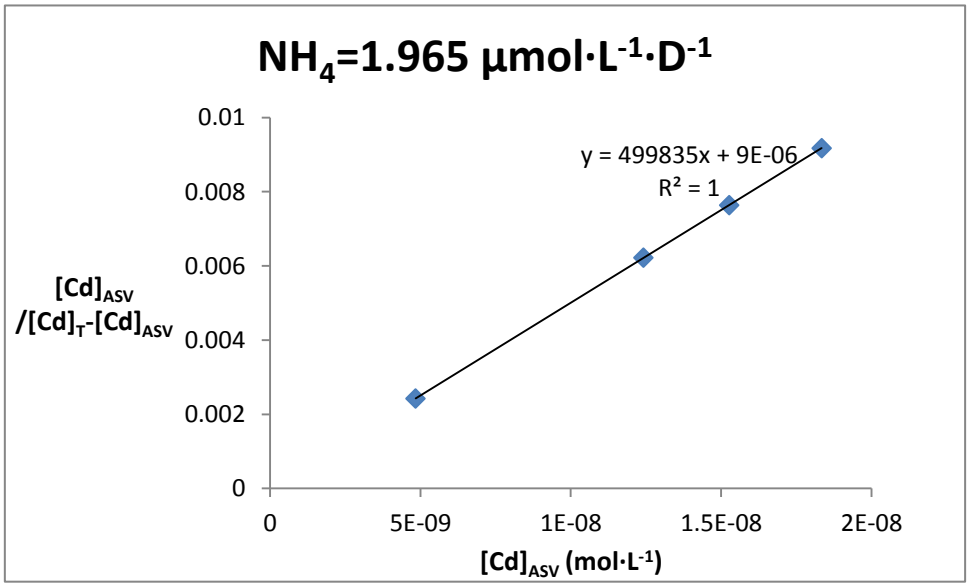

Figure 36 Cd complexation capacity of Cd treatment (with Cd) at ammonia flux 1.965 µmol·L^{-1}·D^{-1} in day 12

Table 26 Cd complexation capacity of Cd treatment (with Cd) at ammonia flux 3.425 µmol·L^{-1}·D^{-1} in day 12

$[Cd]_{ASV}$ (mol·L^{-1})	$[Cd]_T$-$[Cd]_{ASV}$ (mol·L^{-1})	$[Cd]_F/([Cd]_T-[Cd]_F)$
5.30249E-09	1.9947E-06	0.002658293
1.59786E-08	1.99292E-06	0.008017714
2.18327E-08	1.99151E-06	0.010962894
2.59431E-08	1.99185E-06	0.013024602
3.25267E-08	1.98972E-06	0.016347409

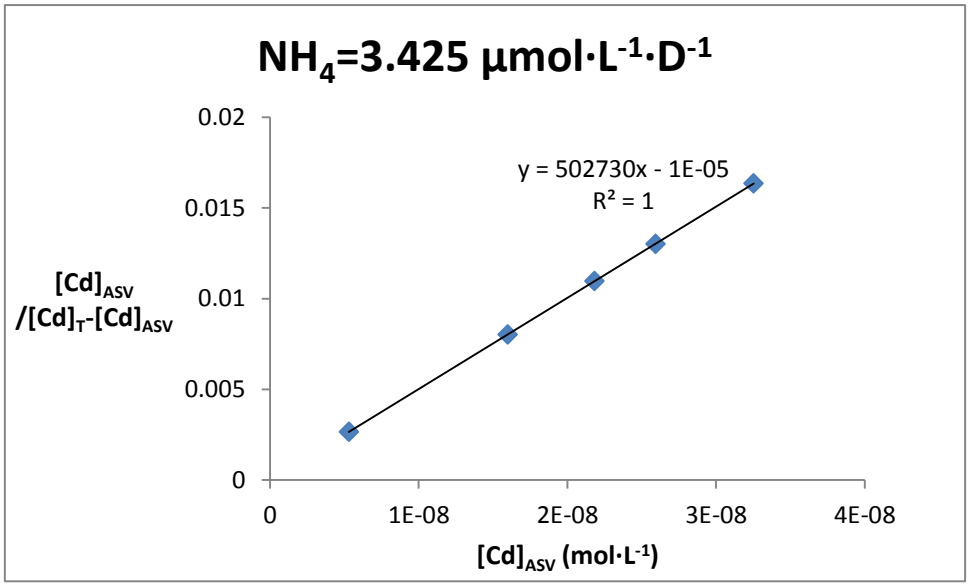

Figure 37 Cd complexation capacity of Cd treatment (with Cd) at ammonia flux 3.425 µmol·L^{-1}·D^{-1} in day 12

Table 27 Cd complexation capacity of Cd treatment (with Cd) at ammonia flux 4.555 µmol·L^{-1}·D^{-1} in day 12

$[Cd]_{ASV}$ (mol·L^{-1})	$[Cd]_T$-$[Cd]_{ASV}$ (mol·L^{-1})	$[Cd]_F/([Cd]_T-[Cd]_F)$
2.30071E-08	1.97699E-06	0.011637431
2.73843E-08	1.97706E-06	0.013851014
3.37011E-08	1.9752E-06	0.017062141
3.99644E-08	1.97338E-06	0.020251749

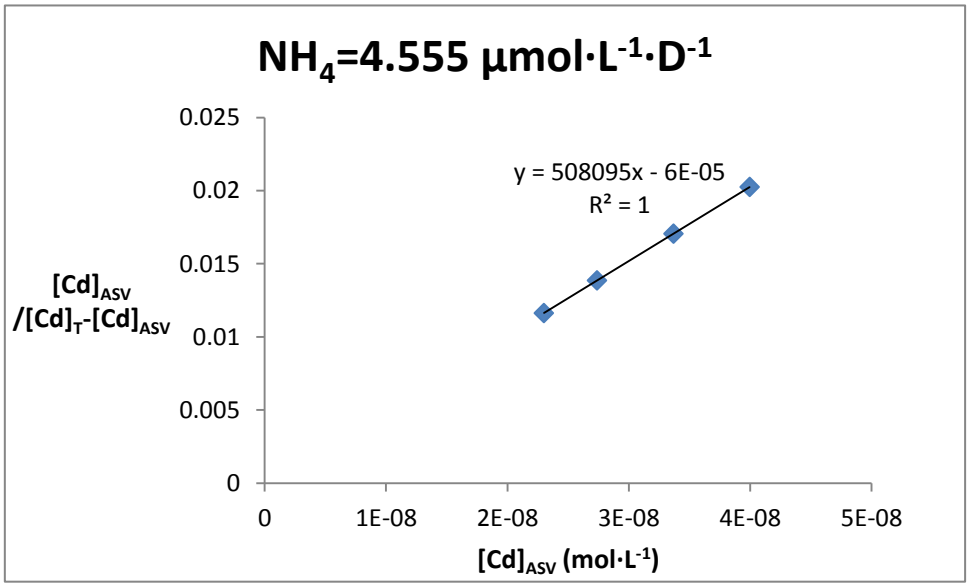

Figure 38 Cd complexation capacity of Cd treatment (with Cd) at ammonia flux 4.555 µmol·L^{-1}·D^{-1} in day 12